Doctoral Dissertation
Doctoral Program in Management Production and Design (35th Cycle)

One-of-a-Kind Design (OKD)
A lean framework for sustainable knowledge-based product development

By

Alberto Faveto

Supervisor(s):
Prof. Franco Lombardi, Supervisor
Prof. Frédéric Segonds, Co-Supervisor

Doctoral Examination Committee:

Prof. B. Rose, University of Strasbourg, ICUBE
Prof. N. Perry, Arts et Métiers Institute of Technology, I2M, Bordeaux Campus
Prof. R. Bandinelli, Università di Firenze
Prof. P. Chiabert, Politecnico di Torino
Prof. G. Bruno, Prolitecnico di Torino

Politecnico di Torino
2022

Declaration

I hereby declare that the contents and organization of this dissertation constitute my own original work and do not compromise in any way the rights of third parties, including those relating to the security of personal data.

Alberto Faveto

2022

* This dissertation is presented in partial fulfillment of the requirements for the **Ph.D. degree** in the Graduate School of Politecnico di Torino (ScuDo).

Tout seul on va plus vite, ensemble, on va plus loin.

African proverb

Acknowledgment

I would like to express my deepest gratitude to my supervisors, Prof. Franco Lombardi and Prof. Frédéric Segonds, for their guidance, support, and encouragement throughout my research journey. Their insightful feedback and expertise have been invaluable in shaping my work's direction and helping me develop as a researcher.

I would also like to extend my thanks to my reviewers, Prof. Bertrand Rose and Prof. Nicolas Perry, for their thoughtful and constructive feedback, which has helped strengthen my research's quality and impact.

I am also grateful to the other examination committee members, Prof. Romeo Bandinelli, Prof. Paolo Chiabert, and Prof. Giulia Bruno, for their time, effort, and valuable feedback during the examination process.

Furthermore, I would like to acknowledge my Italian and French colleagues, who have provided a stimulating and collaborative research environment, and my friends, who have offered their unwavering support and encouragement throughout my studies.

Finally, I extend my heartfelt appreciation to my family and my girlfriend for their constant love, support, and encouragement. Their unwavering belief in me has been my most significant source of strength and motivation throughout my research journey.

Abstract

Increasingly complex and customized products require in-depth life cycle knowledge, which is almost always impossible. This thesis project aims to propose a design support methodology for making informed decisions in all those contexts that can be defined as One-of-a-Kind. In one-of-a-kind production (OKP), the probability of defective products is very high; moreover, designers must test their ideas quickly and inexpensively. In this context, knowledge generation, storage, and reuse play a fundamental role. Scientific research proposed a paradigm that involves the integration of Product Lifecycle Management (PLM) system tools with the Manufacturing Execution Systems (MES), employing a central Knowledge Base System (KBS), allowing communication between designers and the production line in both senses. This way, it is possible to manage design using data from production to minimize defects. For all these reasons, designers need to precognition the optimum process parameters and get insight from the production. Furthermore, a tool to make designers aware of quality's impact on cost and environmental impact is crucial.

The thesis is based on analyzing three different One-of-a-Kind Design problems from various industries and domains. The first challenge involves the deployment of an innovative wireless recharging system for industrial applications. The purpose of the first case study is to create a tool to support the sales teams in forecasting the best positioning of the system, given some customer constraints. The second case study is an application of Additive Manufacturing to find the best parameters to support the designers in considering the quality of the part and its cost and environmental impact. The proposed approach can be used both in small and

big contexts, even if we think that the best-achieved results can be obtained in democratic manufacturing paradigms like Crowdsource Manufacturing, Semi Artisanship Manufacturing, Cloud Manufacturing, Urban Manufacturing, and Social Manufacturing characterized by open or easy-to-share design approach, high personalization, unicity and specificity of products low production volume.

Finally, the third case study is based on a study of the feasibility of an innovative robot-to-parts warehouse picking system with two distinct issues: (A) find the best shape of racks and the minimum number of vehicles needed to manage the warehouse, and (B) study most appropriate.

This case study analysis makes it possible to define a general framework. The framework is composed of four different steps (A) Design Space Definition, (B) Knowledge Generation, (C) Optimization, and (D) Final Decision.

Contents

List of Figures

List of Tables

List of Acronyms and Abbreviations

ABS	Acrylonitrile Butadiene Styrene
AC	Alternating Current
AGV	Automated Guided Vehicle
AHP	Analytical Hierarchical Process
AIC	Akaike's Information Criterion
AM	Additive Manufacturing
AMK	Additive Manufacturing Knowledge
ARMS	Ampere Root Mean Square Error
AS/RS	Automated Storage and Retrieval System
AVS/RS	Automated Vehicle Storage and Retrieval Systems
AWS	Automated Warehouse System
CAD	Computer-Aided Design
CAE	Computer-Aided Engineering
CBAS/RS	Crane-Based Automated Storage and Retrieval System
CMM	Coordinate Measuring Machines
CNC	Computerized Numerical Control
CPU	Central Processing Unit
CT	Computed Tomography
DBD	Decision-Based Design

DC	Direct Current
DEA	Data Envelopment Analysis
DES	Discrete Event Simulation
DfAM	Design for Additive Manufacturing
DIY	Do It Yourself
DMM	Decision-Making Method
DWPT	Dynamic Wireless Power Transfer
EBM	Electron Beam Melting
EDK	Eco-Design Knowledge
ELECTRE	ELimination Et Choix Traduisant la REalité
EV	Electric Vehicle
FFF	Fused Filament Fabrication
FIFO	First In First out
GQFD	Green Quality Function Deployment
HDPE	High-Density Polyethene
HoQ	House of Quality
ICT	Information and Communications Technology
ILP	Integer Linear Programming
IRR	Internal Rate of Return
ISO	International Organization for Standardization
KBS	Knowledge-Based System
KPI	Key Performance Indicator
LCA	Life-Cycle Assessment
LCC	Life-Cycle Cost

LCEA	Life-Cycle Economic Analysis
LCIA	Life-Cycle Impact Assessment
LiDS	Lifecycle Design Strategy
MCDM	Multi-Criteria Decision Method
MES	Manufacturing Execution System
NPV	Net Present Value
OI	Open Innovation
OKD	One-of-a-Kind Design
OKP	One-of-a-Kind Production
OSD	Open-Source Design
PBT	Profit Before Tax
PFC	Power Factor Corrector
PLA	PolyLActide
PLM	Product Lifecycle Management
QFD	Quality Function Deployment
QR	Quick Response code
RAM	Random Access Memory
RMS	Reconfigurable Manufacturing Systems
RP	Rapid Prototyping
SBS/RS	Shuttle-Based Storage and Retrieval System
SDG	Sustainable Development Goals
SJR	Scimago Journal Ranking
SKU	Stock-Keeping Unit
SME	Small-Medium Enterprise

SoC	State of Charge
SWOT	Strength, Weakness, Opportunity, Threat
SWPT	Static Wireless Power Transfer
TBL	Triple Bottom Line
TOPSIS	Technique for Order of Preference by Similarity to Ideal Solution
UL	Unit Load
VDI	Verband Deutscher Ingenieure
VLAB	Valve-Regulated Lead-Acid Battery
VLM	Vertical Lift Modules
VRMS	Voltage Root Mean Square Error
WIP	Work In Progress (or Process)
WPT	Wireless Power Transfer

Chapter 1

Introduction

1.1 Innovation and Design Phases

Part of this introduction is published in the paper "Open product development to support circular economy through a material lifecycle management framework" in the International Journal of Product Lifecycle Management [1]. The product development process can be defined as a finite and coordinated sequence of intellectual, physical, and organizational activities that aim to satisfy customer needs sustainably. According to [2], a generic product development process can be divided into six phases: planning, concept development, system-level design, detail design, testing and refinement, and production and ramp-up.

According to M. Hertwig et al. [3], this complex process can be synthesized into four macro phases: the innovation phase, the development phase, the production phase, and finally, the use phase. Figure 1 displays the correspondence between the four macro phases and the associated activities.

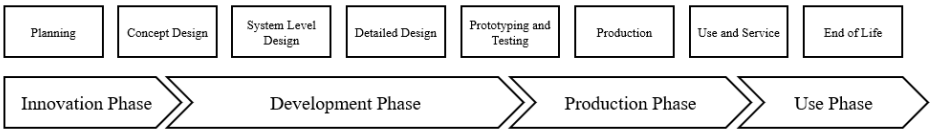

Figure 1 - The Product Development Process

i. The innovation Phase links the applied research field with the product development process. This phase includes the typical product planning and concept design steps where product opportunities are identified, and concepts are generated, evaluated, and selected.
ii. The Development Phase includes system-level and detailed design activities, where product architecture is designed, materials and geometries of all the parts involved in the product are defined, and the production system to be used.

iii. The manufacturing Phase includes testing, refining, and production steps where the product is physically built. It entails the transformation of materials and their assembling to obtain the final product.
iv. Finally, the Use Phase involves all the activities incurred during the use so, maintenance and services, and the management of product disposal and its end of life.

Typically, planning refers to the activity that identifies the product mission and leading targets, and the development process plan is formally set up, too. In this phase, the four main interests focus on the following targets. Planning activity outputs give rise to concept development, where alternative solutions may be envisaged and studied. After an insightful evaluation of developed conceptual designs from all the perspectives, it is possible to spot the best suitable option and take the subsequent development steps. Occasionally, two or more alternative concepts are carried on to the next step to deepen the evaluation through more detailed studies. At the system-level design activity, the concepts selected in the previous stage evolve to a detailed design level, giving rise to the product architectures. So, complex products are decomposed into subsystems with clearly stated interfaces. Each component is designed and evaluated using a sophisticated engineering virtual model to maximize performance and minimize the product lifecycle cost. The solution that passes the system-level design is then subjected to a detailed design activity where each part of the system is accurately studied, analyzed, and designed. The designed configurations of the products are verified during prototyping and testing, in which all the functionalities and performances are assessed. At the end of these activities, the final configuration of the product is defined, and it is ready to be launched at full production. During the Production phase, the manufacturing outputs are monitored. The plants are maintained at a high level of availability and reliability, resource efficiency is assessed, and resource consumption is controlled. The advent of technologies such as Big Data and the Internet of Things enables the possibility to extend the role of the product developer not only at the sale phase but also during the whole usage phase of the product, thanks to the exploitation of sensor networks adequately equipped on the product. Indeed, a 'Use and Service' phase can exploit a significant amount of data to extract precious knowledge using powerful Artificial Intelligence tools. They can feed the previous stages of the product development process to improve the product and process performances and a faster innovation process. A sustainable product development process ends with the End-of-Life phase.

1.2 A New Manufacturing Paradigm

The development of the manufacturing industry is a dramatic sequence of changes in technologies and methodology that started at the beginning of the 20th century with the production chain and mass production. The advent of numerical control machines (CNC) in the 70s triggered the period of flexible manufacturing, making it possible to produce several shapes with the same production line. In the 90s, thanks to the theorization of reconfigurable manufacturing systems () [4], a new brick was added, allowing the production of different product shapes with a variable volume. Nowadays, we face a new revolution in the manufacturing industry, characterized by the democratization of the product that entails several paradigms: Crowdsource Manufacturing [5], Cloud Manufacturing [6], Urban Manufacturing [7], and Social Manufacturing [8]. Although they differ in some aspects, it is possible to find some points in common. These paradigms are characterized by (i) an open or easy-to-share design approach, (ii) high personalization: each user/customer designs and produces his product, creating it himself from scratch, following some design rules, or being supported by an expert designer or a crowd of them, and (iii) low production volume [1]. According to the literature, it is clear that additive manufacturing (AM) is the most suited technology for high complexity, low volume, and high customization application [9]. Moreover, the great majority of the platform that allows the sharing of design data and a democratized approach to manufacturing are based on AM, e.g., Makerbot Thingiverse, RepRap, GrabCAD, etc. [8]

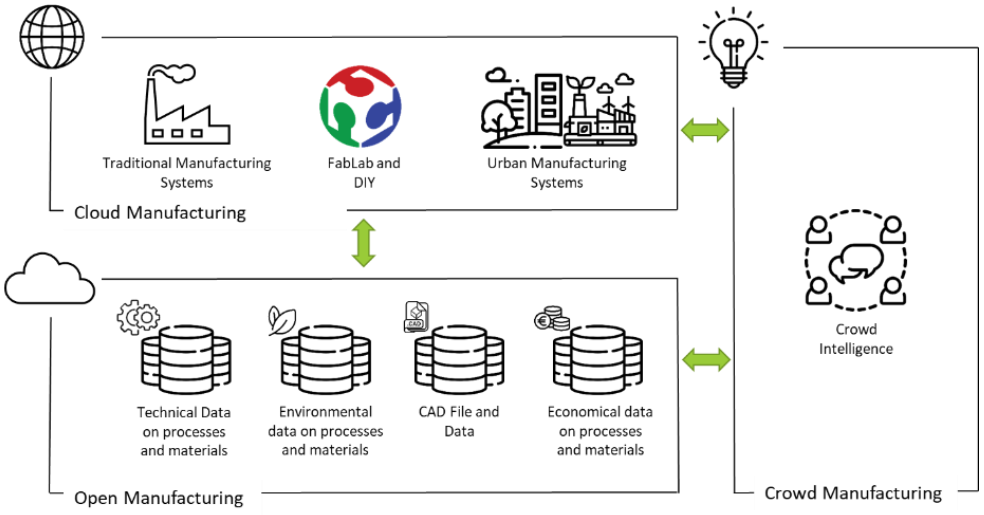

Figure 2 - Distributed Manufacturing Paradigm

The theorized distributed manufacturing paradigm would integrate all the new concepts raised from scientific research in the last decades. It is made of three main elements: a world of physical resources connected all together (cloud manufacturing), a digital world made by open data (open manufacturing), and a world of communities of people where new ideas, concepts, and innovations are developed (crowd manufacturing). These three words work synergically to foster circularity, shorten supply chains, decrease idle times, incentivize innovation, and maximize positive externalities. This paradigm is depicted in Figure 2. Cloud Manufacturing is composed of several machines and resources that are connected, allowing the sharing of production capacity and minimizing idle times. All resources generate data that can be pre-processed using edge computing and then stored in shared databases called Open Manufacturing. These data can entail technical, environmental, design, and economic aspects. Finally, the last part of the paradigm is composed of communities of people, Crowd Manufacturing, through ICT platforms, collaboration among users, makers, and companies can be fostered to generate new ideas and exploit collective intelligence. The concept of distributed manufacturing is not new. In 2016, Srai et al. investigated the presence of several niches in which the use of a distributed approach to manufacturing has already been applied [10]. According to their analysis, manufacturing companies now have unprecedented chances to exchange data, participate in data-driven open innovation, and develop radically original business models with distributed manufacturing. The data-based configuration of distributed manufacturing allows the production, finishing, and installation by the maker, shortening supply chains. Other advantages of distributed manufacturing include personalization, local business expansion, and the use of extra capacity. Distributed manufacturing can also promote closing the loop of production and consumption by recapturing value from waste materials. However, they also highlight several obstacles to the diffusion of such a paradigm. One of the most crucial aspects is the presence of future regulation initiatives from the government that could support the diffusion of distributed manufacturing [10].

In one-of-a-kind production (OKP), the probability of defective products is very high [8]; moreover, designers must test their ideas speedily and inexpensively. On the other side, a distributed approach to manufacturing can cause much waste and significantly impact the environment. Knowledge generation, storage, and reuse play a fundamental role. Bruno et al. have proposed a paradigm that involves the integration of Product Lifecycle Management (PLM) system tools with the Manufacturing Execution Systems (MES), employing a

central Knowledge Base System (KBS), allowing the communication between designers and the production line in both senses [11]. This way, it is possible to manage design using data from production to minimize defects [12]. Figure 3 displays a graphical representation of the described paradigm.

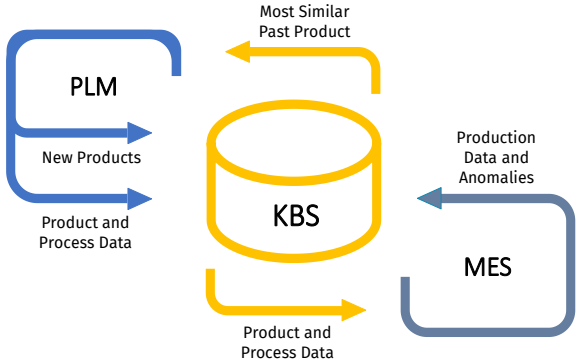

Figure 3 - Integration of PLM and MES through a central KBS, elaboration from Bruno et al. [11]

1.3 An Open Approach to Innovation and Design

Product innovation and design are two core and intertwined activities in product development where most decisions are taken and constrain subsequent steps. Thanks to the digital revolution, new opportunities arise for sustainability-oriented innovation in Industry 4.0. The innovation process can be opened in order to get a broader knowledge and accelerate the innovativeness of products. The last trend in Open Innovation is the so-called quadruple helix model, often referred to as OI 2.0, where participants in the product development process can be grouped into four main categories: government, industry, academia, and society [13]. This model is regarded as suitable for meeting the sustainability challenge under the points of view of its three main pillars: economic, environmental, and social [14]. Jiang et al. proposed a model of the cyber-physical-social system to integrate social intelligence into the product development process through sharing knowledge and capabilities [15]. They described the Reprap example (www.reprap.org), an open-source 3D printer project where users can co-create the printer architecture as well as the library of the interior modules. After that, a community of users can personalize the 3D printer design according to their individual needs, build it utilizing their tools or use other collaborative services available in the community; finally, if desired, they can sell their products via an e-commerce platform. The

same project [16] has been described as an example illustrating how Additive Manufacturing can foster sustainable product development.

[17] proposed a framework for a cloud computing-based collaborative design environment. It supports the collaboration between product designers and various experts to conceive several product design alternatives and select the most environmentally friendly one through the estimation of their Life Cycle Costs directly estimating their Life Cycle Costs on the internet. [18] presented the outcomes of the CloudPyme2 project (http://www.cloudpyme.eu/), where Computer-Aided Engineering (CAE) software, PLM tools, and OI platforms are provided in a supercomputing infrastructure to support the innovativeness and sustainability of Small-Medium Enterprises (SMEs) [19]. Smith, Baille, and McHattie discussed how open design could support a circular economy in the fashion and textile sectors. They envisioned matching waste material from local garments with open-source design data and available production sites to boost redesign strategies reuse of garments and generate recommendations for zero-waste design [19].

In the works of [20] and [21], it is possible to find a methodological framework for facilitating decision-making in design and product upgrade design with a sustainable lifecycle outlook. Moreover, an attractive approach to design is the open-source design detailed by [22] and [23]. The open-source design (OSD) does not necessarily imply environmental sustainability. However, an OSD requires a simple design, standard connections, and modular architecture to facilitate a longer product life. In addition, the products analyzed by the case study always had a short supply chain and local production [22]. Challenges and potentials of the open design process have also been described by Rebensdorf et al. [24] Rosienkiewicz et al. analyzed three important OI-related projects: SYNERGY [1], TRANS3NET[2], and NUCLEI[3]. The main finding of their research was that different organizations have a common need to get information about resources, competencies, and experiences to enhance multidisciplinary collaboration [14].

In the research literature, it is possible to find a multitude of innovation and design decision-support approaches and tools. This lack of a single, well-established practice is a natural barrier to using these tools. The methods of decision

[1] https://synergyplatform.pwr.edu.pl
[2] https://trans3net.webspace.tu-dresden.de
[3] https://www.interreg-central.eu/Content.Node/NUCLEI.html

support open to innovation and design in the literature are manifold. This generates a lack of a unique and well-established approach, which is a natural barrier to the use of these tools. Possible research in this area could be oriented to the attempt to make a map to classify the methods supporting the various stages of the product design process.

1.4 Thesis Structure and Objectives

This work proposes a common framework to support designers in defining a customized tool to make complex decisions in one-of-a-kind (OKD) contexts. The described approach is developed following a bottom-up approach.

The bottom-up approach proposed in this work involves the in-depth exploration and analysis of three particular cases. Case study research has been used extensively in various fields, such as psychology, sociology, business, education, and healthcare, to name a few. Case-study research provided unique insights into the underlying mechanisms and processes that shaped the outcomes of interest in each of these cases. One of the critical strengths of case-study research is its ability to provide rich and detailed descriptions of real-world phenomena. [25] According to Flyvbjerg, case-study research is a valuable tool for gaining a deeper understanding of complex real-world phenomena, but it is also necessary for careful planning and analysis [26]. By focusing on a particular case, researchers can gain a deep understanding of the context, history, and unique characteristics allowing researchers to identify patterns, relationships, and themes that might not be evident in larger quantitative studies. Case-study research also allows for the exploration of complex and dynamic processes over time, which is challenging to capture in traditional experimental designs. However, case-study research is not without its limitations. One of the main concerns is the issue of generalizability. Because case-study research is based on a single case or a small number of cases, it is difficult to generalize the findings to other populations or contexts. Another challenge is the potential for researcher bias, as the researcher's interpretation of the data can influence the findings. To address these concerns, researchers often use multiple cases or use a mixed-methods approach, combining qualitative and quantitative data [25].

The use of multiple case study approach in research has become increasingly popular over the years and has been shown to offer several valuable benefits. By examining multiple cases within a given context, researchers are able to gain a more comprehensive understanding of the phenomenon under investigation [25]. This

approach also provides a way to address the limitations of single case studies, such as the inability to generalize findings to other contexts or to establish causal relationships [27]. A bottom-up approach for the definition of a general framework for decision-aid support tools is a recommended strategy that has been shown to be effective in the development of decision-support systems. Several studies have demonstrated the advantages of a bottom-up approach in this context, including improved system design, flexibility, and scalability. A bottom-up approach based on multiple case studies can lead to more nuanced and comprehensive theories and practical insights that can inform decision-making in various fields. Overall, the multiple case study approaches have been shown to be a valuable research method that can provide rich and diverse data, deepen our understanding of complex phenomena, and contribute to developing generalizable and practical knowledge [25].

The present thesis is divided as follows. Chapter 2 introduces the problem we want to address through a literature review analysis and the main gaps we found. In the third chapter, we present the proposed generic approach. Chapter 4 describes the first case study on wireless power transfer systems in an industrial environment. Chapter 5 presents the second case study on sustainable additive manufacturing, and chapter 6 the third issue about sustainable warehouse robot-to-parts picking system. Finally, chapter 7 draws some conclusions and future works. The described approach has followed a bottom-up strategy, starting from different case studies and finally proposing a generic method. We prefer to introduce the method before presenting the three case studies in this work.

Chapter 2

Decision-Making Method in Product Design

The study of decision-making methods for supporting design sustainability is a particularly thriving area of research. Decision-making support tools in design have three main elements of inquiry: strategic business decisions, holistic engineering evaluation, and operational business process. Each of these general objectives considers different aspects [28]. Figure 4 represents the central aspect to consider based on different goals and proposes possible approaches.

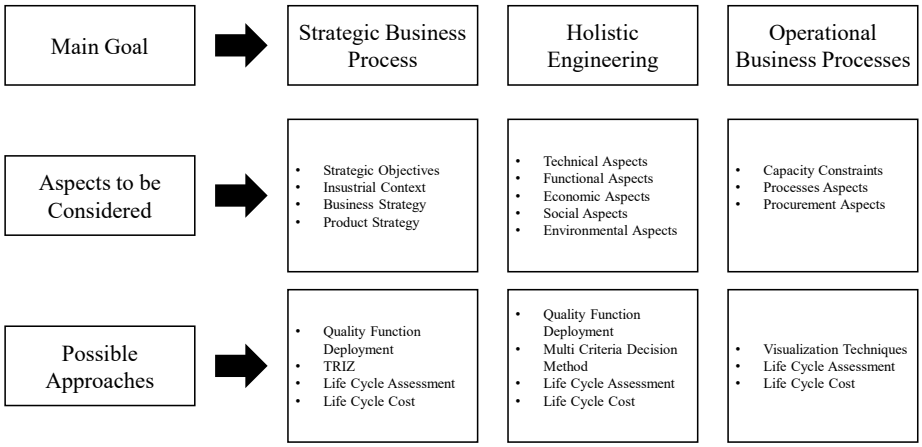

Figure 4 - Decision Making Support Tool goals and main aspects

According to Kengpol et al. [29], a decision-making method consists of three components: a Cost-benefit analysis which explores financial trade-offs among the project. This analysis can be performed by computing the net present value (NPV), the internal return rate IRR, or the cumulative profit before tax (PBT), etc. A second phase, decision-making effectiveness evaluation, is needed to assess the product

launch's success. A criteria assessment that consists of the previous two analyses plus any other tangible and intangible criteria that may affect the company's position. Finally, all data generated from the DMM (decision-making method) are saved in a generic data bank to provide feedback on how well the method works and support subsequent analyses in continuous improvement. Kengpol's paper focuses on how to achieve rapid product development and proposes the evaluation of the three analyses seen above using a multi-criteria technique: Analytical Hierarchical Process (AHP), which is capable of comparing pairwise alternatives among different criteria [29]. Olewnik and Lewis [30] defined the Decision-Based Design (DBD) approach as a set of tools aiming to find the best design solutions. The infinitely large number of alternatives that can be generated and metrics to take into account make this problem extremely complex, which is why different scholars have focused on developing a practical method for it. However, what differentiates all these approaches from one another is the method by which they define the optimum. In any case, A DBD should be logical, use meaningful and reliable information, and not bias the designer, who should ultimately be the one who chooses the design goals. DBD approaches include Quality Function Deployment (QFD), Pugh's Selection Method, Scoring and Weighting Methods, Multi-Criteria Decision Method (MCDM), Multiple Attribute Utility Theory, Taguchi's Loss Function, and Suh's Axiomatic Design [30].

It is very complex to disentangle the methods available to managers and designers, so much so that Stewart et al. proposed a methodology to support the designer and manager in the choice of the best tool to support the design phases. In particular, the selection is mainly based on the product complexity, the desired level of guidance, the design phase, and the main objectives between (a) deployment time, (b) cost reduction, (c) risk management, and (d) market viability [31].

One of the most important goals of DBD is to understand how technical choices impact customer attributes. The latter are genuinely perceived and deemed essential to the customer. Decisions about the product and its process heavily influence product attributes and, thus, the customer's willingness to pay for the good. However, companies often do not solely pursue maximizing economic profit. Still, sometimes long-term corporate strategies and pressures from the policymaker drive the design. In particular, a schematization of the decision-based design framework is proposed in Figure 5. System Design is in charge of choosing different parameters that compose a vector X. System Design takes as input the vector M decided by the system configuration. The vector X has a direct influence on System Attributes (A) and Lifecycle Costs (LC). System attributes are directly visible to

customers, and they influence the customer's Willingness to Pay (W). Not everything is directly controllable by designers: a significant share of Lifecycle Costs, System Attributes, and Willingness to Pay are affected by not manageable Endogenous Variable. For instance, imagine a system deployed on a particularly humid day. This event could impact the final performance and thus not fully satisfy the customer. Lifecycle Costs are composed of two components: Corporate Costs (LCf) and Customer Costs (LCc). LCf usually, can be described as the cost sustained by the company for product design, manufacturing, distribution, and other ancillary operations. On the other side, LCc comprends the usage, maintenance, and disposal costs. Given these two definitions, it is possible to describe Corporate Economic Utility as the difference between the Product Price (P) and the Lifecycle Corporate Costs and Customer Utility as the difference between the Willingness to Pay (W) and all the customer incurred costs (P and LCc). The firm decided the Product Price to maximize its economic utility. Finally, the designers choose the vector X in order to maximize the global utility, as previously stated, also impacted by Strategic Corporate Decisions (S) and Policy Decisions (G).

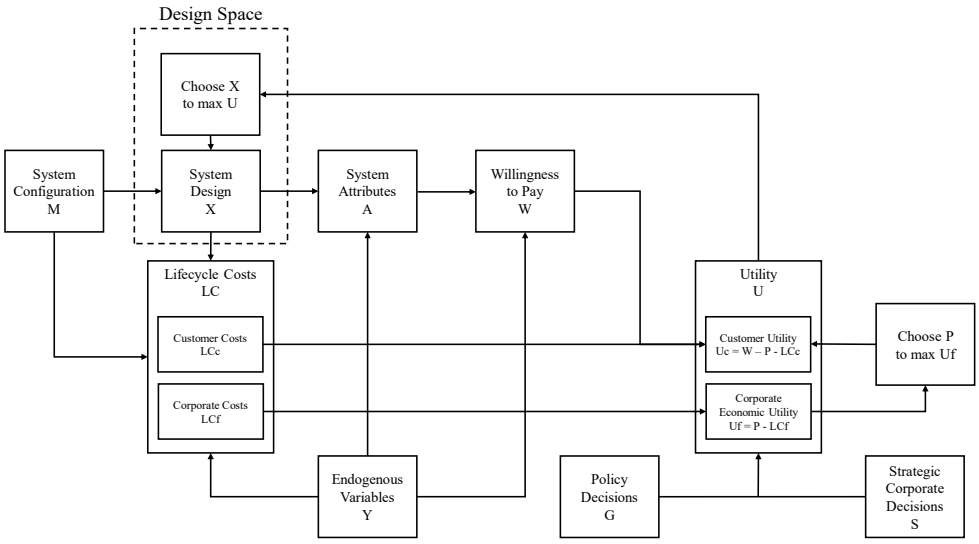

Figure 5 - Framework of Decision-Based Design, elaboration from [32]

2.1 Environmental Decision Design Tools

Sustainability has become an increasingly critical issue in today's world. As the global population continues to grow, so does the resource demand and the strain on the planet's natural systems. In response, there has been a growing movement to

incorporate sustainability principles into all aspects of our lives, from individual consumer choices to global policy decisions. One such approach is the triple bottom line (TBL) [33]., which seeks to balance economic, social, and environmental concerns. Recently, The United Nations proposed 17 Sustainable Development Goals (SDGs) [34] as a blueprint for global sustainable development efforts until 2030. These goals encompass a wide range of issues, including poverty reduction, gender equality, climate action, and sustainable consumption and production. The SDGs acknowledge that these issues are interdependent and require a holistic approach for successful implementation. Achieving the SDGs requires collective action by governments, the private sector, civil society, and individuals worldwide. By addressing the root causes of social, economic, and environmental challenges, the SDGs aim to create a more just and sustainable future for all.

With increasing pressure to address climate change, reduce pollution, and conserve natural resources, it has become increasingly important to have tools and systems in place that can help support environmentally conscious product design. By providing information and data, analytical tools can help designers assess the environmental impacts of their choices. Moreover, these tools can help promote more sustainable practices and policies.

An early example of an environmentally conscious decision support tool developed for product life cycle management was presented in 1999 by Hunkeler et al. The scholars propose a tool called EcoDS. EcoDS is a software for managing the sustainability and risk of lifecycle management through qualitative and quantitative metrics. This proposal focuses on the strategic choice of economical and environmental sustainability projects. Quantitative metrics include, in fact, the net present value (NPV) of the project, i.e., the cash flows that the project is expected to generate in the future discounted. Environmental sustainability is assessed qualitatively, and different risks (i.e., air emissions risk, solid waste risk, etc.) are agglomerated into a single indicator called Residual Risk that can take four levels, e.g., zero, low, medium, and high. The different alternatives are then plotted in a two-axis graph (Economic Risk and Residual Risk) that supports management in project selection. In addition, it is an approach that requires little data and is, therefore, less costly in terms of money and time than a complete LCA [35].

Remaining within the scope of an environmentally conscious design support tool, we cite the work of Lye et al. which propose a design method\ology called ECoDE aiming to assess the environmental impact of a product's components [36]. Differently from the above case, the methods proposed by Lye et al. focus on

environmental aspects by putting the economic element in the background. ECoDE uses the AHP to compare and rank each alternative in ascending order of relative importance. They find ten criteria through a literature review capable of globally assessing the product's environmental sustainability:

1. Component Toxicity
2. Product Cost
3. Product Reliability
4. Material Sustainability
5. Components' Weight
6. Components end-of-life strategy
7. Process efficiency
8. Process environmental Impact
9. Material diversity
10. Component accessibility and reparability

Their approach relies on these ten criteria and evaluates design solutions on these dimensions [36].

One of the most studied DBD approaches to foster sustainability aspects is the Quality Function Deployment. The traditional QFD's House of Quality (HoQ) was extended by Cristofari et al. [37] by adding environmental factors and introducing the Green Quality Function Deployment (GQFD), Zhang et al. led to GQFD-II (Green Quality Function Deployment), which integrates LCA, life cycle cost (LCC), and QFD into an efficient tool that uses customer, environmental, and cost requirements throughout the product development process [38]. Mehta and Wang developed the GQFD-III methodology to integrate life cycle impact assessment (LCIA) into the HoQ and used the analytical hierarchy process (AHP) technique to select the best product concept [39]. Romli et al. proposed an EcoDesign methodology based on an Eco-QFD to support sustainable product development. In particular, they proposed a methodology that considers environmental aspects in each design phase. The approach starts from customer function and identifies the related components and the bill of material. It calculates an environmental assessment, and then it applies a four-stage QFD (product planning, product design, process planning, and production planning) with environmental characteristics combined with functional ones [40]. In [41], the researchers propose a QFD conjoint analysis to connect technical parameters with customer attributes. Their approach is composed of market analysis to retrieve customer importance. Then linear regression discovers a relationship matrix that links technical characteristics

with customer quality perception. In [42], the authors propose a Case-Based Reasoning tool based on Eco-QFD. Their approach is a computational modeling technique based on a Life Cycle Cost (LCC) and Life Cycle Assessment (LCA). It links customer requirements with product characteristics and then designs decisions with environmental impacts. This way, it is possible to assess the environmental effects of customer requirements and make informed decisions. The authors also suggested that the results be stored in a shared library so that future projects can draw on the knowledge [41].

Dell'Anna, Bottero, et al. suggested an approach to support a sustainable approach for construction buildings, in particular, to support decision-making in the transformation of rural facilities into nearly-zero energy buildings. They proposed a multi-stakeholder analysis based on five different criteria. Their approach is particularly fascinating since these criteria (global project cost, primary energy consumption, market value, CO_2 emissions, and indoor comfort of the building) refer directly to the 17 SDGs [43]. In particular, goal 3: good health and well-being, goal 7: affordable and clean energy, and goal 11: good health and well-being [34]. It would be interesting for future work to try to directly link the purpose of sustainable decision-aid tools for new product development to one or a set of the SDGs proposed by the United Nations.

Finally, a fascinating approach is proposed by Keivanpour and Ait Kadi. Their methodology is a data visualization approach based on the definition of a components' eco-efficiency helpful, necessary map for quickly understanding the environmental impact of different components of very complex products [28].

Many of the studies seen in this chapter start with alternatives and criteria. This approach involves prior knowledge about the final outcome of the alternatives. As we describe in the following chapters, it is often not possible to have prior knowledge to support decision-making in OKP design. For this reason, **the central research gap we tried to fill with this thesis is to find a generic framework capable of supporting designers in generating a knowledge-based decision tool. In particular, to find a way to overcome the limitations of lack of knowledge by adding an intermediate step of knowledge generation.**

2.2 One-of-a-Kind Design Support Framework Definition

The approach proposed in this thesis consists of four parts. The first step, called design space definition, investigates the designer's area of interest. Specifically, as

a first activity, the main performances of interest will be chosen, whether these are customer requirements, technical performance, or generic product features that, for some reason, affect product development (e.g., environmental impact). The second step proceeds with evaluating those parameters controllable by the designer. The parameters describe the design space where the product conception can move. Once performance and parameters have been identified, the design space can be considered defined. The two activities described are consecutive but also recursive; once the first set of performances and parameters have been defined, it is possible to examine again what performances are impacted and so on.

Once the design space is identified and described, the second step (knowledge generation) occurs. This step primarily aims to generate new knowledge and relationships between the parameters and the performance chosen. This activity is the most critical and probably the most important for one-of-a-kind design since no previous knowledge is generally available. Through this thesis, we have identified three applicable methodologies for generating new knowledge: a theoretical approach, an entirely empirical approach, and finally, a hybrid approach. The first totally theoretical approach is to be applied when the impact that design variables (parameters) have on performance is already known a priori. This is the case when one is investigating physical and mechanical interactions or when there are known empirical laws already studied. In this case, since all the relationships are already known, it will not be necessary to create new ones, and it will be sufficient to make them explicit and proceed to the next step. The second approach, on the other hand, is empirical. in this case, one has no prior knowledge of how the parameters will impact the product; therefore, experiments must be conducted to make these relationships explicit. This approach is necessary in the case of qualitative performance (e.g., the comfort of a seat or the roughness of a surface). Once an experiment has been generated, it is necessary to proceed with detailed data analysis to generate empirical laws with some degree of confidence. Since this has to be done in tests, there is a cost involved, so it is necessary to perform a number of experiments that will allow for a degree of confidence in the relationships found without increasing costs excessively. Finally, a hybrid approach can generate the relations between design and performance parameters. This approach often takes shape through simulation (finite element method, discrete event simulation, agent-based simulation, computational fluid dynamics, or system dynamics, depending on the domain of study). It is necessary to know some a priori rules and make them explicit to build a simulation model. However, the product's behavior as different parameters change is tested through experiments, and finally, it is possible to

generate new simulation empiric interactions. This approach is necessary when the physical experimentation costs are too high, for example, in the construction of expensive products, buildings, or plants.

The three knowledge generation approaches would result in relationships between design parameters and product performances. These relationships are then used in the third step. This step consists of the definition of an optimization problem in order to find the best values for the parameters in order to maximize the performances. If the goal of the analysis is to maximize (or minimize) a single performance, the optimization operates only on a single objective function. In contrast, it is necessary to apply multi-criteria optimization if the analysis aims to manage multiple objectives. Sometimes it is possible to translate all the objects in a single one (e.g., minimize the costs). However, this approach is sometimes not possible and, other times, misleading. For example, the energy consumption of a product could easily translate into the cost per kWh. However, this value is sure to vary over time, and in the case of multi-period analysis and projects, it could lead to incorrect considerations. Therefore, a multi-objective approach is recommended, even if more complex to manage. Then the defined problem is solved in order to find the best solutions.

The final step consists of the definition of a decision support tool, i.e., a tool to move effortlessly between the solutions found by the optimizer. Often very efficacious methods consist of data visualization as proposed by [28] or multi-criteria decision method as the AHP (Analytic Hierarchy Process), TOPSIS (Technique for Order of Preference by Similarity to Ideal Solution), or ELECTRE (ELimination Et Choix Traduisant la REalité) approaches. A summary of the proposed framework is reported in Figure 6.

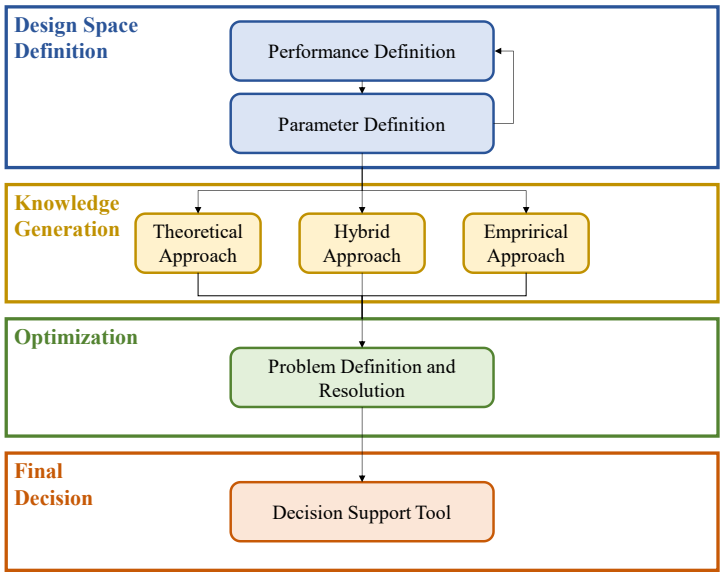

Figure 6 - One-of-a-Kind Design Support Framework

2.3 Application of the proposed Framework on different case studies

The proposed methodology is applied to three different case studies. The first case study aims to find the optimal disposal of a Forklift charging system for warehouses. Analyzing the case study, we decided to focalize on two parameters: the total system cost and the forklifts' state of charge variation. We based our analysis on physics and equations laws in order to study the battery behavior during a working shift. According to Rai and Sahu, this methodology can be considered a Model-Based approach [44]. Finally, we developed a mixed integer linear programming model to find the best solution and study its robustness and impact on input variables. The achieved solution is **a tool to find the system's best position and estimate costs**. The second case stud aims to solve the design problem of assessing the impact of parameters in a fused filament fabrication additive manufacturing (AM) process. We analyze the most interesting key performance indicators in AM processes, choose the more appropriate and categorize them into three clusters:(i) Quality, (ii) Economic, and (iii) Environmental. We develop a Taguchi design of experiments to generate new knowledge and build a data-driven model. Finally, we applied a multi-objective genetic algorithm to find all the non-dominated solutions. Using the frontier of non-dominated solutions, we build a

visual approach to support decision-making. The achieved solution is **a visual-based tool to support designers in the design of additive manufacturing (DfAM) choices**. Finally, the third case study intends to study the best layout of the automated robot-to-parts warehouse picking system. We performed a literature review to find the most used KPI in automated warehouse systems. We categorize them according to the Triple Bottom Line, and we choose the more appropriate for our scope. We generate new knowledge using a discrete event simulation, and this approach could be considered a hybrid approach as previously described. Finally, we applied a multi-criteria decision method (TOPSIS) to the obtained solutions space capable of supporting the designers in their choice. The achieved result is **a tool to support designers in defining warehouse layouts based on SKU storage logic**. Figure 7 summarizes the three case studies and the applied methodologies.

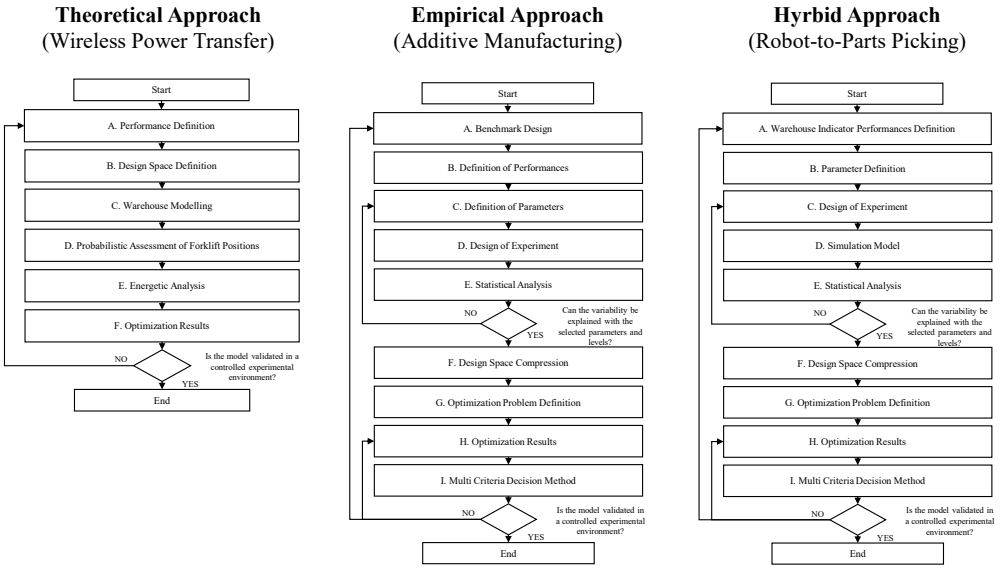

Figure 7 - The proposed methodology and the application of three different case studies

Chapter 3

Wireless Power Transfer in Industrial Environment

3.1 Introduction

The present case study is also published in an article called "Efficient management of industrial electric vehicles by means of static and dynamic wireless power transfer systems" in the International Journal of Advanced Manufacturing Technology [45]

Regulators and corporate policies are more and more pointing attention to climate issues and energy sustainability. For instance, in Europe, the objective is to cut domestic greenhouse gas emissions by at least 80% by 2050 compared to 1990 [46]. These concerns have led to the rapid growth of Electric Vehicles (EVs) due to their ability to reduce pollution and gas emissions and save fuel costs [47,48].

The rapid development of new technologies and applications to develop the EVs automotive field has generated idea spillovers and directed innovation in other sectors where electric engines were already well established, e.g., indoor material handling or airport electric ground support equipment. Vehicles have to be electrically powered to reduce pollutant emissions and guarantee breathable air and workers' safety in these applications. However, the electrification of a large number of vehicles triggers several issues due to the environmental impact and sustainability of batteries. The batteries of electric vehicles need to be recharged quite frequently and require considerable time to reach the desired state of charge. In order to reduce the charging frequency, the capacity of the battery has to be increased. In this case, the battery pack volume rises, which leads to a proportional and substantial increase in the vehicle's weight with a consequent boost in energy consumption per unit of distance traveled [49]. In order to reduce the charging time, the battery swap procedure can be exploited [50,51]. However, this technique requires a more extensive stock of batteries, higher than $n + nR$, where n is the total number of vehicles in service and R is the ratio between the average charging time and the average discharging time. In this case, the impact of the battery life

cycle is quite significant since the efficient recycling of batteries at the end of their life is not consolidated [50,52].

Among others, a promising technology for battery charging is Wireless Power Transfer (WPT), a contactless electrical energy transmission system. It is based on the magnetic coupling between coils installed under the ground level, called the transmitters, and a coil mounted under the vehicle floor, called the receiver [53]. In WPT, the transmitter and receiver are independent, and the recharge process can start automatically when the vehicle is over the transmitter. Moreover, the problem of electrical erosion and deposition of dust, dirt, and chemicals is avoided thanks to the absence of contact and the embedding in the vehicle, which allows the system to have a longer life cycle and less need for intervention and maintenance [53]. For all these reasons, this study aims to propose a model to evaluate the best deployment of a combined static and dynamic WPT charging system within a warehouse to achieve a required level of charge while minimizing plant costs. SWPT systems can be placed in dedicated areas where the vehicles stop and can be recharged, e.g., parking slots, docks, etc. At the same time, DWPT systems can be used to create a charging lane constituted by multiple transmitting coils placed below plant pavement. These coils automatically activate when the forklift is over them [54,55]. The system allows charging the vehicle continuously, eliminating the charging breaks typical of the battery swap method. Moreover, the power needed for this application is similar to the slow charging of batteries. So, it does not require any electrical system improvement, which typically must be realized during the installation of fast charging systems.

The paper is organized as follows. Section 2 presents the literature review available on the topic. Section 3 defines the methodology for installing a WPT system in a warehouse. Firstly, a statistical discretization of the warehouse is performed, then an Integer Linear Programming (ILP) model is applied to evaluate the best positioning of coils inside the plant in order to satisfy project constraints while minimizing the cost. In Section 4, the proposed methodology is applied to a real case study, i.e., a warehouse used as a distribution center by a tire manufacturing company in Europe, while in Section 5, the results of the application are described. Finally, Section 6 presents some conclusions and future works.

3.2 State of the Art

In literature, two types of WPT technologies are defined based on the maximum allowed distance between the transmitter and the receiver: radiative (far-field) WPT and non-radiative (near-field) WPT. The former is concerned about energy transfer at long distances since an antenna transmits the energy to a receiver via electromagnetic waves [56]. The latter concerns the transmission of energy at short distances, and it is based on the near-field magnetic coupling of coils [57]. In this work, we focused on the near-field WPT. For what concerns the applications

devoted to the charge of electric vehicles, the near-field WPT can be indicated as static WPT (SWPT) or dynamic WPT (DWPT) [58,59]. SWPT applies to vehicles stopped or parked during the charge, while DWPT is able to supply power to the vehicle while it continues to move. A general scheme of the main components of a WPT system applied to a forklift is depicted in Figure 8. The system comprises a transmitter pad (i.e. transmitter coil and auxiliary parts), mounted under the floor level, and a receiver pad mounted onboard the vehicle. The AC voltage of the warehouse electric grid is converted to a stable DC voltage through a power factor corrector (PFC) AC/DC converter. Downstream the AC/DC converter, each transmitter is powered via a DC/AC converter giving rise to the variable magnetic field responsible for the wireless power transmission. Finally, onboard the forklift, the AC voltage at the output of the receiver pad is converted again into DC signal to charge the vehicle battery.

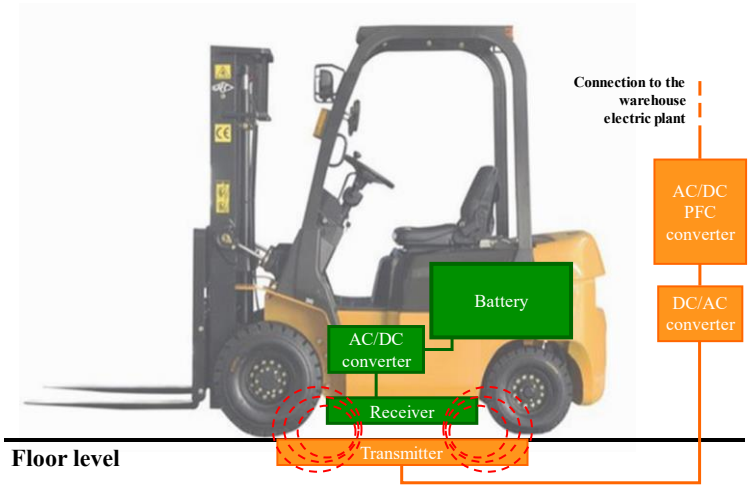

Figure 8 - Scheme of the main components of a WPT system.

WPT involves the use of electromagnetic fields at frequencies that typically range from 10 kHz to 100 kHz in the presence of relevant air gaps between the coils. This is why the assessment of human exposure to the electromagnetic field must be appropriately taken into account during both the design stage of the WPT system and in the management of system operations. In [60], it is possible to find an assessment for the automotive application of a 20 kW DWPT system. As they highlight, the system is safer and compliant with the guidelines if the coil receiver is placed at the center of the vehicle, i.e., in a position in which both the transmitter and receiver coil can be adequately shielded. DWPT has not yet found much use in the automotive industry, even though research in this field is making great strides. In the literature, it is possible to find several works demonstrating technical feasibility [61–63]. Nevertheless, according to the literature, the use of WPT could

find fertile ground in indoor mobility, particularly for industrial warehouse vehicles [64,65].

In fact, according to the lean management perspective, the time spent in the warehouse has no added value; however, stocks are necessary for many reasons (anticipating demand, decoupling processes, buffer production, etc.). Furthermore, the time spent in the warehouse generates additional holding costs, i.e., the daily cost of maintaining the product in the warehouse in terms of energy consumption, overhead, and the risk of perishability and obsolescence of the products [66]. For all these reasons, a green approach to warehouse management is increasing in importance, and it has been the subject of research studies. In recent years, the term Green Warehouse has been defined i.e., as a new management approach to minimize energy consumption and emissions in the holding and handling of warehouse stock [67]. On the other hand, an economic and social management perspective is well established in literature by means of the concept of Lean Warehouse [68]. To the extent of a more sustainable warehouse from an economic, environmental, and social perspective, performance measurement is shifting to a more comprehensive outlook, assessing the pollutant emissions, energy saving, but also the condition of workers, and the ergonomics of the most frustrating tasks [66,69].

Several works have focused on optimizing WPT infrastructure through a mathematical modelization, e.g., in [70], the authors developed a model to find the optimal location of DWPT facilities and design the optimal battery sizes of electric buses and electric public services with multiple lines. While in [71], a methodology is proposed to find the optimal location of a wireless charging system for buses on the airport apron. Finally, [72] and [73] study a model to evaluate wireless transfer technology in vehicular traffic. To the best of our knowledge, no researcher has addressed the problem of WPT systems allocation and optimization in warehouses or other indoor applications. We think this technology could be appealing in an indoor application, and in this paragraph, we present some reasons.

Warehouse forklifts usually employ two kinds of batteries:

- The most used type is valve-regulated lead-acid batteries (VLABs). They are employed due to their low cost and their high reliability. However, lead-acid batteries present some downsides, such as low energy density (35 –50 Wh/kg) and high weight. Although EVs' battery weight represents a drawback, for what concerns the electric forklifts, the weight is not a significant issue because it is used as a counterweight inside them, helping maintain the center of gravity during operational lifts. [74–76].
- Lithium-ion batteries are the most modern solution. They are lighter and present superior energy density (114-125 Wh/kg), a longer life cycle, and

greater efficiency. However, they are still not widely adopted as, on the counterpart, they are more expensive [75,76].

One of the most diffused methods to execute the recharge consists of the battery swap procedure [50,77]. The exhausted battery is substituted with a charged one. Though, this operation requires skilled personnel and introduces many safety risks [77]. It is possible to use a single battery that should be frequently partially charged using a particular power supply, providing a current up to three times higher than the nominal charging one. However, the drawback of this solution is represented by the high number of breaks needed for frequently charging the battery and, as aforementioned, the more significant number of battery stock required. On the other hand, thanks to DWPT, it is possible to create a charging lane constituted by multiple transmitting coils placed below plant pavement. These coils activate automatically when the forklift passes over. This system allows to continuously charge the vehicle by keeping a constant state of charge and eliminating the charging breaks typical of the battery swap method. Moreover, the power needed for this application is similar to the one for the slow charging of batteries, and so it does not require any electrical system improvement, which typically must be realized during the installation of fast charging [78].

As aforementioned, DWPT can potentially solve the trade-off between battery autonomy and charging time. In a DWPT system, the batteries can have a smaller capacity and therefore be cheaper. Besides, as there is no need to stop vehicles for recharging, the total number of forklifts (and batteries) can be lower in indoor applications like plants or warehouses. Both of these advantages mean that the system has a lower environmental impact. Fewer vehicle breaks and greater utilization of batteries can drive a service life intensification. In our opinion, this phenomenon can have an extraordinary effect on warehouse sustainability because a small number of resources are needed and operate more efficiently. Additionally, this sustainable approach positively affects warehouse economic performances: fewer pauses mean greater productivity, and fewer resources mean a minor use of the company’s funds.

3.3 Methodology

The proposed methodology for the WPT systems installation in a warehouse is composed of seven phases Figure 9. The first and second phases' purpose is to define the measured performance and the decision variables. In our analysis, we focalize on the final system cost and the energy provided to the forklifts as the central performances. In contrast, the design space defines the best positioning of the system inside the industrial environment.

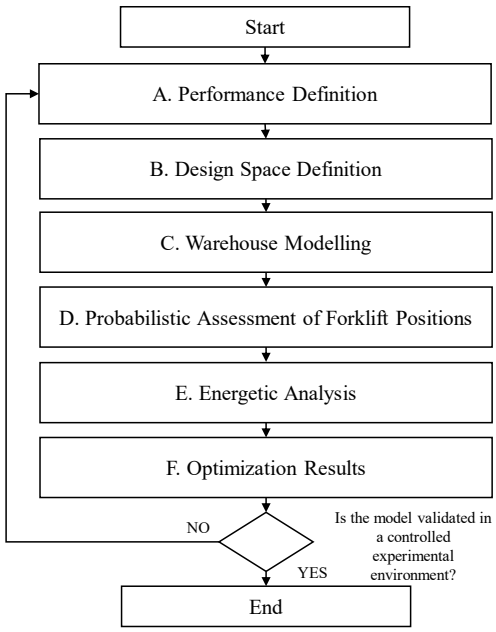

Figure 9 – Methodology of wireless power transfer case study divided into 7 steps

The third phase is the mathematical definition of the warehouse. The warehouse is modeled as an undirected graph by using nodes and edges placed on the discretized working area. All the operations carried out by the electric forklifts must be defined, and the definition of DWPT system to be installed.

The fourth phase is the probabilistic assessment of the forklift positions, which is carried out based on the time spent by the forklifts in the different working zones during a working shift. Such computation has a twofold purpose; on the one hand, the time distribution of the forklifts represents the criterion by which the optimization algorithm computes the whole WPT system layout, including both SWPT and DWPT systems. On the other hand, the knowledge of each temporal contribution relating to the different service phases, which are the travel time in unloaded conditions, the operational time in the storage/retrieval point, the travel time in loaded conditions, the operational time in the docking area and the waiting time in the docking area, allows the assessment of the energy demand in a working shift.

The fifth phase is the energetic analysis in order to compute the State of Charge (SoC) variation of the forklifts after a working shift. It includes the energy spent by the forklifts during their different service phases, as well as the energy absorbed due to charging systems by means of WPT. The SoC variation is a customer requirement, so the WPT system layout must be able to guarantee the residual energy required by the customer at the end of the working shift.

The sixth phase is the formulation of the optimization problem. The output of the optimization problem is the computation of the WPT systems displacement layout that allows the fulfillment of the problem constraints, the satisfaction of the SoC requirement, and the cost minimization of the system.

Finally, the last phase consists of analyzing and evaluating the obtained solution.

According to the general framework proposed in Figure 6 in the second chapter, this first use case's proposed methodology can be structured as follows. The design space definition is completed in phases A and B. In this first case, the parameter definition is not essential since the only decision variable is the placement of the WPT system inside the warehouse. The core of knowledge generation through a theoretical approach is done with the four phases, C, D, E, and H. Some fundamental rules are generated in these phases, and all future decisions rely on these assumptions. Finally, the use case ended with optimization phase I. Since we have a single performance (cost) to be minimized and a single performance (energy provided to the forklifts) as a constraint to be satisfied, we get an optimal solution, so the designer will not need tools to support the choice. Figure 10 displays through a dashed line the main elements of the general framework validated with this first case study.

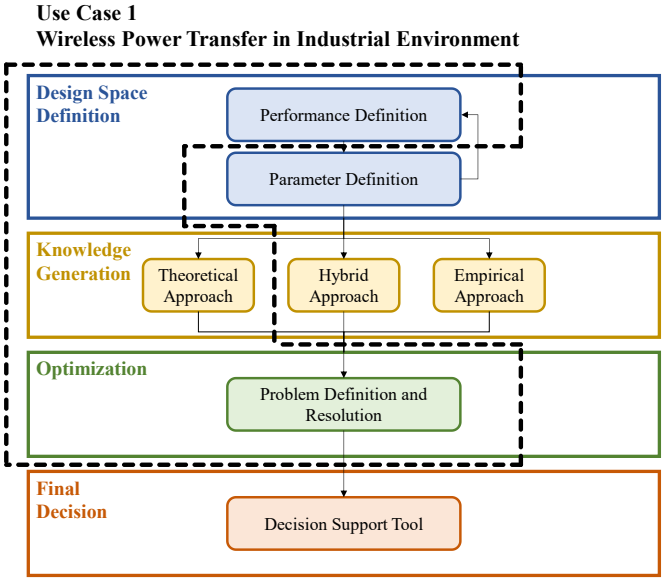

Figure 10 - General framework on the WPT use case

The present chapter takes as a reference for the WPT systems the data provided by Enermove s.r.l. (http://www.enermove.com/), an Italian company partner of this work. In the upcoming sections, all the phases of the methodology are described in detail.

3.3.1 Warehouse Modelling

In this phase, in order to design a mathematical model of the warehouse, the following items are defined: (i) warehouse map, (ii) DWPT, and (iii) forklift operations. These three elements and their definitions are exhaustively detailed in the three subsequent subparagraphs.

4.3.1.1 Warehouse map model

A warehouse can be defined as a set of corridors, i.e., paths along with the forklifts move to store items in the racks or retrieve items from them. Each corridor has an orientation: if it is parallel to the x-axis, it is called a horizontal corridor; otherwise, it is a vertical corridor. For instance, in the warehouse depicted in Figure 11, three corridors are present, two vertical and one horizontal.

It's possible to define $\mathcal{H}$ the set of all the horizontal corridors in the warehouse, and $|\mathcal{H}| = H$ its cardinality. In a similar way, $\mathcal{V}$ is the set of all the vertical corridors in the warehouse, and $|\mathcal{V}| = V$ its cardinality.

$$\mathcal{H} = \{1, 2, \dots, H\} \tag{1}$$

$$\mathcal{V} = \{1, 2, \dots, V\} \tag{2}$$

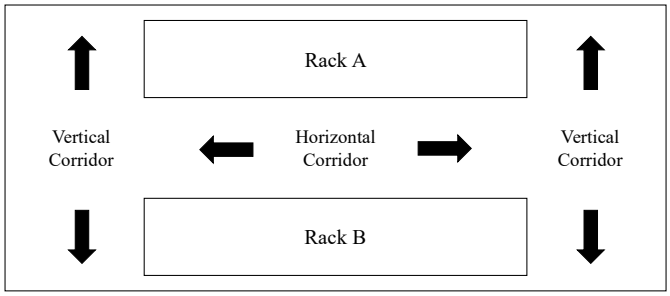

Figure 11 - Warehouse with three corridors.

In order to discretize each warehouse corridor, it is possible to define a set $\mathcal{N}$ of warehousing nodes with cardinality $|\mathcal{N}| = N$, equal to the number of all the nodes within the discretized warehouse, excluded the entry docks ones:

$$\mathcal{N} = \{1,2, \dots, N\} \tag{3}$$

The corridors are discretized into smaller areas using warehousing nodes. Any point of the aisle that the forklift can traverse is associated with a node if that node is the closest to that. In this way, we reduce the warehouse into a simple graph of

nodes and edges. All the events that happen in a bidimensional warehouse area are associated with the single closest unidimensional node.

Each warehousing node belongs to one of the following categories, as shown in Figure 11:

1. *Horizontal node*: a node belonging to a horizontal corridor, where a DWPT module can be installed just along the x direction;
2. *Vertical Nodes*: a node belonging to a vertical corridor, where a DWPT module can be installed just along the y direction;
3. *Cross Nodes*: a node belonging to both a horizontal and a vertical corridor, where a DWPT module can be installed in both directions;
4. *Impossible Nodes*: a node where no DWPT module can be installed because, in that area, it is not possible to insert a coil.

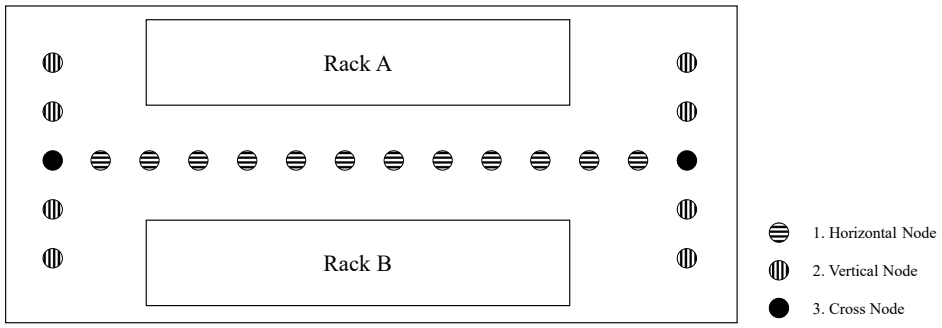

Figure 12 - Warehouse representation with node categories.

For each warehousing node i, the following properties are defined:

- n_i: a sequential integer number starting from 1 representing the node identifier.
- (x_i, y_i): the cartesian coordinates of the node in accordance with the chosen reference system.
- $cat_i \in \{1,2,3,4\}$: the category of the node.
- $horc_i \in \mathcal{H} \cup \{0\}$: the horizontal corridor to which the node belongs to (0 otherwise).
- $verc_i \in \mathcal{V} \cup \{0\}$: the vertical corridor to which the node belongs to (0 otherwise).
- $onf_i \in \{0,1\}$: the operational node flag with value 1 if an operation of storage or retrieval can be executed in the node, 0 if it is only a passing node.

Each couple of adjacent nodes is connected by a non-oriented edge, and DWPT modules can be placed only across the defined edges. As all the nodes within the warehouse map are equally spaced, all the edges have the same length, and since a DWPT module developed by Enermove has a length of 2.5 m, we have decided on an edge length of 0.5 m as a trade-off between the flexibility of DWPT module

placement and graph complexity. In a similar way, as done for the warehousing nodes, it's possible to define a set of edges $\mathcal{E}$ with cardinality $|\mathcal{E}| = E$.

$$\mathcal{E} = \{1,2,\dots,E\} \tag{4}$$

Each edge $e \in \mathcal{E}$ is identified by an edge ID e_e: a sequential integer number starting from 1.

An additional element to fully represent the warehouse is the docking node, defined as the closest node to the docking area. The docking node has the same properties as the warehousing nodes, but no DWPT module can be placed on it; thus, all docking nodes belong to the 4th category. The docking areas deal with the loading and unloading operations of the items from the truck. We have defined a set of docks Δ with cardinality $|\Delta| = D$:

$$\Delta = \{1,2,\dots,D\} \tag{5}$$

Each dock $j \in \Delta$ is identified by the following parameters:

- d_j: a sequential integer number starting from 1 representing the dock identifier.
- $dn_j \in N$: it identifies the docking node, i.e., the closest node to the working area.
- $dnf_j \in \{0,1\}$: a docking node flag. This property is 1 if an SWPT charging point can be potentially installed on the dedicated area within the dock area, otherwise is 0.

As aforementioned, a docking node is a node nearer to the docking area. Any events that happen in the docking area are allocated to the corresponding docking node. It's assumed that SWPT chargers are mounted in dedicated areas where the forklift can remain stationary without impeding the execution of other operations. Figure 13 shows an example of dock configuration. The red dot represents the docking node, the big gray area represents the Docking area, whereas the red square represents the transmitting part of an SWPT charger mounted on the dock area.

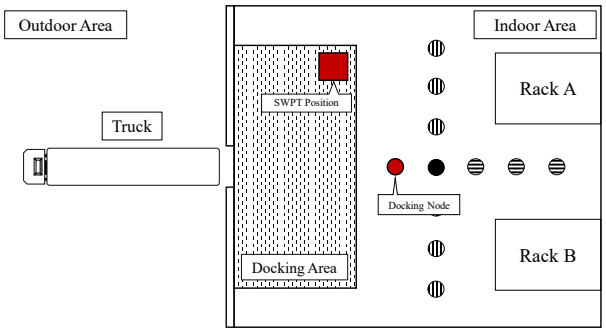

Figure 13 - Warehouse dock schematization (top view). The red square represents the possible position for the static coil, while the red dot represents the Docking Node, the node nearest to the docking area.

4.3.1.2 DWPT modeling

As a transmitting DWPT module is 2.5 m long, and the node spacing in the warehouse is 0.5 m, each transmitting DWPT module is composed of five consecutive nodes. It's convenient distinguishing the five nodes forming a DWPT module to correctly define a set of constraints that make the module physically installable. To this purpose, DWPT Center is defined as the central node of the five consecutive nodes, whereas each of the other four nodes is identified as DWPT Part. Moreover, a DWPT module can be oriented along the x-axis or y-axis.

According to the node category defined earlier, when all the nodes belonging to a DWPT module/section/transmitting section are horizontal or cross nodes, the module is called Horizontal DWPT. When all the nodes belonging to a DWPT module are vertical or cross nodes, the module is called Vertical DWPT. It turns out that a DWPT module can be uniquely identified by the position and orientation of its DWPT Center.

Figure 14 shows an example of a possible DWPT module configuration. Red nodes are DWPT Centers, whereas the blue ones are DWPT Parts. Based on the above definition, it's possible to identify the DWPT sections displayed in Figure 14 as a Vertical DWPT with ID center 22, and a Horizontal DWPT with ID center 12.

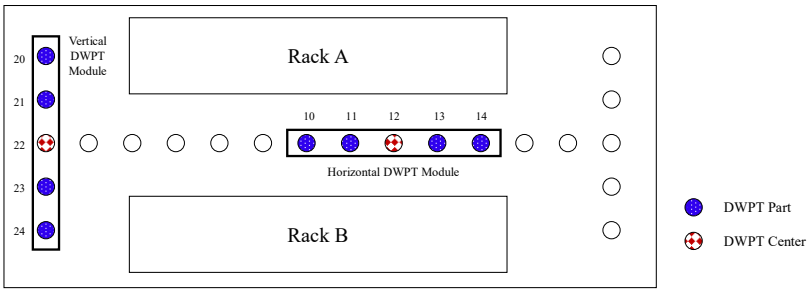

Figure 14 - DWPT configuration with vertical and horizontal DWPT modules, in blue DWPT part node, in red DWPT center node.

3.1.3 Warehouse operations modeling

The two types of operations considered in this work are storing and retrieval operations. An operation starts and ends in the same docking node. Retrieval operations begin with the movement of the unloaded forklift from the loading dock to the retrieval point, i.e., the operational warehousing node (a warehousing node with onf equal to 1). Once arrived on it, the retrieval operation is executed, and the forklift is loaded with the item to be shipped. Finally, the forklift goes back to the loading dock and deposit the item on the truck. Conversely, storage operations begin with the movement of the loaded forklift from the docking node to the operational warehousing node. The item is stored in the warehouse, and then the unloaded forklift returns to the loading dock. The time spent by the forklift to cross a node in loaded and unloaded mode is assumed to be independent of the operation and depending only on the speed of the forklift; these quantities are respectively identified as loaded travel warehousing node time $ltwnt$ and unloaded travel warehousing node time $utwnt$.

The path followed by the forklift during the execution of an operation can be the shortest between the two nodes, or it might be another one according to the warehouse policy. Anyway, neglecting the time difference between loading and unloading the item from the truck, as well as from the storage/retrieval point, from a temporal standpoint, the two types of operations can be treated as equivalents. So, it's possible to define a set of all the operations $\mathcal{O}$ with cardinality $|\mathcal{O}| = O$:

$$\mathcal{O} = \{1,2,\dots,O\} \tag{6}$$

Each operation $k \in \mathcal{O}$ is characterized by the following properties:

- o_k: a sequential integer number starting from 1 representing the operation identifier.
- $odn_k \in \Delta$: the operational docking node, i.e., the dock where the item is loaded or unloaded during the operation.

- $own_k \in \mathcal{N}$: the operational warehousing node, i.e., the node where the item is stored or retrieved during the operation.
- $LWNP_k \subseteq \mathcal{N}$: the loaded warehousing nodes path, i.e., the set of nodes crossed during the path of the forklift in loaded conditions.
- $UWNP_k \subseteq \mathcal{N}$: the unloaded warehousing nodes path, i.e., the set of nodes crossed during the path of the forklift in unloaded conditions.
- $ownt_k$: the operational warehousing node time (in seconds), i.e., the time spent by the forklift in the operational warehousing node to store or retrieve the items.
- $odnt_k$: the operational docking node time (in seconds), i.e., the active time spent by the forklift in the dock to load or unload the item from the truck.
- ot_k: operation time, i.e., the total time of the operation (in seconds), that is the time spent by the forklift to move from the dock to the operational warehousing node and return to the dock, computed as follows:

$$ot_k = ownt_k + odnt_k + ltwnt \cdot |LWNP_k| + utwnt \cdot |UWNP_k| . \quad (7)$$

- $op_k \in \{0,1\}$: operation probability, which depends on the arrivals and retrievals of items in the warehouse.

Once Nodes, Edges, and Operations have been characterized, the next methodological step is the probabilistic assessment of the electric forklift positions in a working shift within the modeled warehouse.

3.3.2 Probabilistic assessment of the forklift positions

The WPT modules are placed along with the most used nodes by the forklifts within the warehouse. In order to do that, the forklift's probability of being at a specific node must be assessed. This can be done by computing the time spent by the forklifts in each node during the execution of the operations. Such data can be collected in different ways, e.g., analytically through the study of the forklift paths if only the orders of the items to store/retrieve are known, numerically by means of a simulation model, or by embedding the forklifts with sensors to directly obtain the time spent in each position. Nevertheless, the methodology is suitable regardless of the system used for data collection activity.

3.3.2.1 Warehousing node probabilities

Assuming there is a set of forklifts $Z = \{1, \dots, F\}$ in the warehouse, for each of them $f \in Z$, it is possible to define a vector of N elements called Warehousing Node Probabilities (WNP_f), a vector containing the probabilities to find a forklift located on warehousing nodes.

$$WNP_f = \left[(wnp_1)_f, \dots, (wnp_i)_f, \dots, (wnp_N)_f\right]^T \quad (8)$$

The probability of having a forklift in a warehousing node can be further divided into three parts. The Operational Warehousing Node Probabilities $OWNP_f$, i.e., the probability of having the forklift performing a storing or retrieval operation in the warehousing node, the Loaded Travel Warehousing Node Probabilities $LTWNP_f$, i.e., the probability of having the forklift moving in loaded conditions across the space covered by the warehousing node without stopping and, finally, the Unloaded Travel Warehousing Node Probabilities $UTWNP_f$ i.e., the probability of having the forklift moving in unloaded conditions across the space covered by the warehousing node without stopping. Thus, WNP_f can be written as the sum of such three terms:

$$WNP_f = OWNP_f + LTWNP_f + UTWNP_f \quad (9)$$

Each element of such vectors can be computed starting from the operation probability (op_k), the operation time $(ot_k)_f$, the operational warehousing node time $(ownt_k)_f$, the loaded travel warehousing node time $(ltwnt_k)_f$, and the unloaded travel warehousing node time $(utwnt_k)_f$, as reported below.

$$(ownp_i)_f = \begin{cases} \sum_{k=1}^{O} \frac{(ownt_k)_f}{(ot_k)_f} op_k, & if\ i = own_k, \\ 0, & otherwise \end{cases} \quad \forall\ i \in \mathcal{N}, f \in Z \quad (10)$$

$$(ltwnp_i)_f = \begin{cases} \sum_{k=1}^{O} \frac{(ltwnt)_f}{(ot_k)_f} op_k, & if\ i \in LWNP_k \\ 0, & otherwise \end{cases} \quad \forall i \in \mathcal{N}, f \in Z \quad (11)$$

$$(utnp_i)_f = \begin{cases} \sum_{k=1}^{O} \frac{(utwnt)_f}{(ot_k)_f} op_k, & if\ i \in UWNP_k \\ 0, & otherwise \end{cases} \quad \forall i \in \mathcal{N}, f \in Z \quad (12)$$

3.3.2.2 Docking Node Probabilities

A vector of D elements called Operational Docking Node Probabilities $(ODNP)_f$ can be defined for each forklift $f \in Z$ as a vector containing the forklift's probability of being located on docking nodes during the operational phase.

$$ODNP_f = \left[(odnp_1)_f, \dots, \left(odnp_j\right)_f, \dots, (odnp_D)_f\right]^T \tag{13}$$

Each element of such vector can be computed starting from the operation probability op_k, the operation time $(ot_k)_f$, and the operational docking node time $(odnt_k)_f$. Mathematically:

$$\left(odnp_j\right)_f = \begin{cases} \sum_{k=1}^{O} \frac{(odnt_k)_f}{(ot_k)_f} op_k, & if\ j = odn_k, \quad \forall\ j \in \Delta, f \\ 0, & otherwise \end{cases} \in Z \tag{14}$$

Moreover, the probability of finding a forklift on a dock in waiting time can be collected in a vector called Waiting Docking Node Probabilities $WDNP_f$. Note that waiting time can be exploited by the forklift to statically recharge on a dock if there is an SWPT charging point on the dock.

3.3.2.3 Forklift's average behavior computation

After having carried out all the previous calculations, the mean behavior of the forklift must be assessed to build the future optimization problem. To this aim, the following average vector is computed.

$$WNP = [wnp_1, \dots, wnp_i, \dots, wnp_N]^T \tag{15}$$

WNP is the mean Warehousing Node Probabilities vector, and its elements are evaluated as average over the values of forklifts.

$$wnp_i = \frac{1}{F} \sum_{f=1}^{F} (wnp_i)_f \qquad \forall i \in \mathcal{N} \tag{16}$$

In the same way, the vectors pertaining to Loaded Travel Warehousing Node Probabilities $LTWNP$, Unloaded Travel Warehousing Node Probabilities $UTWNP$, Operational Warehousing Node Probabilities $OWNP$, Operational Docking Node Probabilities $ODNP$, and Waiting Docking Node Probabilities $WDNP$ are computed as average over the forklifts.

The six computed vectors characterize the mean behavior of the forklifts in the warehouse, and they will be used for the energetic balance described in the upcoming paragraph.

3.3.3 Energetic Analysis

The most important constraint of the methodology is fulfilling the battery State of Charge (SoC) variation of the forklifts in a working shift. So, the optimization algorithm would place the WPT module as the layout that satisfies the SoC variation required by the user, minimizing the cost based on the probabilistic assessment of the average forklift position discussed in the previous section.

Battery SoC, at any instant time, is defined as follows:

$$SoC = \frac{E_{batt}}{E_{batt,max}} \tag{17}$$

E_{batt} is the amount of energy stored in the battery at the considered instant time, whereas $E_{batt,max}$ is the maximum capacity of the battery. It's possible to compute the SoC variation in a working shift ΔSoC_{shift} as the difference between the absorbed energy $E_{IN,shift}$ and the consumed energy $E_{OUT,shift}$ in a working shift divided by the maximum capacity of the battery.

$$\Delta SoC_{shift} = \frac{\Delta E_{shift}}{Ebatt,max} = \frac{E_{IN,shift} - E_{OUT,shift}}{E_{batt,max}} \tag{18}$$

The optimization algorithm will have to fulfill the following condition:

$$\Delta SoC_{shift} \geq \Delta SoC_{shift,desired} \tag{19}$$

3.3.3.1 Absorbed Energy

During a working shift, the forklifts can be recharged in three different ways: (i) inside the warehouse on DWPT modules, (ii) during the waiting time on docks

if the docks have an SWPT charging point, and, finally, (iii) during the break time if the forklifts are placed on SWPT charger in docks.

The absorbed energy taken directly from the DWPT module can be computed as follows:

$$E_{IN,dyn} = \eta_{dyn} \cdot P_{nom} \cdot ST_{eff} \cdot \sum_{i=1}^{N} (wnp_i * x_i) \quad (20)$$

Where η_{dyn} is the efficiency of the DWPT system, P_{nom} is the nominal DWPT system charging power, ST_{eff} is the effective working shift duration, x_i is a binary variable equal to 1 when a DWPT module is placed on the i-th node, 0 otherwise. x_i represents a variable to be optimized during the optimization process.

The absorbed energy during the waiting time in docks $E_{IN,static,waiting}$ in a working shift is computed similarly.

$$E_{IN,static,waiting} = \eta_{static} \cdot P_{nom} \cdot ST_{eff} \cdot \sum_{j=1}^{D} (wdnp_j \cdot xd_j) \quad (21)$$

Where η_{static} is the efficiency of the SWPT system, ST_{eff} is the effective working shift time, whereas xd_j is a flag equal to 1 when an SWPT system is placed on j-th dock, 0 otherwise. Note that xd_j is an optimization variable, too.

The absorbed energy during the breaks $E_{IN,static,breaks}$ can be computed as follows:

$$E_{IN,static,breaks} = k_{breaks} \cdot \eta_{static} \cdot P_{nom} \cdot BT \quad (22)$$

Where k_{breaks} accounts for the effective proportion of forklifts that can be recharged during the breaks, and BT is the breaks time duration in a working shift.

Finally, the three contributions are summed up:

$$E_{IN,shift} = E_{IN,dyn} + E_{IN,static,waiting} + E_{IN,static,breaks} \quad (23)$$

3.3.3.2 Consumed Energy

In a working shift, four sources of energy consumption are modeled in this work; (i) the execution of an operation in the dock, (ii) the execution of an operation in the warehousing node, (iii) the forklift motion within the warehouse in loaded conditions, and (iv) the forklift motion within the warehouse in unloaded conditions.

The energy lost during the loading/unloading phase in docks ($E_{OUT,odn}$) can be computed in the following way.

$$E_{OUT,odn} = P_{cons,odn} \cdot ST_{eff} \cdot \sum_{j=1}^{D} odnp_j \tag{24}$$

$P_{cons,odn}$ is the electrical power required for the execution of an operation in dock.

In an analogous way can be assessed the energy spent during the forklift motion in loaded conditions $E_{OUT,ltwn}$ and unloaded conditions $E_{OUT,utwn}$, as well as the energy spent by the forklift during the execution of an operation in warehousing nodes $E_{OUT,own}$.

$$E_{OUT,own} = P_{cons,own} \cdot ST_{eff} \cdot \sum_{i=1}^{N} ownp_i \tag{25}$$

$$E_{OUT,ltwn} = P_{cons,ltwn} \cdot ST_{eff} \cdot \sum_{i=1}^{N} ltwnp_i \tag{26}$$

$$E_{OUT,utwn} = P_{cons,utwn} \cdot ST_{eff} \cdot \sum_{i=1}^{N} utwnp_i \tag{27}$$

$P_{cons,own}$, $P_{cons,ltwn}$, and $P_{cons,utwn}$ are respectively the electric power needed to carry out an operation in warehousing nodes, the electric power needed by the forklift to travel within the warehousing nodes in loaded conditions, and the electric power needed by the unloaded forklift to travel within the warehousing nodes.

As for the acquired energy, all the contributions are summed up.

$$E_{OUT,shift} = E_{OUT,odn} + E_{OUT,own} + E_{OUT,ltwn} + E_{OUT,utwn} \quad (28)$$

3.3.4 Optimization Problem

The objective of the optimization problem is to define a mathematical model to be optimized based on the definitions discussed in the previous section. The final goal is to find a physically installable placement of the WPT systems layout to fulfill the energetic constraint required by the customer to minimize the cost of the system. The problem is modeled as an Integer Linear Programming (ILP) problem in which a linear function must be minimized by fulfilling a set of constraints made of linear equalities and inequalities.

Because the working area is discretized in N warehousing nodes and D docking nodes, the following set of optimization variables θ can be defined.

$$\theta \in \mathbb{R}^{5N+D} : \theta = \{\theta_1, \dots, \theta_{5N+D}\} \quad (29)$$

Each optimization variable is a binary variable that can be equal to 0 or 1, and because of this, the problem is defined as Integer Linear Programming (ILP). The set θ of optimization variables can be split into six subsets and arranged in the following column vector.

$$\theta = \begin{bmatrix} x_1, \dots, x_N, h_1, \dots, h_{N,}, hc_1, \dots, hc_N, v_1, \dots, v_N, \\ vc_1, \dots, vc_N, xd_1, \dots, xd_D \end{bmatrix}^T \quad (30)$$

Each subset variable has the following meaning:

- x_i is 1 if a DWPT module is placed on node i, otherwise is 0.
- h_i is 1 if a Horizontal DWPT Part is placed on node i, otherwise is 0.
- hc_i is 1 if a Horizontal DWPT Center is placed on node i, otherwise is 0.
- v_i is 1 if a Vertical DWPT Part is placed on node i, otherwise is 0.
- vc_i is 1 if a Vertical DWPT Center is placed on node i, otherwise is 0.
- xd_j is 1 if an SWPT module is placed on dock j, otherwise is 0.

Note that if one of the optimization variables h_i, hc_i, v_i, vc_i is 1, so x_i must be 1 too.

The cost function of the optimization problem is a linear function representing the overall cost of the WPTs system; it's defined as follows.

$$f(\theta) = c^T\theta \tag{31}$$

c is the cost vector representing the cost of each optimization variable. It can be arranged as follows.

$$c = [c_1, \dots, c_i, \dots, c_{5N+D}]^T \tag{32}$$

With:

$$c_i = c_{dyn} \quad i \in \mathcal{N} : 1 \leq i \leq N \tag{32a}$$

$$c_i = 0 \quad i \in \mathcal{N} : N+1 \leq i \leq 5N \tag{32b}$$

$$c_i = c_{static} \quad i \in \mathcal{N} : 5N+1 \leq i \leq 5N+D \tag{32c}$$

c_{dyn} is the cost of a DWPT module, c_{static} is the cost of an SWPT module.

The final formulation of the cost function, considering only the non-null costs, is reported below.

$$f(\theta) = \sum_{i=1}^{N}(c_{dyn} \cdot x_i) + \sum_{j=1}^{D}(c_{static} \cdot xd_j) \tag{33}$$

The model is subjected to a set of constraints, many of which are topological.

If a node is a Horizontal node, then it can just be a Horizontal Part or Horizontal Center of a DWPT module (38a). The same happens for what concerns the vertical direction modeled (38b), whereas if a node is a cross node, both directions are allowed, and that node could be a Horizontal Part, or Horizontal Center, or Vertical Part, or Vertical Center (38c).

If a node belongs to the 4th category, no DWPT module can be installed on that node (38d).

Relating to corridors, in any Horizontal corridor, the sum of all the Horizontal DWPT Parts must be 4 times the sum of all the Horizontal DWPT Centers (38e). The same condition must be applied for Vertical corridors, too (38f).

Additionally, some constraints must be described to force the creation of the DWPT module as a strip of five consecutive nodes. To this aim, we define the

distance matrix of the node of the graph as $C = (c_{i_1 i_2})$, C is a positive and symmetric $N \times N$ matrix. Each value represents the minimum distance in steps between the two nodes i_1 and i_2, and all the entities on the main diagonal are equal to 0. For each $\bar{\imath} \in \mathcal{N}$ it is possible to define four different sets of nodes: *Radius-2 Horizontal Neighbours* of node $\bar{\imath}$ ($R_{\bar{\imath}}^{2h}$), *Radius-2 Vertical Neighbours* of node $\bar{\imath}$ ($R_{\bar{\imath}}^{2v}$), *Distance-5 Horizontal Neighbours* of node $\bar{\imath}$ ($L_{\bar{\imath}}^{5h}$), and *Distance-5 Vertical Neighbourhood* of node $\bar{\imath}$ ($L_{\bar{\imath}}^{5v}$)

$$R_{\bar{\imath}}^{2h} = \{\forall\, i \in \mathcal{N}: i \neq \bar{\imath}, horoc_i \neq 0,\ horoc_{\bar{\imath}} = horoc_i, c_{\bar{\imath}i} \leq 2\} \tag{34}$$

$$R_{\bar{\imath}}^{2v} = \{\forall\, i \in \mathcal{N}: i \neq \bar{\imath}, verc_i \neq 0,\ verc_{\bar{\imath}} = verc_i, c_{\bar{\imath}i} \leq 2\} \tag{35}$$

$$L_{\bar{\imath}}^{5h} = \{\forall\, i \in \mathcal{N}: i \neq \bar{\imath}, horoc_i \neq 0,\ horoc_{\bar{\imath}} = horoc_i, c_{\bar{\imath}i} = 5\} \tag{36}$$

$$L_{\bar{\imath}}^{5v} = \{\forall\, i \in \mathcal{N}: i \neq \bar{\imath}, verc_i \neq 0,\ verc_{\bar{\imath}} = verc_i, c_{\bar{\imath}i} = 5\} \tag{37}$$

Following such definitions, when a node is a *Horizontal DWPT Center*, it must have four *Radius-2 Horizontal Neighbours*, and all of them must be *Horizontal DWPT Parts*, as well as when a node is a *Vertical DWPT Center*, it must have four *Radius-2 Vertical Neighbours*, all of them must be *Vertical DWPT Parts*. These constraints are respectively represented in equations 38g) and 38h). Equations 38i) and 38j) force each DWPT part to have precisely one DWPT Center among the nodes belonging to its *Radius-2 Neighbourhood*. The DWPT module length for horizontal DWPTs is constrained in equations 38k) and 38l), whereas the DWPT module length for Vertical DWPTs is constrained in equations 38m) and 38n). In some docks, it is not possible to install any SWPT module. This is defined in 38o). The energetic constraint required by the customer is modeled in 38p). Finally, the constraint pertaining to the binary integer values of the optimization variables is defined in the last constraint 38q).

$$3x_i - 3h_i - 3hc_i - v_i - vc_i = 0 \qquad \forall\, i \in \mathcal{N}: cat_i = 1 \tag{38a}$$

$$3x_i - h_i - hc_i - 3v_i - 3vc_i = 0 \qquad \forall\, i \in \mathcal{N}: cat_i = 2 \tag{38b}$$

$$x_i - h_i - hc_i - v_i - vc_i = 0 \qquad \forall\, i \in \mathcal{N}: cat_i = 3 \tag{38c}$$

$$x_i + h_i + hc_i + v_i + vc_i = 0 \qquad \forall\, i \in \mathcal{N}: cat_i = 4 \tag{38d}$$

$$\sum_{i=1}^{N}(h_i) - 4\sum_{i=1}^{N}(hc_i) = 0 \qquad \forall\, i \in \mathcal{N} : horc_i = h, \quad h \in \mathcal{H} \tag{38e}$$

$$\sum_{i=1}^{N}(v_i) - 4\sum_{i=1}^{N}(vc_i) = 0 \qquad \forall\, i \in \mathcal{N} : verc_i = v, \quad v \in \mathcal{V} \tag{38f}$$

$$4hc_i - \sum_{z} h_z \leq 0 \qquad \forall\, i \in \mathcal{N}, \forall\, z \in R_i^{2h} : \left|R_i^{2h}\right| = 4 \tag{38g}$$

$$4vc_i - \sum_{z} v_z \leq 0 \qquad \forall\, i \in \mathcal{N}, \forall\, z \in R_i^{2v} : \left|R_i^{2v}\right| = 4 \tag{38h}$$

$$h_i - \sum_{z} hc_z \leq 0 \qquad \forall\, i \in \mathcal{N}, \forall\, z \in R_i^{2h} : cat_i \in \{1,3\} \tag{38i}$$

$$v_i - \sum_{z} vc_z \leq 0 \qquad \forall\, i \in \mathcal{N}, \forall\, z \in R_i^{2v} : cat_i \in \{2,3\} \tag{38j}$$

$$hc_i - \sum_{z} hc_z \leq 0 \qquad \forall\, i \in \mathcal{N}, \forall\, j \in L_i^{5h} : cat_i \in \{1,3\}, \; L_i^{5h} \neq \emptyset \tag{38k}$$

$$hc_i = 0 \qquad \forall\, i \in \mathcal{N} : cat_i \in \{1,3\}, \; L_i^{5h} = \emptyset \tag{38l}$$

$$vc_i - \sum_{z} vc_z \leq 0 \qquad \forall\, i \in \mathcal{N}, \forall\, j \in L_i^{5v} : cat_i \in \{2,3\}, \; L_i^{5v} \neq \emptyset \tag{38m}$$

$$vc_i = 0 \qquad \forall\, i \in \mathcal{N} : cat_i \in \{2,3\}, \; L_i^{5v} = \emptyset \tag{38n}$$

$$xd_j = 0 \qquad \forall j \in \Delta : dwf_j = 0 \tag{38o}$$

$$E_{IN,SHIFT} \geq E_{OUT,SHIFT} \tag{38p}$$

$$x_i, h_i, hc_i, v_i, vc_i, xd_j \in \{0,1\}\ \forall i, \forall j \tag{38q}$$

The optimal solution corresponds to the overall cost of the whole WPT system.

$$f_{MIN} = \min\left(\sum_i c_d x_i + \sum_j c_s x d_j\right) = cost_{tot} \tag{39}$$

$$\sum_i c_d x_i = cost_{dyn} \tag{39a}$$

$$\sum_j c_s x d_j = cost_{stat} \tag{39b}$$

Such an optimization model has been implemented in Matlab (https://mathworks.com/)

3.4 Case Study

The proposed approach was applied in an industrial case study to optimize the installation of a WPT system (SWPT + DWPT systems) in the full-scale dimension warehouse used as a distribution center by a tire manufacturing company. The case study is appropriately modified to protect the company's privacy; nevertheless, the study does not lose its significance.

3.4.1 Warehouse Description

The warehouse object of this work is displayed in Figure 15. It has a rectangular shape: the long side measures 245 m, and the short one is 183 m. It presents 16 docks (they are evidenced with a capital D in the figure), 8 on each of the long sides. The docks are directly connected to the outside, and each one can accommodate a truck waiting to be loaded. There are two different forklift parking spaces on the warehouse's left side (marked with a capital P). The building is divided into two zones separated by a central wall. It is possible to change the zone using one of the four gates. These wall passages are placed at the bottom, one at the top, and two in the middle of the warehouse (in the figure, they are highlighted with two opposing arrows). The warehouse has 94 racks 60 m long, 8.4 m tall, and depth between 1.5 m and 9 m. In the figure, racks are represented by white boxes. Each rack has 6 levels and 24 bays. The unit load (UL) is composed of eight pairs of tires fastened by belts and placed on a pallet. The maximum volume of each UL is 1.728 m^3, a cube with each edge 1.2 m long. The warehouse can store 41.184 ULs.

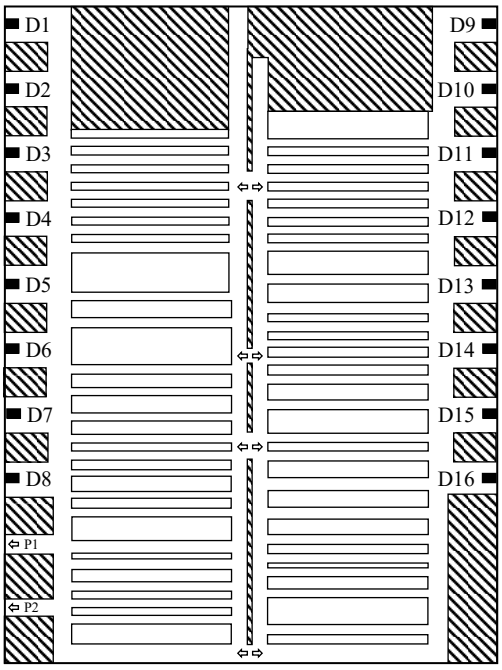

Figure 15 - Warehouse Layout.

3.4.2 Experimental Tests of Forklift Consumption

The electric forklift taken as a reference is the Toyota Traigo 48 [79], and all parameters are based on this model. These forklifts have a load capacity of 1600 kg, and their weight (battery included) is equal to 3002 kg. According to the technical specifications, Toyota Traigo mounts two traction motors with nominal power equal to 6 kW each and a lifting motor with nominal power equal to 11 kW. Each vehicle mounts a 48V battery with a capacity of 30 kWh.

According to the VDI (Verband Deutscher Ingenieure) cycle [80], the average power is 4.3 kWh/h. However, this cycle is particularly energy-intensive; it involves a series of movements and lifts to obtain a power parameter that can indicate an average energy consumption. This average consumption is obtained by simulating a too-stressful use that, in practice, is never found. For this reason, a battery charge cycle analysis is performed; real charge and discharge data of the batteries have been collected on two forklifts in a real operating environment

through the control unit of the forklift instrumentation. The studied forklifts were equipped with a 48 V hermetic lead-acid battery consisting of 24 cells with a capacity of 30 kWh. The obtained results have been averaged and reported in Table 1.

Table 1 - Experimental Results of Forklift Consumption.

	Value
Average Consumed Energy per Cycle	26.17 kWh
Maximum Consumed Energy	52.15 kWh
Minimum Consumed Energy	3.23 kWh
Average Experimental Total Power	2.82 kWh/h
Average Experimental Traction Power	2.48 kWh/h
VDI Cycle Power	4.30 kWh/h

These vehicles have a maximum speed of 16 km/h. However, 5 km/h is the most common speed limit in an indoor warehouse where pedestrians are present. The vehicle's lift speed is 0.50 m/s.

3.4.3 WPT Parameters

In this section, all the WPT systems parameters used in the case study are described. Such data is provided by the Italian company Enermove srl. Figure 16 shows the forklift analyzed in this study equipped with a WPT system developed by Enermove. The SWPT module is shown in the figure, resulting in a square base with a size 45 cm x 45 cm at the same floor level.

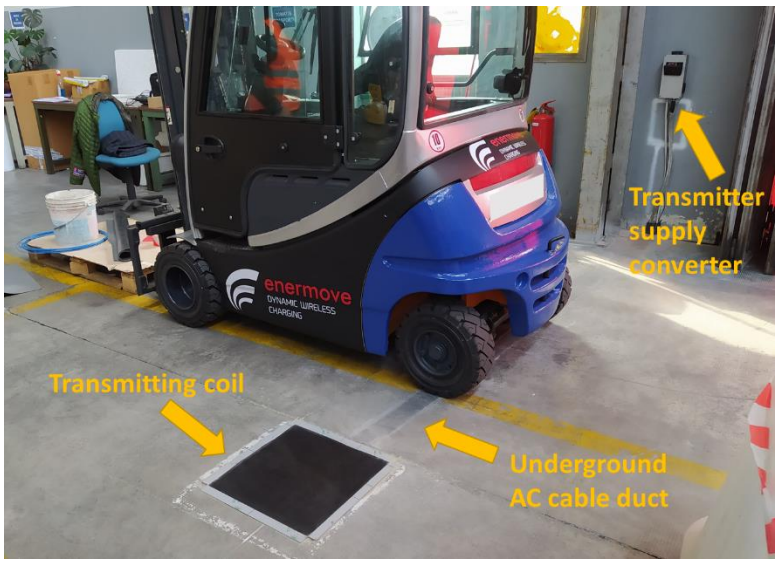

Figure 16 - Forklift in an industrial environment whit a detail of an SWPT charging point.

The transmitting pad of the DWPT system has a length of 120 cm and a width of 20 cm. The forklift operates with both static and dynamic WPT systems through the same receiver, having a square shape with each side 35 cm wide, and it is mounted underneath the vehicle chassis. In the analyzed case study, each WTP module (both dynamic and static) has a rated charging power equal to 3.5 kW. The efficiency of the DWPT transmission is around 85%, while SWPT is about 90%. The deployment of dynamic transmitting coils requires a minor cut on the concrete superficial layer to create a slot to place the coil. Then, the coil is molded in a specific resin and subsequently covered by concrete or a layer of resin for industrial pavements. Hence, no further maintenance operations are required on the coils as they remain embedded in the pavement during the whole service life of the WPT system. On the other side, a static transmitter may also be mounted without creating any slot in the concrete in the so-called above-ground installation mode in which the receiver coil assembly is directly bolted to the pavement.

As the DC/AC converter can simultaneously manage two transmitting coils mounted sequentially and adjacent to each other, a length of 2.5 m has been chosen for the DWPT module. A medium gap of 0.1 m has been considered to allow the correct assembly of the components on the floor. Note that the dimension of the transmitters listed at the beginning of this section, the DWPT module length, can vary slightly according to the specific application. The cost of each DWPT transmitting module is 2500 €. An SWPT transmitter costs 3000 €, while the cost of the receiver to be mounted on the forklift is 1500 €.

Table 2 - WPT systems' parameters.

Parameter	Value
DWPT module dimension	2.50 m x 0.20 m
DWPT module power (P_{nom})	3.5 kW
DWPT efficiency (η_{dyn})	0.85
DWPT module cost (c_{dyn})	2500 €
SWPT module dimension	0.45 m x 0.45 m
SWPT module power (P_{nom})	3.5 kW
SWPT efficiency (η_{stat})	0.90
SWPT module cost (c_{static})	3000 €

3.4.4 Model application

In order to evaluate the model in different warehouse conditions, a discrete event simulation model of the full-scale dimension warehouse was developed by using the Flexsim software (https://www.flexsim.com). The whole warehouse is modeled using 11094 nodes (11078 warehousing nodes and 16 docking nodes) and 11264 edges. In Figure 17, we present the build warehouse model during a simulation run.

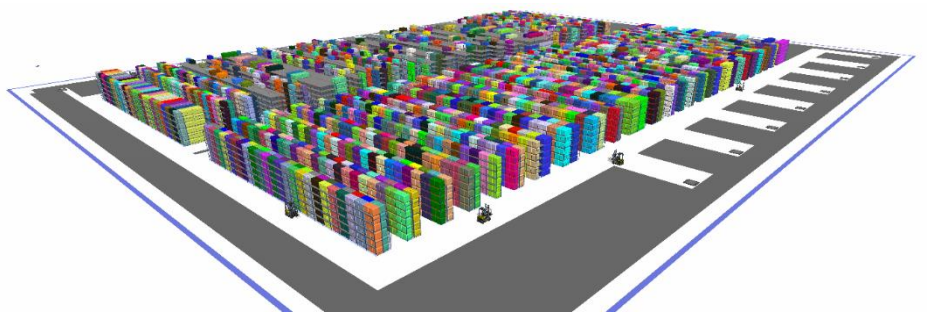

Figure 17 - Warehouse Simulation Model

In order to simulate the warehouse, we have had to specify some logic and behaviors. Moreover, we have based on some previously described assumptions. In this paragraph, we report all the parameters and the logic used to model the warehouse.

Each replication represents a stand-alone shift from 8 A.M to 4 P.M., at the beginning of the shift, the total units stored are 30.888 (75% of the full capacity). We decided to simulate only retrieval tasks performed by 4 forklifts. Orders arrive following an exponential distribution with an expected value of $1/\lambda$. When an order comes, if there is space, a dock is reserved. Otherwise, the order waits until one of the sixteen docks is back available. When an order enters the port, the forklift is called back to the dock to receive the details. Forklifts retrieve the items in the warehouse according to a minimum travel distance law. Each order is composed of a single homogeneous unit load. Tasks are managed according to a FIFO rule.

Loading and unloading procedure time follows a log-normal distribution with an expected value equal to 20 s and a variance equal to 16 s^2. The vehicles move in straight lines and 90° curves; diagonal movements are not allowed. This behavior is in line with the traffic rules of the existing warehouses and the general safety requirements. A forklift moves from point A to point B via the shortest path in each task. The shortest path is computed using the A* algorithm [81]. We have modeled a forklift driver break behavior. On average, the drivers take a break every 90 minutes. When a task is finished, the driver stops the forklift near the dock if 90 minutes are passed from the previous break. The pause time follows an exponential distribution with an expected value equal to 15 minutes. We let the possibility of skipping breaks. If the driver is performing a particularly long task and the break time has already passed by several minutes at the end of this task, the driver will continue working. This behavior makes the model more realistic and less mechanistic.

From the energy point of view, we based the energy consumption on the Average Experimental Total Power (2.82 kWh/h) and the Average Experimental Traction Power (2.48 kWh/h) and the VDI Cycle Power (4.30 kWh/h) described previously. In order to be as conservative as possible, we decided to use a power equal to 4.30 kWh/h as the average power travel loaded ($P_{cons,ltwn}$). In order to figure the energy consumption of each shift, we need to find the three missing powers: (i) average power travel unloaded ($P_{cons,utwn}$), (ii) average power for warehouse operations ($P_{cons,own}$), and (iii) average for dock operations ($P_{cons,odn}$). It has been assumed that an equal power value for $P_{cons,own}$ and $P_{cons,odn}$ since the forklift operations are the same, it only changes the area they are completed. Then, $P_{cons,utwn}$ and $P_{cons,own}$ have been computed by solving the following equations:

$$\begin{cases} \frac{UTWNP}{LTWNP + UTWNP} P_{cons,utwn} + \frac{LTWNP}{LTWNP + UTWNP} P_{cons,ltwn} = 2.48 \text{ kWh/h} \\ \frac{UTWNP}{WNP + ODNP} P_{cons,utwn} + \frac{LTWNP}{WNP + ODNP} P_{cons,ltwn} + \frac{OWNP}{WNP + ODNP} P_{cons,own} + \\ \frac{ODNP}{WNP + ODNP} P_{cons,odn} = 2.82 \text{ kWh/h} \end{cases} \quad (40)$$

The main warehouse parameters used in the simulation model are described in Table 3, while Table 4 shows the forklift parameters.

Table 3 - Warehouse Parameters

Parameter	Value
Warehouse Dimensions	240 m – 183 m
Total Unit Load Capacity	41184
Space Utilization	75%
Standard Unit Load Volume	1.728 m^3

Table 4 - Forklift Parameters

Parameter	Value
Max Speed	5 km/h
Lift Max Speed	0.5 m/s
$P_{cons,ltwn}$	4.30 kWh/h
$P_{cons,utwn}$	1.23 kWh/h
$P_{cons,own}$	3.92 kWh/h
$P_{cons,odn}$	3.92 kWh/h
Battery Capacity	30 kWh

In order to assess the methodology and its robustness in different operating conditions of the warehouse, we define two distinct scenarios (A and B), depending on the order interarrival rate of orders and the storage logic of SKUs in the warehouse. Scenario A has a high interarrival rate, while scenario B has a low interarrival rate. In scenario A, items are placed randomly with three degrees of freedom, while in scenario B, the degrees of freedom are only two: objects in the same bay must be homogeneous. A scheme of these two logics is represented in Figure 18. Having three degrees of freedom allows the management of more SKU types than the logic with only two degrees of freedom since, in the same space, it is possible to store a more significant number of unique SKUs. So, another difference between scenarios A and B is the number of unique SKUs stored.

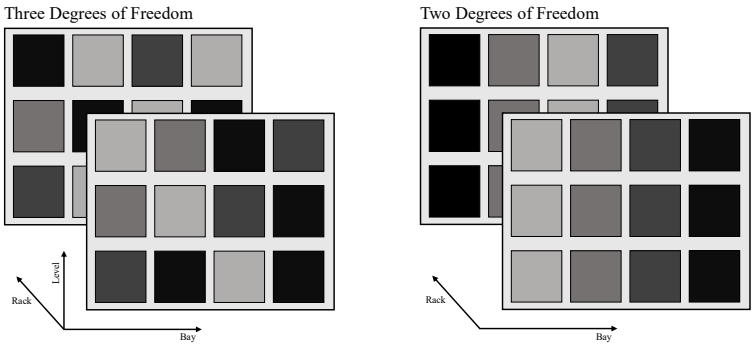

Figure 18 – The two warehouse storage logics

An outline of the two scenarios is reported in Table 5.

Table 5 - Explored Scenarios

Parameter	**Scenario A**	**Scenario B**
Interarrival (1/λ)	70 s	10 s
SKU number	500	100
Storage DoF	3	2

The simulation output is a warehouse heatmap: we have simulated positioning sensors that update the forklift positions every 0.25s. On each update, sensors record the forklift ID, its x and y position in the warehouse, the state in which the forklift is (idle, travel empty, loading, travel loaded, unloading, and on break), and the total travel distance from the beginning of the simulation.

For each analyzed scenario, 60 simulations were run: 30 of them were used to assess the probabilities of the forklift positions to feed the optimizer, while the other 30 simulations were used to validate the optimizer results, keeping track of the state of charge of the forklifts' battery.

3.5 Results and Discussion

This section presents the work results, i.e., the optimal WPT layout with the associated cost and the state of charge verification of the forklifts. In order to achieve the optimal solution, we use the Matlab function *intlinprog*. The results have been obtained with a computer HP 290 G4 Microtower, with CPU intel core

i7-10700 2.90 GHz and RAM 64 GB. The average time required by the computer to generate the entire graph and build the constraints was approximately 4 hours and 15 minutes. The algorithm managed to find the optimal solutions in about 5 minutes and 26 seconds

Section 5.1 reports the results obtained by the optimizer. As previously described, the optimizer needs as input five different elements. (i) The discretized warehouse, an un-oriented graph composed of N node, E arcs, and D docking node. (ii) The four vectors defining the forklifts' status: $OWNP_f$ defining the probability of having the forklift operating a specific warehousing node, $LTWNP_f$ representing the probability of having a loaded forklift moving across the space covered by the warehousing node, $UTWNP_f$ i.e., the probability of having the forklift moving unloaded across the space covered by the warehousing, and finally, the vector $ODNP_f$ defining the probability of having the forklift operating in a particular dock. To estimate these four vectors, we use the first set of 30 simulations, (iii) The system specification: the DWPT and SWPT model dimension, power efficiency and cost. (iv) The forklift consumption behavior, in particular, the average power needed to move the forklift loaded ($P_{cons,ltwn}$), unloaded ($P_{cons,ltwn}$), and to handle UL in the warehouse($P_{cons,own}$) and the docking ($P_{cons,odn}$) and finally (v) the energetic constraint. In our case study, we have imposed a change in the battery state of charge equal to 0 during a shift ($E_{IN,SHIFT} \geq E_{OUT,SHIFT}$). The output of the optimizer is the decision variables x_i and xd_j indicating if the DWPT or SWPT systems are present in the i-th node and j-th docking node.

Section 5.2 presents the validation of the obtained solution. We validate our solutions by analyzing the second set of 30 simulations, each lasting eight hours. We give as input for the simulator the obtained optimal distribution of DWPT and SWPT, and we compute the state of charge time series of the 4 forklifts present in each simulation. The model is validated if, on average, the consumption of the forklifts is equal to the energy recharged. Furthermore, knowing the trend of all 120 SoC curves (30 simulations for 4 forklifts) allows us to evaluate the robustness of the obtained solution. If the SoC drops to zero, even a single time for a shift, the obtained solution fails. As previously mentioned, the analysis is performed on two separate scenarios.

3.5.1 WPT Layout and Cost

For the analyzed scenarios in this work, the optimizer has computed the whole WPT system layouts schematically represented in Figure 19. It is possible to observe, for both scenarios, that it is placed the SWPT charger in each docking area. Moreover, the figure displays that DWPT modules are mainly located in the two lateral corridors and at the end part of the aisles between racks. This behavior is due

to using the shortest path logic assumed by forklifts in the simulation; the vehicles transit mainly near the docking area and the adjacent area.

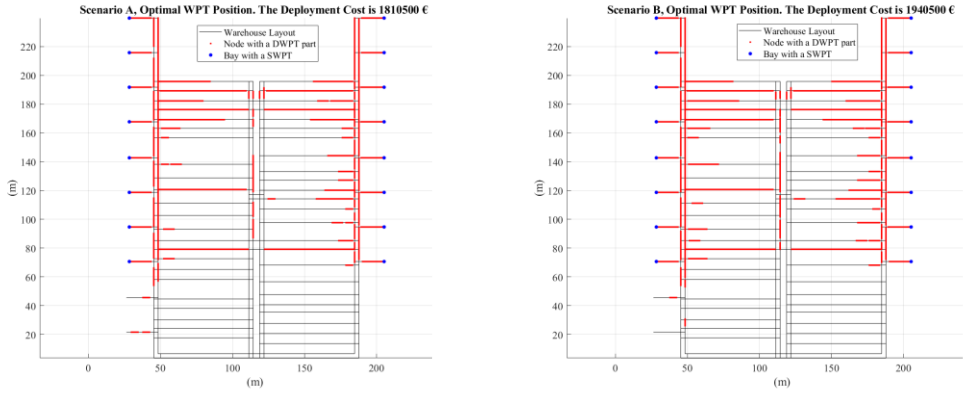

Figure 19 - Optimal WPT Layout, Scenario A (1/λ = 70 s) on the left, Scenario B (1/λ = 10 s) on the right.

Notably, for what concerns scenario A, 705 DWPT modules have been placed inside the warehouse, corresponding to a total length of 1762.5 m and associated cost of 1762500 €, while 16 SWPT chargers are needed in docking areas with a cost of 48000 €. Regarding scenario B, 757 DWPT modules have been calculated by the optimizer, corresponding to a total length of about 1892.5 m and an associated cost of 1892500 €, while 16 SWPT chargers in docking areas and a cost of 48000 €. We analyzed two extreme scenarios where the order frequency between scenarios A and B increased seven times. Despite this radical difference, the final result in terms of cost differs by less than 10% (7.18%). This result shows the remarkable robustness of the obtained solution. If the warehouse has an extreme variable demand with interarrival of orders very different every day, there is a shallow risk of having an insufficient WPT number. Table 6 - Optimal Results summarizes the achieved results.

Table 6 - Optimal Results

Parameter	Scenario A	Scenario B
Number of DWPT Modules	705	757
Number of SWPT Chargers	16	16
Length of DWPT System	1762.5 m	1892.5 m

Cost of DWPT System	1762500 €	1892500 €
Cost of SWPT System Cost	48000 €	48000 €

Concerning the case study analyzed in this work, the methodology developed and the results obtained lead to consider the use of WPT charging systems as very promising. Compared to the current charging procedure used (battery swap and fast charging), the wireless method has numerous advantages over its operational life cycle, despite a higher initial investment cost. In particular, both battery swap and fast charging require the use of one or more operators who have to deal with a non-added value activity for a considerable time. In the case of battery swap, there is also a significant safety concern in battery connection, disconnection, and handling procedures. Furthermore, both traditional systems also require considerable investment. Fast charging needs installing a higher-powered electrical system and a series of fast charger points. Moreover, the utilization of forklifts will be lower, which means that a more significant number of forklifts will be needed. Finally, with regard to the battery swap, a considerable investment is the set of spare batteries to be purchased, stored, and managed. A complete economic comparison between the WPT charging system and traditional ones will be the object of future studies.

3.5.2 State of Charge Verification

Once the optimal distribution of SWPT and DWPT modules was obtained, we analyzed the outputs of 30 simulations for each simulated scenario for a total of 60 simulations. The aim is to monitor the evolution of the SoC variation for each forklift and check if the methodology proposed in this work is effective. Each scenario has been averaged on its 30 working shifts to track the forklifts' mean behavior. The results are shown in Figure 20 and Figure 21, respectively, for Scenarios A and B. On average, all forklifts have an SoC variation within ± 0.5 %, which can be considered a satisfactory result. Moreover, almost all forklifts are generally characterized by charging spikes, this behavior is due to driver breaks.

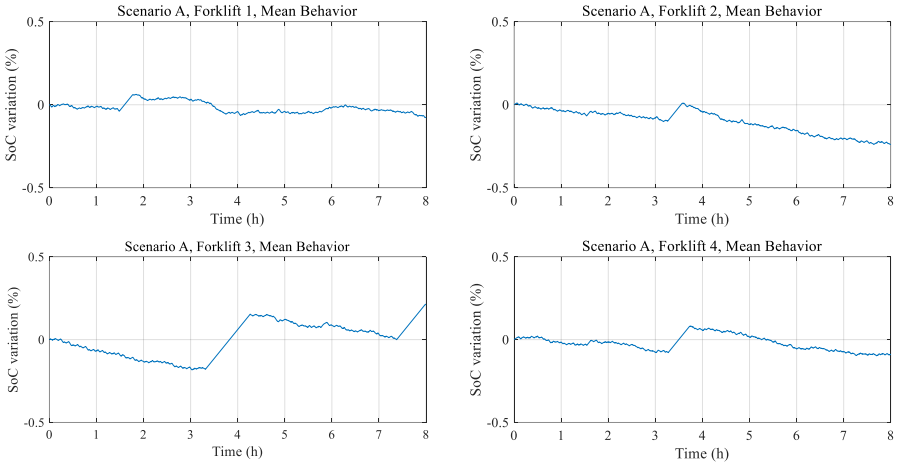

Figure 20 - SoC variation in the average working shift for Scenario A

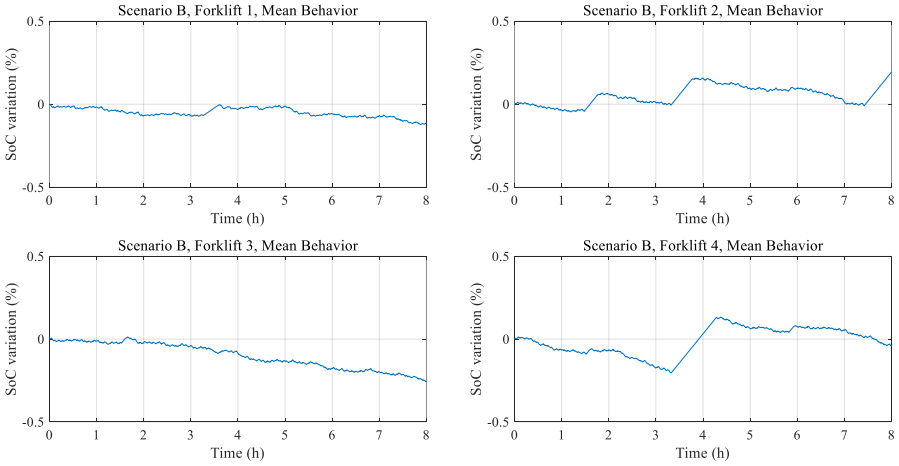

Figure 21 - SoC variation in the average working shift for Scenario B

Analyzing the 120 forklifts' SoC, we noticed that the battery never dropped to zero. Moreover, Table 7 summarizes the maximum and minimum SoC variation detected for each scenario. As it's possible to observe, the proposed methodology guarantees a constant availability of electric vehicles. Indeed, in the worst case, the minimum SoC variation is –15.86%, and, assuming an initial reference SoC of about 50%, it led to a residual SoC of the forklift above 30%. This behavior is highly reassuring; the most extreme cases are far above a level of risk, so the possibility of forklifts ending up mid-shift with a dead battery is very low, considering the positioning of the coils obtained from the optimizer.

Table 7 - Maximum and minimum SoC variation detected for each scenario

	Scenario A	**Scenario B**
Max	+ 18.63 %	+ 22.98 %
Min	- 11.95 %	- 15.86%

Since the analyzed warehouse is very complex and has a considerable dimension, the obtained results reveal an excellent performance of the proposed methodology. In smaller warehouses, the difference between the behavior of the single forklift and the mean behavior of the forklifts is likely limited, and so the current methodology is expected to be reliable also in a warehouse with reduced size.

3.6 Conclusions and Future Improvements

This work proposes a design methodology for the computation of the optimal static and dynamic WPT systems layout based on the usage map of the electric vehicles within the working area. The procedure has been virtually applied to a case study involving a real warehouse layout, real electric forklifts data, as well as real static and dynamic WPT systems data. The results show the technical feasibility of such battery recharge technology by ensuring, on average, a state of charge of the forklifts is approximately constant. This work also gives an indication of the involved costs for the adoption of such technology in an industrial context and can constitute a reference study for future research in this field. After the current study about the performance of the system, the proposed work could be developed through several subsequent research projects. On the one hand, the authors will investigate the affordability of such technology in industrial contexts by carrying out an economic comparison with other battery recharging solutions, such as battery swapping systems and fast recharging systems. On the other hand, the application of the DWPT system has excellent potential in AGV applications since AGVs need fewer breaks than forklifts. It is possible to test if such a system can work continuously without stopping for recharges.

However, the proposed model can be further improved through different approaches. Firstly, as addressed above, the used model can only handle warehouses with orthogonal aisles. An improvement would be made by removing this constraint, although most warehouses have a plant layout with vertical and horizontal corridors [82]. A second improvement would be to parameterize the size of the WPT module and the edge length. These values are currently fixed under certain conditions (2.5 m for the DWPT module and 0.5 m for the edge length), and it is not straightforward to change them. A second future improvement of the

presented work could be to analyze how the intermediate variables impact the final result, i.e., what are those variables between order arrival frequency, power and efficiency of the WPT system, warehouse storage logic etc. that most impact the distribution of coils and thus the total cost of the system. Finally, the last improvement would be to include the number of connected components in the cost function, e.g., by using the zeroth number of Betti in the solution graph. Keeping track of the gaps between components is extremely important, as digs need to be made on the floor. It would be more convenient and energy-efficient to place the system as contiguous as possible. However, such a solution would make the model more complex to optimize.

The following chapter presents the proposed framework applied in the additive manufacturing context. In particular, we develop a tool to study the impact of different parameters on product quality and environmental sustainability performances.

Chapter 4

Sustainable Additive Manufacturing

4.1 Introduction

This chapter focuses on a novel approach to managing OKD in additive manufacturing. As highlighted by Bikas et al., AM designers need to precognition the optimum process parameters and get insight from the production [83]. Furthermore, a tool to make designers aware of quality's impact on cost and environmental impact is crucial [84]. **The main research question we want to address is to study a simple and effective methodology that can provide, in early design stage, adequate user insight into costs, environmental impacts, and additive manufacturing product quality**. Our method is proper in distributed or small one-of-a-kind production contexts, which cannot rely on overly onerous tools. In particular, we decided to focus our analysis on Fused Filament Fabrication (FFF) since, according to the literature, it is the most widely diffused AM technology for its cost-effective ratio [85]. This additive manufacturing technique is based on a continuous filament of thermoplastic material, heated, melted, and extruded through a nozzle. The nozzle deposits each layer, and the semi-liquid material hardens and adheres to the layers below. According to the literature, this technique is characterized by low cost and high manufacturing speed. However, the final results lack mechanical properties and surface quality [86]. Despite these limitations, it is the most promising additive manufacturing technology [85].

The section is divided as follows: Section 2 presents the state-of-the-art and the main gaps, and Section 3 details the proposed methodology. Section 4, the first part of the method, is applied in a case study to find empirical relations. Section 5

presents the multi-objective optimization model. Finally, Section 6 presents some conclusions, impacts, and future developments of the study.

4.2 State of the Art

In this section, we present the most relevant literature related to the study of different aspects of sustainability in AM design. In particular, the first subsection is related to product quality. This work evaluates product quality through three AM characteristics: Accuracy, Resolution, and Surface Texture [87]. Customers' product quality specification is the main issue to be satisfied. The second subsection presents the central literature on environmental sustainability in additive manufacturing. In the third subsection, we cover the economic topic. Sub-paragraph 2.3 shows some sustainability methods linked to the early stages of design, and finally, in the last subsection, we describe the main gaps we have found and want to fill with the present chapter.

4.2.1 Product Quality Issue

Additive manufacturing generates new issues in terms of the method of managing and verifying product specifications. The definition of tolerances and specifications in additive manufacturing processes is more complex than in subtractive manufacturing since new process-driven issues and capabilities have to be specified along the product life cycle [88]. In particular, Ameta et al. identified five process-driven issues (build direction and location, layer thickness, support structures, use of heterogeneous materials, and scan/track direction while printing) and three process capabilities (complex geometry, topology optimized shapes features, and internal part infills). E.g., since the build direction or the infill pattern has a significant impact on product mechanical proprieties and surface quality, the designers have to specify this information with all geometric specifications [89].

In order to exploit the unique possibilities of this additive manufacturing and consider its limits and criticalities, designer support methods have been developed that fall under the Design for Additive Manufacturing (DfAM) methodologies, i.e., design in the service of AM [90]. In this context, more complex figures and new possibilities arise, but also new constraints and problems. In [91], four conventional guidelines are presented: the risk of warping, surface roughness, the use of supports, and the analysis of possible toppling and small parts manufacturability, and they proposed a tool to give graphical insights to the designers about the crucial issue of

the part. While in [90], the author suggests and tests a five-step procedure to promote AM-oriented designs from the early product design stages.

On the other side, many studies have been proposed to estimate additive manufacturing product quality by investigating the effect of materials, technologies, and processes. Most of these studies focus on analyzing the effect of factors on surface roughness, mechanical proprieties, and dimensional accuracy [92]. Cojocaru et al., in their work, propose a deep analysis of the impact of process parameters on different mechanical proprieties of PLA products manufactured through FFF [93]. In [94], the authors analyze various FFF parameter optimization articles, classifying them based on the feedstock filament. They also show that additive manufacturing research focusing on product cost, process cost, and environmental factors is still a minority. Similar conclusions are presented in [92] and [95]. In particular, Mohamed et al. highlight missing optimization techniques to find the optimal combinations for a certain set of process parameters and the lack of studies focusing on production time and product cost [92]. Most studies that analyze the influences of design and manufacturing factors on product quality are process dependent and show a lack of generality and maturity, reflecting a shortage of reliability and reusability.

4.2.2 Environmental Sustainability Issue

One of the three main pillars of our analysis is the environmental sustainability of additive manufacturing processes. In the literature, it is possible to find a significant amount of research articles and reviews on this particular topic, meaning that the interest in knowing the future implications of additive manufacturing in an environmentally sustainable manufacturing paradigm is elevated. From a circular perspective, to decrease the impact of manufactured products on the environment, three different goals have to be pursued: (i) reduce the waste during the product lifecycle (narrow the loop), (ii) increase the lifespan of products (slowing the loop) and finally, giving new life to products (closing the loop) [96].

In scientific literature, the main object of analysis in environmentally sustainable additive manufacturing is the direct consumption of machinery. This concern is probably since material waste in additive manufacturing is inferior to traditional manufacturing, mainly in metal additive processes like electron beam melting (EBM)[97]. In [98], the influence of the principal manufacturing parameters on energy consumption, material wastes, and mechanical proprieties is studied. What is clear from many studies is that the main factor influencing energy

consumption is process time: the longer the process takes, the more machine components will have to be heated and consume energy. Hence, layer height and infill strategy significantly impact energy consumption since they can enlarge the needed building time [98,99]. Electric energy consumption is also studied in rapid prototyping (RP) applications. Mongol et al., for instance, examined the impact of different parameters such as orientation and height of the part, presence of supports, layer height, etc., on energy consumption in several RP additive manufacturing processes: FFF, thermojet, and selective laser sintering [100]. In [101], the authors perform a literature review on additive rapid prototyping and rapid tooling environmental impact, pointing out the importance of studying the recoverability of the materials.

The study of the materials and their recyclability is another topic in recent scientific literature. Acrylonitrile butadiene styrene (ABS) and nylon are two of the most common materials used in FFF processes. These materials are derived from crude oil, and their recyclability is not widely spread [102]. For these reasons, the use of bio-based and biodegradable plastic in additive manufacturing is becoming increasingly important. Polylactic acid (PLA) is a widely used plastic filament for FFF applications. As the two precedent materials, PLA is not considered recyclable, although some studies on its recyclability are in progress. Nevertheless, it is bio-based since it is produced by corn starch and is biodegradable in industrial conditions. For this reason, its environmental impact is lower. In the literature, it is possible to find several examples of procedures and methodology to recycle material for FFF applications [102,103] and how the material behaves as a result of several recycling cycles [103].

Recently scholars have been investigating the usage of commonly recyclable and recycled materials. For instance, in [104], the authors present profound research on the effect of several parameters on the mechanical properties of high-density polyethene HDPE. This plastic is widely used in consumer applications like cosmetics and detergent flasks, and recyclable plants of HDPE are spread on a large scale. Finally, another way to reduce additive manufacturing's material environmental impact is by preventing waste by ensuring the product quality, for example, by monitoring the product quality in real-time through defects image recognition [12,105]. Ullah et al. proposed an index to evaluate the environmental impact of additive manufacturing in RP applications, considering the carbon footprint, material, and energy consumption [106]. At the same time, in [107], the authors proposed a multi-criteria decision analysis based on 25 parameters, both traditional and environmental (e.g., mechanical properties, manufacturing

efficiency, economics, process emission, and footprints, etc.), to produce a ranking of the best AM technique for rapid prototyping.

A helpful tool that is becoming increasingly used is the Life Cycle Assessment (LCA). Some works present methodologies to support the designer in choosing the AM machine and selecting production parameters to minimize the product impact during its lifecycle based on environmental strategy decisions [108,109].

4.2.3 Economic Issue

The final goal of the manufacturer is to produce a product that satisfies the quality standards and minimizes production costs. For this reason, the economic point of view is indissoluble from a comprehensive analysis. Khorram et al. [110] studied in which context AM technology is sustainable from an economic perspective and the main organizational and operational factors that impact its sustainability. Their analysis shows that additive manufacturing is mainly suitable for small companies that produce in small batches. Furthermore, AM can bring a vast advantage to these companies thanks to this technology. They can make inside what previously was outsourced. In this context, Baldinger et al. propose a profound cost estimation methodology to evaluate in a make-or-buy scenario if it is more convenient to design the part and produce it inside using AM or outsource it [111]. Finally, Life Cycle Costing (LCC) is a tool not yet widely used in the study of AM. It might be intriguing to study the costs of the product manufactured in additive along its life cycle and perhaps study possible impacts on the circular economy. One example of Life Cycle Economic Analysis (LCEA) can be found in [112]. In their study, the authors evaluate the economic impact of distributed manufacturing on US household users. They consider energy cost, filament cost, the time to produce, and the return on investment, and they finally eventually confirm the feasibility and cost-effectiveness of building products at home.

4.2.4 Early Design Stage Methodology

In the literature, although still an under-explored argument, some works propose tools, methodologies, or frameworks to support designers in the AM early design stages to make decisions based on sustainability parameters (principally environmental). These stages are proposed by Segonds et al. in [113] and

correspond to the innovation phase described in Figure 1 in the first chapter of this thesis.

In [114], the authors proposed a methodology to facilitate sustainable design thinking with an outlook on the product lifecycle. The proposed method is based on a Lifecycle Design Strategy (LiDS) wheel, two technical cards containing information on additive manufacturing processes and materials to support convergent thinking, and a SWOT (Strength, Weakness, Opportunity, Threat) framework to evaluate the obtained solutions. Laverne et al. developed a tool to support eco-additive manufacturing. In particular, their prototype is intended to guide the designer through a user interface in the machine choice that satisfies the product specifications and the machine parameters able to drive the decided resource minimization strategy [108]. Rocheton et al. proposed a similar tool to assist designers in making conscious environmental choices. The tool inputs the user skills, the mesh file, the design rules, and the strategy the user wants to follow (minimize energy or material consumption), and it gives the ideal machine to produce the prototype, the printing orientation, and parameters [115].

Agrawal proposes an approach, suggesting a combination of Design for Additive Manufacturing and Design for Environment rules. In particular, he found 26 design guidelines clusterized into four groups, i.e., (i) accuracy, (ii) layer thickness, (iii) Strenght, and (iv) environmental and end of life, and he ranked the 26 guidelines with a TOPSIS-based multi-criteria decision method to facilitate the designers in their choice [116].

4.2.5 Gaps

In this final paragraph, we decided to highlight the principal gaps we want to fill with the present work. It is clear that the interest in studying a methodology to support the AM designer in decision-making in the early design stages [117]. Nevertheless, we have perceived two main gaps: (i) the lack of a simple, standardized methodology to create and capitalize the knowledge in the additive manufacturing process to allow quicker and wasteless prototyping, and (ii) the lack of a method to generate knowledge related to the product cost and its environmental

impact as well as the product quality, in order to foster its sustainability all along the lifecycle with a particular outlook on circularity.

4.3 Methodology

A design optimization tool can be based on different approaches, in particular: (a) use the computer simulation to test design aspects' impact on final product performances (hybrid approach), (b) use an analytical model based on physical law (theoretical approach) to build a full optimization model, and (c) use an experimental data-driven approach (empirical approach) to estimate the relationships statistically. Since the primary purpose of this work is to suggest an easy-to-replicate approach, the first two approaches (a-b) are not suitable candidates. Computer simulation needs previous knowledge and can be expensive in terms of costs and time. An analytical approach allows for achieving results in a fast and inexpensive manner. Nonetheless, an analytical approach needs a deep understanding of physical phenomena and complex mathematics to build deterministic functions. For these reasons, we decided to develop an experimental data-driven methodology to estimate the relationships between parameters and performances.

A possible idea for making an empirical approach work would be to integrate it with the knowledge of process experts. The model would optimize qualitative and quantitative performances, i.e., manufacturing cost and environmental impact (like manufacturing, use, etc.). Each of the decided performances has to be weighted according to design decisions.

The proposed methodology is displayed in Figure 22. It consists of two main phases: STEP 1 – Knowledge Generation, whose goal is to define an experimental space assisted by experts to generate new knowledge, and STEP 2 - Optimization, whose primary purpose is to capitalize on the acquired knowledge and define an automatized tool to support designers in choosing the best parameters and avoiding defects and wastes.

According to de Pastre et al., creating a general standardized benchmark for experimentation is impossible. The design choice must be made by evaluating the experimental decisions and the metrological limits and specificity of the production process [87]. Nevertheless, several guidelines exist, i.e., ISO 52902 [118]. For all these reasons, the first step of our proposed methodology is to generate a new benchmark in order to satisfy three distinct aspects: (i) design choice, (ii)

manufacturing constraints and (iii) metrological limitations. After that, it is necessary to define some performances to be analyzed and the relative parameters we want to assess. Then, according to all these variables, we define a Design of Experiment (DoE) to investigate the impact of the selected parameters on the performances. STEP 1 finishes with the statistical analysis of the obtained dataset in order to generate an empirical regression model to link the parameters mathematically with the performances. STEP 2 starts with the compression of the design space. If some parameter has no impact, they have to be removed. The same has to be done with performances that remain constant for all the experiments. Then, a multi-objective optimization problem is defined, and thanks to the obtained results, the designer can make his choice with precognition.

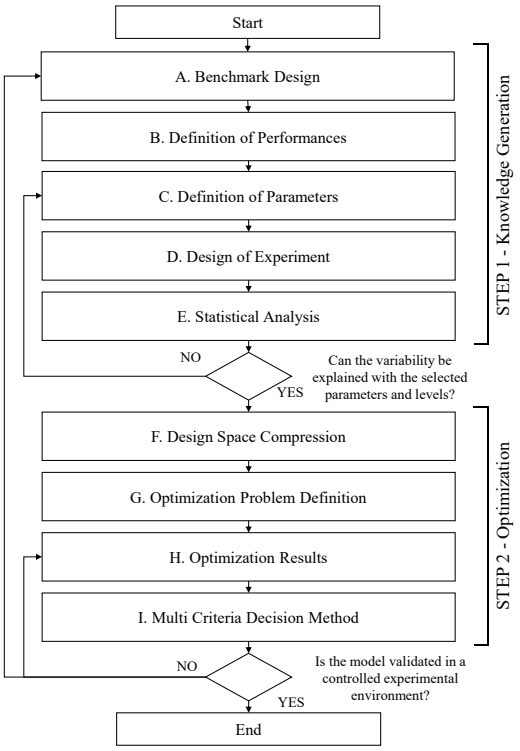

Figure 22 - Proposed Methodology divided into nine different stages

A similar approach is already used in the literature. For instance, in [119], the authors apply an empirical methodology to evaluate and estimate the optimum drilling rate and electrode wear ratio in electric discharge machining drilling, while in [120], a comparable method is used to identify the best parameters to maximize product performances (warpage, weld line, and clamp force) in plastic injection

molding processes. We applied the proposed approach to a real case study in the following two sections of this chapter.

According to the general framework proposed in chapter 2 (Figure 6), we applied the proposed guidelines from the design space definition to the support tool definition. In particular, as previously stated, we used this use case to validate the empirical approach to knowledge generation. In particular, there is a correlation between the proposed methodology described in Figure 22 and the general framework. The phases between A to C compose the design space definition, then we proceed with the empirical approach through phases D and E. Phases G and H are intended to find the optimal solutions, and finally, phase I is needed to support the designers in decision-making. In Figure 23, a dashed line highlights the general framework's parts validated through the sustainable additive manufacturing case study.

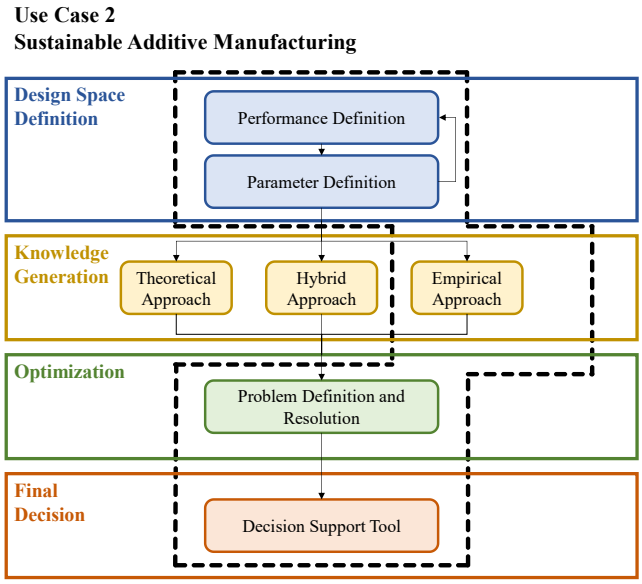

Figure 23 - General framework on the additive manufacturing use case

4.4 Methodology Application – Knowledge Generation

This chapter presents a real application of the first part of the proposed methodology conducted in an experimental environment. Each sub-paragraph describes the application of each methodology stage (A to E) straightforwardly. As

previously mentioned, this first part of the methodology is intended to generate new knowledge about the process to support the designers in their decisions.

4.4.1 Setup

The experimentation is performed in the Arts et Metiers Institute of Technology's Laboratoire Conception de Produits et Innovation (LCPI) using a Raise 3D E2 (https://www.raise3d.com), a desktop additive manufacturing machine for FFF application with two independent extruders. This tool is economical and adapted to DIY or FabLab applications. The benchmark is designed with FreeCad (v0.19), an open-source parametric 3D Computer-Aided Design (CAD) modeler. Finally, the G-code generation is performed using the Raise 3D E2's proprietary slicer IdeaMaker (v4.2.3). The material used for this experiment is black PLA with a 1.75 mm diameter and a density equal to 1.24 g/cm^3, bought from the french company DailyFil (www.dailyfil.fr).

4.4.2 Benchmark Design

The design choice matches the experimental goals, production, and metrological limits, using ISO 52902 as a reference [118]. The benchmark is defined in collaboration with additive manufacturing experts, knowing the machine's capabilities. On the other side, we decided on the dimension and position of different features to be capable of measuring them straightforwardly. The benchmark is adapted for prototyping assessment, and in particular, it contains the

most frequent elementary shapes. Figure 24 displays the benchmark orthogonal projection of left, right, frontal, and top views emphasizing the key quotas.

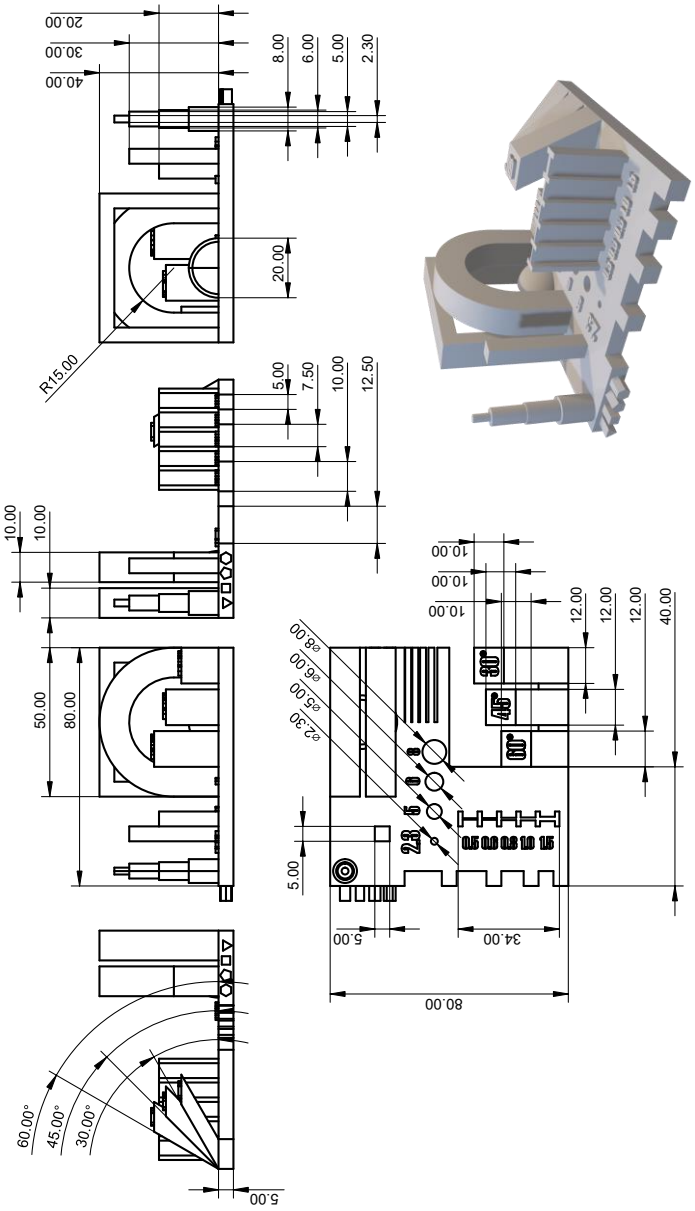

Figure 24 - Benchmark orthogonal projection (left, frontal, right, and top view) and 3D representation with the main dimensions.

The benchmark comprises eleven subparts: Bridge, Arc, Sphere, Holes, Pins, Side, Ribs, Slots, and three different Slopes (30°,45°, and 60°). The subparts are intended to assess various geometrical shapes' accuracy, resolution, and surface texture. Accuracy is the capability of the machine to build an object as close as possible to the reference value. The resolution is the potential to manufacture small dimension features, and finally, the surface texture is the capability to create a smooth surface without irregularities and nasty overhangs. In Figure 25, the eleven subparts are defined and highlighted using different colors. Table 8 specifies the purpose of each subpart.

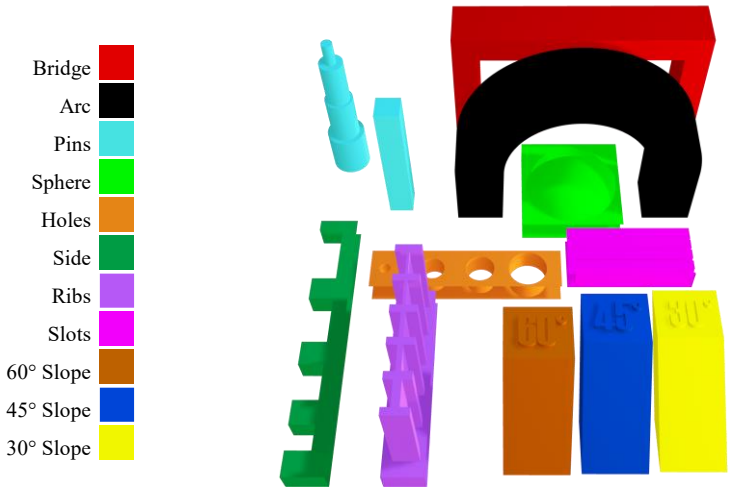

Figure 25 - Benchmark's subparts graphical representation

Table 8 - Benchmark subparts' goal definitions

Subparts	Goals
Bridge	Accuracy and surface texture
Arc	Accuracy and surface texture
Sphere	Accuracy and surface texture
Holes	Accuracy and surface texture
Pins	Accuracy, resolution, and surface texture
Side	Accuracy, resolution, and surface texture
Ribs	Accuracy, resolution, and surface texture
Slots	Accuracy and surface texture
60°, 45° and 30° Slopes	Accuracy and surface texture

4.4.3 Definition of Performances

We can split the performances into two separate classes: (i) environmental-related performances and (ii) quality-related performances. About the first group, we focused on energy consumption during manufacturing, material consumption needed to produce the part, and time necessary to make the part. At the same time, the quality of the object is evaluated through three different metrics. Each metric is intended to evaluate one specific goal for any subpart and uses various means. To assess the surface texture, we decided to analyze the part through a subjective assessment made by a sample of experts in diverse fields of product design. To evaluate the resolution of subparts, we analyze the different dimensions through a manual caliper and compute a global metric. Finally, we used a scanner to generate a product's cloud of points to compare the adherence between the produced part and the CAD. This final process is made to estimate a metric of the accuracy of the process. In the next sub-paragraphs, we detailed how all (i) related environmental performances and (ii) quality-related performances are computed.

We decided to keep the economic aspect outside our analysis since all the presented performances can be cost-related. The direct impact of some of them, like energy or material consumption, can be effortlessly calculated. On the other hand, the economic impact of quality is hard to define. Moreover, each cost depends on the company ecosystem, suppliers, and stakeholders. Therefore, we prefer to leave out the pure cost so that our analysis retains its value while changing the conditions of time and space. However, this study also has indirect economic aspects: higher material and energy consumption will result in higher costs for the company and a more significant environmental impact.

Table 9 summarises the seven performance indexes used for our experimentation and the measurement unit, classified into two groups: (i) environmental-related performances and (ii) quality-related performances.

Table 9 - Performance Definition

Class	Performance	Unit
Environmental-Related Performance	Energy Consumption (PE_i)	VAh
	Material Consumption (w_i)	g
	Processing Time (PT_i)	s
	Carbon Footprint ($totC_i$)	kg CO2eq
Quality-Related Performance	Accuracy Index ($\hat{A}_{ik}$)	%
	Resolution Index (R_{ik})	%

Qualitative Index ($\hat{Q}_{ik}$)	%

The following sub-paragraph illustrates each index's primary purpose and computation procedure.

4.4.3.1 Energy Consumption

In order to measure the energy consumption, we installed an amperemeter in series and a voltmeter in parallel on the machine alimentation circuit. The sensors are the AC5712 current sensor and the ZMPT101B voltage sensor. Using an Arduino board (https://www.arduino.cc/), we measured the VRMS and ARMS each second to compute the apparent power in VA. After that, we used this value to calculate the whole energy consumption in VAh. VAh represents the apparent energy absorbed by the machine, and this value takes into account the active energy used by the device and the reactive power losses. Reactive power generates extra load, and the network must be appropriately sized. Furthermore, in industrial applications, reactive energy consumption can directly impacts energy cost, and from an environmental perspective, a VAh-based bill is preferable. Analyzing the phase shift between system voltage and current, when the machine is stopped, the cos φ is around 0.89, while when the device is running, it drops as low as 0.4. This significant variation is justified by the use of induction motors inside the machine that draw reactive power to operate.

According to the literature, the energy consumption in AM can be computed per piece, weight, or volume of extruded material [21]. We decided to use the energy per piece since the produced part is a benchmark and has the same geometrical characteristics every time. Moreover, in FFF applications, it is more common to use this indicator.

4.4.3.2 Material Consumption and Processing Time

We measured the total processing time needed to produce any part. After the production, we weigh each piece to consider the total amount of PLA used. We compute the total amount of material used for the model and supports. The scale used for the analysis is a PCB 1000-2 by KERN & SOHN GmbH. The scale resolution is equal to 0.01 g. The slicer also estimates these two values.

Nevertheless, an average error on these valuations of 1337s (4.06%) and 1.68g (3.6%) is detected.

4.4.3.3 Carbon Footprint

In order to evaluate the environmental impact of each product, we decided to estimate the production carbon footprint assessed in kg of CO_2eq. However, it is hard to consider a complete LCA in the first stages of product development since the information is missing. In contrast, the data is extensive in the advanced stages, but the possibility of significant product changes is minimal [121]. We proposed a semi-quantitative approach by estimating the kg of CO_2eq to give some insights to designers even if the knowledge of the process is still low. We decided to analyze the impact of the production in the first two steps of the product lifecycle: raw material extraction and manufacturing. In our experiment, the environmental impact of the i-th part is mainly composed of four elements: (i) the embodied energy committed to creating the needed quantity of plastic material. (ii) The kg of CO_2eq emitted in the atmosphere to produce that amount of plastic, and (iii) the direct energy consumed by the AM machine to produce the part. We decided not to evaluate the impact of the supply chain since we use a single supplier for raw material, and so the kg of CO_2eq emitted in the atmosphere for transportation, in our experiment, is a constant. Usually, the energy consumption in LCA analysis is not directly translated into kg of CO_2eq since the carbon footprint of electricity depends on the energy source used to make it. For instance, in the United States, energy is mainly produced from coal, oil, and gas. A considerable share of Germany's electric energy is produced from solar and wind plants, while France's is 78% nuclear [122]. Nevertheless, our analysis made some assumptions about the energy production mix. We used the average French ones since the experiment was performed in France, and the material used was produced in the same country. France's energy mix is composed of 10% fossil fuel, 78% nuclear, and 12% renewable. The emission of such a combination is equal to 0.06 CO_2eq kg/kWh [123]. According to the literature, polylactic acid has an embedded energy of 15.28kWh/kg (55 MJ/kg), producing 2.8 CO_2eq kg/kg. In comparison, the recycled counterpart has embedded energy equal to 5 kWh/kg (18 MJ/kg) and produces 0.95 CO_2eq kg/kg [123]. All the used values must be used with extreme caution, and for this reason, we defined our analysis as semi-quantitative. According to Ashby, a

standard deviation of 10% on all average CO_2eq values must be considered [123]. Finally, the amount of kg of CO_2eq emitted for any i-th parts ($totC_i$) is equal to:

$$totC_i = ke\ EE\ w_i + C\ w_i + ke\ PE_i \tag{41}$$

Where ke is the amount of CO_2eq emitted to produce a kWh of energy (0.06 CO_2eq kg/kWh), EE is the embedded energy of the used material (e.g., for not recycled PLA 15.28kWh/kg), w_i is the total amount of material used to produce the part (model + supports), C is the quantity of CO_2eq emitted to produce a kg of material (e.g., for not recycled PLA 2.8 CO_2eq kg/kg), and finally, PE_i is the total energy consumed by the machine to produce the i-th part.

4.4.3.4 Qualitative Index

The first quality analysis is a quantitative one. We composed a panel of 8 design experts. Their domain is various: computer-aided design (CAD), industrial engineering, and augmented and virtual reality design, and we ask them to evaluate each part qualitatively. Some tools have been provided to facilitate their task: plates of the exact size of the slots and four different gauges with the precise diameter of the four holes. Moreover, we ask them to consider with particular notice the surface texture and the roughness of each part. We give them an evaluation sheet and ask them to assess each sub-part using a Likert scale between 1 and 7, with 1 for the highest quality and 7 for the worst. After that, we composed an Index for each of the 11 subparts by averaging the nine evaluations. E.g., the quantitative index Q_{ik} of the k-th sub-parts present on the i-th part is calculated as:

$$Q_{ik} = \frac{\sum_{j=1}^{N} q_{ikj}}{N} \tag{42}$$

Where q_{ikj} is the evaluation given by the j-th evaluator on the k-th subpart present on the i-th produced piece, and N is the number of evaluators. In order to compare each indicator, we normalize them by dividing each value by the maximum value found using the formula:

$$\bar{Q}_{ik} = \frac{Q_{ik}}{\max(Q_{ik})} \tag{43}$$

According to Yu et al., the proposed method is the best to normalize positive values since it can maintain the minimum and the maximum value and the relative

difference between series elements [124]. Thus, we ranged all indices between 0 and 1, where 0 indicates the best quality while 1 is the worst. In this way, both Environmental-Related Performances and Quality-Related Performances are concordant: the best performance is achieved with the minimum value.

4.4.3.5 Resolution Index

The second quality analysis is related to the achievable resolution. We performed this analysis only for 3 of the 11 sub-parts: Pins, Side, and Ribs. These three elements are designed to assess the minimum resolution of the machine in manufacturing specific features. In particular, the first Pin is designed to determine the resolution of producing vertical cylinders with a diameter of 8, 6, 5, and 2.3 mm. The second Pin has a square base 5 mm wide and 35 mm in height. The Side can assess the manufacturing of an interlock 5, 7.5, 10, and 12.5 mm. Finally, the Ribs are intended to evaluate the production of a straight rib of 5 mm between two supports with a thickness of 1.5, 1, 0.8, 0.6, and 0.5 mm. In order to evaluate the resolution index, we measure all the presented dimensions with a manual caliper with 0.01 mm precision. For the three aforementioned k-th subparts present on the i-th produced piece, we calculate two different metrics: the average relative error ARE_{ik}, and the maximum relative error MRE_{ik}.

The resolution Index for the k-th sub-part on the i-th piece is the average of the metrics normalized using the previously presented method:

$$\bar{R}_{ik} = \frac{\overline{ARE}_{ik} + \overline{MRE}_{ik}}{2} \tag{44}$$

4.4.3.6 Accuracy Index

The experimentation is composed of different steps: (i) CAD modeling, (ii) 3D model generation, (iii) Slicing, (iv) Production Process, (v) Scanning, and (vi) Sampling. Figure 26 displays the six tasks and the associated outputs (digital or physical). Moreover, the image shows where Accuracy Index ($\bar{A}_{ik}$) and the Resolution Index ($\bar{R}_{ik}$) are measured. The $\bar{R}_{ik}$ is calculated between the produced part and CAD quotas. In contrast, $\bar{A}_{ik}$ is evaluated between the mesh file (.stl), considered as a reference and the final cloud of points (.asc). In this paragraph, we detail the different steps we followed in computing this index. Each intermediate

step can generate variability, so it would be impossible to know where the measured error is generated.

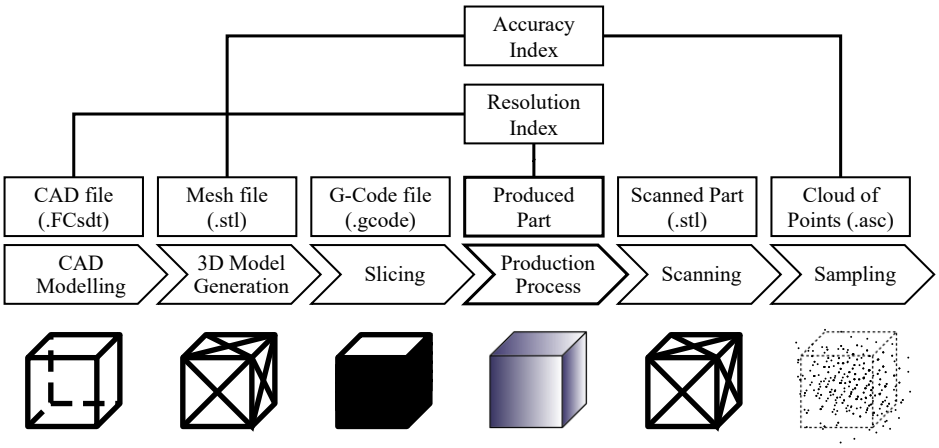

Figure 26 - Experiment Process Steps.

To evaluate the accuracy of the part, we propose an automated methodology by scanning the produced part and comparing it with the mesh reference in .stl format, in addition to the qualitative and quantitative methods presented above. According to the literature, there are no industrial applications of scanning procedures to evaluate product quality, and the most used methods are traditional calipers or coordinate measuring machines (CMM) [125]. However, it is possible to find some applications in scientific research. E.g., in [12], the authors proposed integrating a quality scan control system at the shop-floor level with the Manufacturing Execution System, while [126] proposed an online quality monitoring methodology to detect defects in material extrusion AM processes. A widely used technology in additive manufacturing quality assessment is computed tomography (CT) to assess material distribution, porosity, and lack of fusion [127], du Plessis et Al. proposed a standardized procedure to use CT scans in metal additive manufacturing applications [128].

We decided to test the application of a micro CT scanner, and the result was mesmerizing. To perform this analysis, we used a µCT 100 produced by SCANCO Medical AG (www.scanco.ch/). However, a CT machine is costly (about 250 k€), the scanning time is long, and the final images require extensive post-treatment. Moreover, the final mesh obtained is heavy to manage. In our case, it was composed of 6.8 million points and was about 0.6 GB. Indeed, this analysis could be used in applications where the internal structure and the product's mechanical properties

are crucial. Figure 27 displays a section of the benchmark part obtained using a micro CT scanner. In the figure, it is possible to see the internal infill pattern and its density.

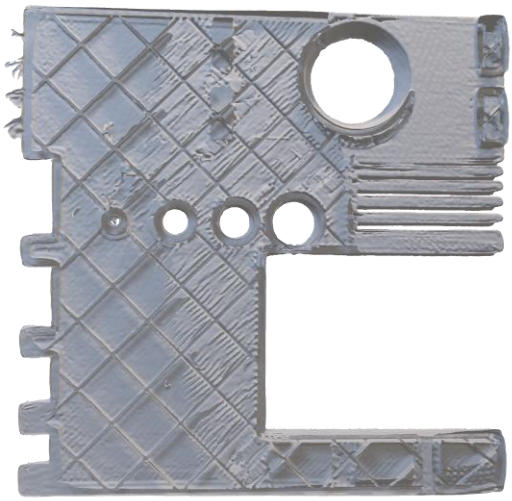

Figure 27 - microCT benchmark scan section.

The application of the micro CT scanner was interesting, and it helped us demonstrate the proposed approach's theoretical feasibility with this more precise technology. Moreover allowed us to analyze the material's internal structure. However, since we are not interested in internal product structure and its mechanical properties in this first analysis, we decided to use an optical scanner, the Einscan-SP (www.einscan.com), a 3D desktop scanner with a declared accuracy of 0.05 mm.

The produced parts were scanned using an established procedure: each piece was covered by a layer of mattifying white spray to allow a clean and more detailed image. Then the part was scanned five times in different positions to analyze each side properly (see Figure 28). The part was positioned on a turning table, and the

scanner took a picture each 10°. Finally, the five different files were merged to create a single .stl file.

A. flat | B. upside down | C. on flat side | D. on arc | E. on uneven side

Figure 28 - The five different scanning positions used.

In a second moment, we used the open-source software CloudCompare (www.cloudcompare.org) to generate a produced part cloud of points, each of which has approximately 10M points. The cloud of points was then aligned to the reference mesh. Finally, we computed the signed distance between each point and the reference mesh. We can consider the mesh as a reference since the average error between the mesh surface, and the CAD surface is 0.011 μm with a standard deviation of 18.63 μm.

Using these distances between the scanned part and the reference mesh, we computed three metrics: the number of points outside the tolerance T_{ik}, the range between the two farthest points D_{ik}, and the standard deviation S_{ik}. According to the literature, in FFF applications, a satisfying accuracy is ± 0.5%, with a lower limit of ± 0.5 mm [129]. For these reasons T_{ik} was computed as the percentage of points outside the interval ± 0.5 mm. We also calculated the distance distribution's average, skewness, and kurtosis. These three other values could be used in further analysis. Finally, we computed the accuracy index $\bar{A}_{ik}$ for the k-th subpart present on the i-th piece, by averaging the three metrics normalized using the same methodology presented previously.

$$\bar{A}_{ik} = \frac{\bar{T}_{ik} + \bar{D}_{ik} + \bar{S}_{ik}}{3} \tag{45}$$

4.4.4 Definition of Parameters

We have considered some parameters related to Product Material, Manufacturing Parameters, and Product Finesse. According to Laverne et al., users

who have scarce Additive Manufacturing Knowledge (AMK) and Eco-Design Knowledge (EDK) prefer to have simple guided parameters so they can spend the most time on creative design [108]. For this reason, we decided to focus only on easily accessible parameters. In particular, we decided to analyze the impact of using a Recycled PLA instead of a normal one. Then we decided to investigate the parameter present on the first page of the Slicer Software used to create the Gcode (presence of support, presence of base, layer height, infill rate, shell number), and all the parameters suggested by the filament producer (working temperature, plate temperature, and working speed). Table 10 displays the experiment parameters levels (Factors).

Table 10 - Design of Experiment Levels

Factors	Level (-)	Level (+)
Material (M)	Recycled PLA	Not Recycled PLA
Working Temperature (WT)	200°	215°C
Plate Temperature (PT)	T_a	50°C
Working Speed (WS)	40 mm/s	80 mm/s
Support (S)	No	Yes
Base (BAS)	No	Yes
Layer Height (LH)	0.1 mm	0.3 mm
Infill Rate (IR)	10%	60%
Shell Number (SN)	1	3

The parameters WT, PT, and WS levels have been decided using the material manufacturer's suggested ranges as a reference. At the same time, the parameters LH, IR, and SN have been chosen by defining a wide range in order to explore as much as possible design space while avoiding too extreme and unsuitable values. We agreed not to analyze the infill pattern. According to the literature, the infill pattern mainly affects part mechanical properties, weight, and process time [130], but no significant impact on product quality is proven. Nevertheless, it is demonstrated that the gyroid infill pattern confers on the piece the best mechanical properties [130]. For this reason, we used this infill pattern for all our experiments. Finally, in order to avoid failure, such as completely detaching the piece from the heating plate, we covered the plate with a thin layer of solvent-free starch-based

glue. Despite being very cheap and suitable for children's use, this glue worked very well, and it can be easily washed without the use of soaps or detergents.

4.4.5 Design of Experiment

Since we have nine parameters on two levels, a full factorial Design of Experiment (DoE) would require 2^9 (512) tests. We, therefore, opted for an experimental plan with the Taguchi method formed by 32 orthogonal vectors (L32). Table 11 shows the entire experiment through 32 arrays based on the nine factors on two levels. The Taguchi method allows us to investigate the impact of different parameters with a small set of experiments. Moreover, this methodology is widely used in additive manufacturing scientific research [131]. In other applications, with higher budgets or fewer factors, the application of a full factorial is not to be ruled out.

Table 11 - L32 Taguchi Design of Experiment

Experiments	M	WT	PT	WS	S	BAS	LH	IR	SN
E1	−	−	−	−	−	−	−	−	−
E2	−	−	−	−	+	−	+	+	+
E3	−	−	−	+	−	+	−	+	+
E4	−	−	−	+	+	+	+	−	−
E5	−	−	+	−	−	+	+	−	+
E6	−	−	+	−	+	+	−	+	−
E7	−	−	+	+	−	−	+	+	−
E8	−	−	+	+	+	−	−	−	+
E9	−	+	−	−	−	+	+	+	−
E10	−	+	−	−	+	+	−	−	+
E11	−	+	−	+	−	−	+	−	+
E12	−	+	−	+	+	−	−	+	−
E13	−	+	+	−	−	−	−	+	+
E14	−	+	+	−	+	−	+	−	−
E15	−	+	+	+	−	+	−	−	−
E16	−	+	+	+	+	+	+	+	+
E17	+	−	−	−	−	+	+	+	+
E18	+	−	−	−	+	+	−	−	−
E19	+	−	−	+	−	−	+	−	−
E20	+	−	−	+	+	−	−	+	+
E21	+	−	+	−	−	−	−	+	−
E22	+	−	+	−	+	−	+	−	+
E23	+	−	+	+	−	+	−	−	+
E24	+	−	+	+	+	+	+	+	−
E25	+	+	−	−	−	−	−	−	+
E26	+	+	−	−	+	−	+	+	−
E27	+	+	−	+	−	+	−	+	−
E28	+	+	−	+	+	+	+	−	+

E29	+	+	+	−	−	+	+	−	−
E30	+	+	+	−	+	+	−	+	+
E31	+	+	+	+	−	−	+	+	+
E32	+	+	+	+	+	−	−	−	−

4.4.6 Statistical Analysis

Once all the experiments were performed, we studied the results in order to find the relations between the parameters and the measured performance. Since we have 11 qualitative indexes ($\hat{Q}_{ik}$), 3 resolution indexes ($\hat{R}_{ik}$), 11 accuracy indexes ($\hat{A}_{ik}$) and 4 Environmental-Related Performances (PE_i, w_i, PT_i, and $totC_i$) for each i-th part, we have to find 29 different functions. However, since the $totC_i$ equation is a combination of PE_i, w_i and constants, it was not necessary to estimate it by a regression. Therefore, we tried to develop 28 regression models in order to analyze the relations between the parameters and the performances. We decided to evaluate the qualitative, resolution and accuracy models separately since these indexes represent different objectives. For instance, $\hat{Q}_{ik}$ and $\hat{A}_{ik}$ are pretty correlated. However, these two metrics do not represent precisely the same thing; geometric analysis of the cloud of points can detect any deviation from the reference. On the other hand, the visual-qualitative assessment examines the surface quality, smoothness of structures and overhangs, and the aesthetic of the parts, features not detectable through the scanner.

In order to find the best model to predict the impact of parameters on performances, we used a methodology composed of 3 different steps: (i) outliers analysis, (ii) stepwise bidirectional regression fitting minimizing the model AIC [132], (iii) and finally a backward elimination of the less significant predictors to avoid overfitting. In order to prevent multicollinearity, the three binomial variables (S, BAS, and RE) have been substituted with three binary variables (S_Y, BAS_Y, and RE_Y), indicating if supports are used, if a base is used and if the part is produced with recycled material. Finally, each model's normality and homoscedastic residuals have been tested using a Shapiro-Wilk test [133] and the studentized Breusch-Pagan test [134]. The models' reliability varies greatly depending on the sub-part being evaluated. We decided to place a 40% R^2 threshold on the models. All models that explain less than 40% of the variance are not reported, so these features cannot be evaluated in our case study. We unsuccessfully build a satisfactory model for seven performances: Arc $\bar{Q}$, Pin $\bar{R}$, Side $\bar{A}$, Rib $\bar{Q}$, 60° $\bar{Q}$, 30°$\bar{Q}$, and 45°$\bar{Q}$. Although these models cannot be used to predict, they still have interest, as they can express which factors among those studied have an impact

(albeit minimal) on performance. Lastly, we managed to compute 21 out of 28 regression models. In the different models we represent the t-test significativity of each variable using the following convention: *** < 0.1%, ** < 1%, * < 5%, and † < 10%. The Adjusted R^2 and the p-value from the F statistics of the full model.

Table 12 - Bridge Models

Dep. Variable	Predictors	β	Sig	Adj-R^2	p-value
Bridge $\hat{A}_B$	Constant	0.97379	***	78.85%	1.45E-09
	S_Y	-0.56082	***		
	LH	-0.56170	**		
	SN	-0.06975	*		
	$S_Y \times SN$	0.08170	*		
Bridge $\hat{Q}_B$	Constant	0.75909	***	70.97%	9.64E-08
	RE_Y	-0.09091	*		
	WS	0.00278	**		
	S_Y	-0.25909	***		
	LH	-0.84091	***		

Table 12 displays the obtained model for the bridge Accuracy Index and the bridge Qualitative Index. The two indexes have a strong correlation (0.846). As previously explained, the better the subpart's performance, the lower the indicator. The two indicators are both strongly impacted by the presence of support and layer heights. On both hands, the use of support improves the final quality of the sub-part.

Regarding the layer height, we have a counterintuitive result. The thicker the layer, the better the quality of the bridge. Visually examining the parts produced, it is immediately apparent that this is especially true of unsupported bridges: the thicker the layer, the lower the bridge's collapse. In addition, the bridge having all straight sides and no curvatures is little impacted by stair error, and the visible layers do not seem to make the part of shallow quality. Another very interesting parameter is the number of shells. In many sub-parts, this parameter has an effect. In the bridge, the higher the number of shells, the better the part is.

Table 13 - Arc Model

Dep. Variable	Predictors	β	Sig	Adj-R^2	p-value
Arc $\hat{A}_A$	Constant	0.52291	***	58.69%	1.01E-04
	RE_Y	-0.18445	**		
	WS	0.00473	***		
	S_Y	-0.21279	***		
	IR	-0.00166	*		

$BAS_Y \times WS$	-0.00476	***
$BAS_Y \times S_Y$	0.22654	**
$BAS_Y \times RE_Y$	0.18686	*

Table 13 shows the model for the arc Accuracy Index. It is interesting to notice that better accuracy is reached with recycling material, supports, and a higher infill rate. At the same time, it drops with a higher printing speed. Nevertheless, if the base is present, the effect of the other variables, both positive and negative, is compensated, and the final arc only depends on the infill rate value.

Table 14 - Sphere Models

Dep. Variable	Predictors	β	Sig	Adj-R^2	P-value
Sphere $\hat{A}_{Sp}$	Constant	-0.07086		62.51%	2.36E-04
	WT	0.00324	†		
	PT	-0.00652	*		
	WS	0.00127	*		
	S_Y	-0.42845	***		
	LH	-1.37713	**		
	LH × PT	0.03026	**		
	LH × S_Y	1.10383	***		
	PT × S_Y	0.00410	*		
Sphere $\hat{Q}_{Sp}$	Constant	-0.77312		47.52%	2.37E-04
	WT	0.00657	*		
	SN	-0.06777	**		
	LH × WS	0.00816	**		

Table 14 displays the sphere quality model. The two main parameters that impact its accuracy are the layer height and the support, which positively impact the final quality of the sub-part. However, if support is combined with a high layer height, a negative interaction fixes the accuracy at a level. In practice, the maximum possible accuracy is achieved when either parameter has a positive effect. When both are present, there is no significant increase. On the other hand, it appears that the qualitative model of the sphere is very different from the accuracy one. This is not surprising since the sphere often has asperities and roughness on its surface that are not detectable by the scanner. Remarkably, the surface quality of the sphere increases when more shell numbers are used, while working at too high a

temperature, too fast and using a thick layer causes surface harshness and irregularity in spherical structures.

Table 15 - Pins Models

Dep. Variable	Predictors	β	Sig	Adj-R^2	P-value
Pin $\hat{A}_P$	Constant	0.43845	***	59.40%	1.20E-05
	PT	-0.00251	**		
	WS	0.00140	**		
	LH	-0.34794	**		
	IR	-0.00157	***		
Pin $\hat{Q}_P$	Constant	-1.96121		44.28%	1.95E-03
	RE_Y	3.13450			
	WT	0.01250	*		
	WS	0.00326	*		
	SN	-0.05028	*		
	RE_Y × WT	-0.01486	*		
	LH × PT	-0.01320	*		

Table 15 details the pins models. Pin accuracy is determined mainly by four factors. Being on the upper left side, it is affected by warping, which is a shrinking of the plastic that occurs during cooling and disconnects the 4 sides of the model. this phenomenon can be avoided by creating a base or incrementing the temperature of the plate that help adhesion. Using a higher plate temperature, this error does not occur, and pin accuracy improves. Note that this effect is only valid for the benchmark as designed. The other three parameters are pretty straightforward. Higher print speed causes lower accuracy, while higher layer height and infill rate improve it.

As for the qualitative index, quality deteriorates significantly when recycled material is used and printing speed and temperature increase. At the same time, there is a positive effect as the number of layers increases.

Table 16 - Side Models

Dep. Variable	Predictors	β	Sig	Adj-R^2	p-value
Side $\hat{Q}_{Sd}$	Constant	0.09507		57.50%	7.21E-05
	WS	0.00131	*		
	LH	-0.69415	*		
	SN	-0.05635	*		
	LH × SN	0.47083	***		

	RE_Y × LH	0.29911	*		
Side $\hat{R}_{Sd}$	Constant	0.30483	***	63.35%	4.97E-07
	LH	0.57648	*		
	LH × WS	0.00954	*		

Table 16 presents the two side models. The accuracy of the side depends very strongly on the height of the layers and the number of shells. Since these are straight and sharp structures, a similar phenomenon occurs for the bridge. Also, we have a cap effect due to the interaction of these two factors. Increasing one and the other together does not have an increasing linear impact. Regarding side resolution, this worsens with increasing layer thickness, and this worsening effect is even increased when the manufacturing speed is raised.

Table 17 - Holes Models

Dep. Variable	Predictors	β	Sig	Adj-R^2	p-value
Hole $\hat{A}_H$	Constant	0.50310	***	45.97%	2.51E-04
	WS	-0.01003	*		
	LH × WT	-0.00197	***		
	WS × WT	0.00004	*		
Hole $\hat{Q}_H$	Constant	0.43806	***	46.75%	7.69E-05
	LH	0.85751	***		
	SN	0.04167	*		

Table 17 shows the holes models. The accuracy of holes in the benchmark is improved by printing speed. A speedy production probably allows for the creation of accurate circles, while moving the extruder slower would result in more defects. A thicker layer also helps in the production of more accurate holes. On the other hand, there are opposite results regarding the subjective quality tested by the expert panel. Not surprisingly, the correlation between these two parameters is about 0%. The layer height impacts the quality of the holes very negatively. Also, because the holes are in direct contact with the plane, the base has a negative effect, generating "elephant feet" and a partial fusion of the model.

Table 18 - Slot Models

Dep. Variable	Predictors	β	Sig	Adj-R^2	p-value
Slot $\hat{A}_{Sl}$	Constant	0.16499	***	71.26%	1.53E-07
	LH	2.38415	***		
	LH × SN	-0.51907	***		
	RE_Y × SN	0.07145	**		
	RE_Y × LH	-1.14278	***		

Slot $\hat{Q}_{Sl}$	Constant	0.27139	***	55.78%	1.09E-05
	BAS_Y	0.16479	***		
	LH	0.92009	***		

Slot quality models are detailed in Table 18. Three parameters determine slot accuracy. Layer height, shell number and recyclable PLA. The more each layer is coarse, the worst the accuracy of slots. This phenomenon is easily understandable since slots are thin structures where great precision is needed. However, this effect is modified if the material used is recycled or if the number of shells is sufficiently high. On the other hand, as far as qualitative performance is concerned, only two parameters impact layer height and base. as far as the layer height is concerned, the effect is identical to what happens with the accuracy of the same sub-part. On the other hand, as far as the base is concerned, since this feature is in contact with the plane, an "elephant foot" effect is generated, and a partial fusion with the base partially degrades the aesthetic quality of the sub-part.

Table 19 - Ribs Models

Dep. Variable	**Predictors**	**β**	**Sig**	**Adj-R^2**	**p-value**
Ribs $\hat{A}_R$	Constant	1.01471	***	72.39%	1.36E-08
	BAS_Y	-0.34764	**		
	LH	-2.44407	***		
	BAS_Y × LH	0.99662	*		
Ribs $\hat{R}_R$	Constant	0.01307		58.81%	3.41E-06
	BAS_Y × LH	0.74182	**		
	LH × WS	0.02013	***		
	RE_Y × LH	-0.41887	†		

Ribs Models are detailed in Table 19. The accuracy of Ribs is mainly due to the presence of an adhesion aid base. This behavior is probably due to the position of the sub-part on the benchmark. External corners are subjected to warping defects, and this kind of error is mainly eased with a base. The Ribs are placed on the left bottom corner, and probably the use of a base prevents deformation of that corner and facilitates the production of Ribs. Another critical parameter is LH. The higher the layer, the more significant the accuracy of the ribs. The interaction of the two parameters damps these two effects. In terms of resolution, the Ribs are mainly impacted by three interactions. The coarse layer and fast printing cause negative parts. As for the accuracy index, the interaction between base and layer height

results in difficulty in obtaining good resolution. Nonetheless, it seems that there is a positive interaction between the use of recycled material and layer height.

Table 20 - Slope Models

Dep. Variable	Predictors	β	Sig	Adj-R^2	p-value
60° $\hat{A}_S$	Constant	-2.82137	***	64.23%	8.07E-07
	RE_Y	2.94402	***		
	WT	0.01549	***		
	RE_Y × WT	-0.01481	***		
45° $\hat{A}_F$	Constant	0.42493	***	39.68%	4.14E-04
	S_Y	-0.07680	**		
	PT × SN	0.00084	**		
30° $\hat{A}_T$	Constant	0.59589	***	80.33%	5.53E-10
	BAS_Y	-0.08056	**		
	LH	-0.88281	***		
	S_Y × SN	-0.09045	***		
	LH × SN	0.66164	***		

The three accuracy index slope models are presented in Table 20. It is interesting to observe how the three models have little in common. The presence of support positively impacts 45° and 30° slopes. The 60° slope is not affected by this parameter since we only inserted supports for inclinations greater than 45°. The accuracy of the 60° slope is primarily due to the use of recycled material and the working temperature. Using recycled material and a high fusion temperature would result in imperfect 60° shapes. This effect is not linear since the interaction of the two parameters has an opposite sign. The 45° slope accuracy model cannot predict well since the adjusted R^2 is lower than 40%. Since it is precisely on the decided threshold, we decided to keep this model even if its reliability is low. As previously reported, the 45° slope's accuracy is meanly impacted by the presence of support and the interaction between plate temperature and shell number, which negatively affect this performance. The layer height mainly impacts the 30° slope accuracy. With thick layers, the accuracy increase. Nevertheless, this effect is reduced as the number of shells increases promoting a ladder effect on the piece. Finally, the accuracy of the 30° slope is positively affected by the presence of the base. This behavior is probably due to the position of the 30° slope in the benchmark. Since

the sub-part is placed on the corner of the square base on narrow support, it is prone to warping, as previously described for the Ribs' accuracy.

Table 21 - Environmental-Related Performances Models

Dep. Variable	Predictors	β	Sig	Ad-R^2	p-value
PT	Constant	26559.33	***	98.80%	2.20E-16
	WS	-62.36	***		
	S_Y	5016.69	***		
	BAS_Y	1196.56	***		
	LH	-51749.37	***		
	IR	757.3	***		
	SN	4458.51	***		
	LH × SN	-7974.69	*		
	LH × IR	-1785.44	***		
	IR × SN	-53.15	*		
PE	Constant	697.213	***	93.67%	6.35E-15
	PT	11.978	***		
	WS	-2.802	*		
	S_Y	149.375	**		
	LH	-2012.881	***		
	IR	19.546	***		
	LH × IR	-54.093	***		
w	Constant	11.34462	***	95.35%	2.20E-16
	S_Y	9.5	***		
	BAS_Y	10.55	***		
	LH	42.45	***		
	IR	0.26823	***		
	SN	3.01313	***		

Finally, Table 21 details the three environmental-related models. These three models are highly significant and explain more than 90% of the variability. In particular, process time increases if base and support are required and if shell number and infill rate rise. On the other hand, process time decreases as working speed augments or if layer height increases. In addition, layer height also has a mitigation effect on infill rate and shell number since fewer layers have to be manufactured. Another interesting interaction is between the infill rate and shell number. Since less infill is needed as the number of shells increases and vice versa, the two factors are connected. The increase in production time by raising one of the two parameters is not linear but is slightly mitigated by the fact that it is not needed to produce the other element.

According to the literature, energy consumption is proportional to the processing time [99]. This relation can also be inferred from the variables composing the second model: all variables having a significant impact on time also impact energy consumption. It is also interesting to note that the working temperature does not significantly affect energy consumption, at least in the narrow range we evaluated (15°C). Conversely, as the plate temperature increases, more energy is consumed.

Finally, the effect of parameters on material consumption is also quite clear. Producing the base and the support would require more plastics and a higher layer height, shell number and infill rate impact on material usage. As expected, the obtained models on energy, time and material consumption are excellent, while the models on quality are variable. Some have good significativity and can explain a significant part of the dataset variance, while others have poor performances. According to the literature, additive manufacturing processes, in particular, have considerable variability, and the same parameters can drive different product outputs[12].

Nevertheless, thanks to this analysis, we also manage to understand what are the more critical parameters. The crucial parameter is layer height (LH). It is present on 14 models out of 21. A higher layer height often results in greater accuracy but lower surface and aesthetical quality. Moreover, the layer height massively increases the material used. Its interaction with working speed (WS) is also interesting. In different subparts manufacturing at elevated speed while using a thick layer height worsens the surface quality. Another quite impactful parameter is the shell number. Using more than one shell often improves the quality of the part. Finally, it is evident that the presence of support (S_Y) significantly impacts product quality, the variable is present in 8 models out of 21, and if present, it enhances the qualities of the subpart. It is not surprising that in scientific research, these parameters are the most studied and almost always present. Another frequently studied parameter is the infill rate (IR). From the results obtained, this seems to have little effect on the final product quality, and according to the scientific literature, its impact is definitely more related to the mechanical properties [93].

Table 22 shows a summary of the presented analysis. In particular, it is represented the occurrence of each factor with more than a single occurrence with two different percentages indicating how many time an increase of the parameter has a beneficial or detrimental effect on the studied performances.

Table 22 - Factors occurrences and their impacts.

Factor	Occurrences	Beneficial Effect	Detrimenal Effect
LH	14	64%	36%
WS	9	33%	67%
S_Y	8	63%	38%
SN	7	57%	43%
BAS_Y	5	40%	60%
IR	5	40%	60%
RE_Y	4	50%	50%
WT	4	0%	100%
LH×SN	4	50%	50%
PT	3	67%	33%
LH×WS	3	0%	100%
REY×LH	3	67%	33%
SY×SN	2	50%	50%
BASY×LH	2	0%	100%
REY×WT	2	100%	0%
LH×PT	2	50%	50%
LH×IR	2	100%	0%

4.5 Methodology Application - Optimization

In this section, we presented the application of the second part of the proposed methodology from G to I in Figure 22. Stage F, design space compression, was unnecessary since all the parameters were significant at least once, and we did not have regular performances. In particular, in 5.1, we defined the optimization problem. In subsection 5.2, we explained the resolution method and displayed the obtained solutions. Finally, in 5.3, we proposed a visual multi-criteria decision method to apply the obtained solution in an actual application.

4.5.1 Optimization Problem Definition

In this paragraph, the optimization problem is defined. Equation 45 represents all 22 objectives to be minimized. As previously mentioned, all variables presented reach their optimum in the minimum value. Equations 46a-u are precisely the 21 empirical regression models obtained by the statistical analysis of the 21

performances presented in the previous chapter. Equation 46v represents the kg of CO2eq emitted in the atmosphere to produce the parts. This equation is derived from the general one presented before. In particular, in this mathematical function, it is inserted the binary variable RE_y, equal to 1 if recycled PLA is used, 0 otherwise, and the parameters are specified: ke is the CO2eq emitted to produce a kg/VAh (in this analysis, we approximate this value as 0.06 CO2eq kg/kWh, considering equal the CO2eq released to generate a kWh or a kVAh), EE_{NRE} is the embedded energy in non-recycled PLA (15.28 kWh/kg), while EE_{RE} is the embedded energy in recycled PLA (5 kWh/kg). C_{NRE} is the CO2eq released to produce 1 kg of non-recycled PLA (2.8 CO2eq kg/kg) and C_{RE} for recycled one (0.95 CO2eq kg/kg). Finally, equations 47a-i represent the decisional variables' lower and upper bound. The range is the same as the experimental plan. Since we have studied only this space, we can infer only inside it.

$$\min PT, PE, w, totC, \bar{A}_B, \bar{Q}_B, \bar{A}_A, \bar{A}_{Sp}, \bar{Q}_{Sp}, \bar{A}_P, \bar{Q}_P, \bar{Q}_{Sd}, \bar{R}_{Sd}, \bar{A}_H, \bar{Q}_H, \bar{A}_{Sl}, \bar{Q}_{Sl}, \bar{A}_R, \bar{R}_R, \bar{A}_S, \bar{A}_F, \bar{A}_T \tag{45}$$

$$PT = k_{PT} - \hat{\beta}_{1PT} \cdot WS + \hat{\beta}_{2PT} \cdot S_y + \hat{\beta}_{3PT} \cdot BAS_y + \hat{\beta}_{4PT} \cdot LH + \hat{\beta}_{5PT} \cdot IR + \hat{\beta}_{6PT} \cdot SN + \hat{\beta}_{7PT} \cdot LH \cdot SN + \hat{\beta}_{8PT} \cdot LH \cdot IR + \hat{\beta}_{9PT} \cdot IR \cdot SN \tag{46a}$$

$$PE = k_{PE} + \hat{\beta}_{1PE} \cdot PT + \hat{\beta}_{2PE} \cdot WS + \hat{\beta}_{3PE} \cdot S_y + \hat{\beta}_{4PE} \cdot LH + \hat{\beta}_{5PE} \cdot IR - \hat{\beta}_{6PE} \cdot LH \cdot IR \tag{46b}$$

$$w = k_w + \hat{\beta}_{1w} \cdot S_y + \hat{\beta}_{2w} \cdot BAS_y + \hat{\beta}_{3w} \cdot LH + \hat{\beta}_{4w} \cdot IR + \hat{\beta}_{5w} \cdot SN \tag{46c}$$

$$\bar{A}_B = k_{\bar{A}_B} + \hat{\beta}_{1\bar{A}_B} \cdot S_y + \hat{\beta}_{2\bar{A}_B} \cdot LH + \hat{\beta}_{3\bar{A}_B} \cdot SN + \hat{\beta}_{4\bar{A}_B} \cdot S_y \cdot SN \tag{46d}$$

$$\bar{Q}_B = k_{\bar{Q}_B} + \hat{\beta}_{1\bar{Q}_B} \cdot RE_y + \hat{\beta}_{2\bar{Q}_B} \cdot WS + \hat{\beta}_{3\bar{Q}_B} \cdot S_y + \hat{\beta}_{4\bar{Q}_B} \cdot LH \tag{46e}$$

$$\bar{A}_A = k_{\bar{A}_A} + \hat{\beta}_{1\bar{A}_A} \cdot RE_y + \hat{\beta}_{2\bar{A}_A} \cdot WS + \hat{\beta}_{3\bar{A}_A} \cdot S_y + \hat{\beta}_{4\bar{A}_A} \cdot IR + \hat{\beta}_{5\bar{A}_A} \cdot BAS_y \cdot WS + \hat{\beta}_{6\bar{A}_A} \cdot BAS_y \cdot S_y + \hat{\beta}_{7\bar{A}_A} \cdot BAS_y \cdot RE_y \tag{46f}$$

$$\bar{A}_{Sp} = k_{\bar{A}_{Sp}} + \hat{\beta}_{1\bar{A}_{Sp}} \cdot WT + \hat{\beta}_{2\bar{A}_{Sp}} \cdot PT + \hat{\beta}_{3\bar{A}_{Sp}} \cdot WS - \hat{\beta}_{4\bar{A}_{Sp}} \cdot S_y + \hat{\beta}_{5\bar{A}_{Sp}} \cdot LH + \hat{\beta}_{6\bar{A}_{Sp}} \cdot LH \cdot PT + \hat{\beta}_{7\bar{A}_{Sp}} \cdot LH \cdot S_y + \hat{\beta}_{8\bar{A}_{Sp}} \cdot PT \cdot S_y \tag{46g}$$

$$\bar{Q}_{Sp} = k_{\bar{Q}_{Sp}} + \hat{\beta}_{1\bar{Q}_{Sp}} \cdot WT + \hat{\beta}_{2\bar{Q}_{Sp}} \cdot SN + \hat{\beta}_{3\bar{Q}_{Sp}} \cdot LH \cdot WS \tag{46h}$$

$$\bar{A}_P = k_{\bar{A}_P} + \hat{\beta}_{1\bar{A}_P} \cdot PT + \hat{\beta}_{2\bar{A}_P} \cdot WS + \hat{\beta}_{3\bar{A}_P} \cdot LH + \hat{\beta}_{4\bar{A}_P} \cdot IR \tag{46i}$$

$$\bar{Q}_P = k_{\bar{Q}_P} + \hat{\beta}_{1\bar{Q}_P} \cdot RE_y + \hat{\beta}_{2\bar{Q}_P} \cdot WT + \hat{\beta}_{3\bar{Q}_P} \cdot WS + \hat{\beta}_{4\bar{Q}_P} \cdot SN + \hat{\beta}_{5\bar{Q}_P} \cdot RE_y \cdot WT + \hat{\beta}_{6\bar{Q}_P} \cdot LH \cdot PT \tag{46j}$$

$$\bar{Q}_{Sd} = k_{\bar{Q}_{Sd}} + \hat{\beta}_{1\bar{Q}_{Sd}} \cdot WS + \hat{\beta}_{2\bar{Q}_{Sd}} \cdot LH + \hat{\beta}_{3\bar{Q}_{Sd}} \cdot SN + \hat{\beta}_{4\bar{Q}_{Sd}} \cdot SN \cdot LH + \hat{\beta}_{5\bar{Q}_{Sd}} \cdot RE_y \cdot LH \tag{46k}$$

$$\bar{R}_{Sd} = k_{\bar{R}_{Sd}} + \hat{\beta}_{1\bar{R}_{Sd}} \cdot LH + \hat{\beta}_{2\bar{R}_{Sd}} \cdot LH \cdot WS \tag{46l}$$

$$\bar{A}_H = k_{\bar{A}_H} + \hat{\beta}_{1\bar{A}_H} \cdot WS + \hat{\beta}_{2\bar{A}_H} \cdot LH \cdot WT + \hat{\beta}_{3\bar{A}_H} \cdot WS \cdot WT \tag{46m}$$

$$\bar{Q}_H = k_{\bar{Q}_H} + \hat{\beta}_{1\bar{Q}_H} \cdot LH + \hat{\beta}_{2\bar{Q}_H} \cdot SN \tag{46n}$$

$$\bar{A}_{Sl} = k_{\bar{A}_{Sl}} + \hat{\beta}_{1\bar{A}_{Sl}} \cdot LH + \hat{\beta}_{1\bar{A}_{Sl}} \cdot LH \cdot SN + \hat{\beta}_{1\bar{A}_{Sl}} \cdot RE_y \cdot SN + \hat{\beta}_{1\bar{A}_{Sl}} \cdot RE_y \cdot LH \tag{46o}$$

$$\bar{Q}_{Sl} = k_{\bar{Q}_{Sl}} + \hat{\beta}_{1\bar{Q}_{Sl}} \cdot BAS_y + \hat{\beta}_{2\bar{Q}_{Sl}} \cdot LH \tag{46p}$$

$$\bar{A}_R = k_{\bar{A}_R} + \hat{\beta}_{1\bar{A}_R} \cdot BAS_y + \hat{\beta}_{2\bar{A}_R} \cdot LH + \hat{\beta}_{3\bar{A}_R} \cdot BAS_y \cdot LH \tag{46q}$$

$$\bar{R}_R = k_{\bar{R}_R} + \hat{\beta}_{1\bar{R}_R} \cdot LH \cdot BAS_y + \hat{\beta}_{2\bar{R}_R} \cdot LH \cdot WS + \hat{\beta}_{3\bar{R}_R} \cdot RE_y \cdot LH \tag{46r}$$

$$\bar{A}_S = k_{\bar{A}_S} + \hat{\beta}_{1\bar{A}_S} \cdot RE_y + \hat{\beta}_{2\bar{A}_S} \cdot WT + \hat{\beta}_{2\bar{A}_S} \cdot RE_y \cdot WT \tag{46s}$$

$$\bar{A}_F = k_{\bar{A}_F} + \hat{\beta}_{1\bar{A}_F} \cdot S_y + \hat{\beta}_{2\bar{A}_F} \cdot PT \cdot SN \tag{46t}$$

$$\bar{A}_T = k_{\bar{A}_T} + \hat{\beta}_{1\bar{A}_T} \cdot BAS_y + \hat{\beta}_{2\bar{A}_T} \cdot LH + \hat{\beta}_{3\bar{A}_T} \cdot S_y \cdot SN + \hat{\beta}_{4\bar{A}_T} \cdot SN \cdot LH \tag{46u}$$

$$totC = ke \cdot EE_{RE} \cdot w \cdot RE_y + C_{RE} \cdot w \cdot RE_y + ke \cdot EE_{NRE} \cdot w \cdot (1-RE_y) + C_{NRE} \cdot w \cdot (1-RE_y) + ke \cdot PE \tag{46v}$$

$s.t$

$$\{RE_y \in \mathbb{N} | 0 \leq RE_y \leq 1\} \tag{47a}$$

$$\{WT \in \mathbb{R} | 200 \leq WT \leq 215\} \tag{47b}$$

$$\{PT \in \mathbb{R} | 25 \leq PT \leq 50\} \tag{47c}$$

$$\{WS \in \mathbb{R} | 40 \leq WS \leq 80\} \quad (47d)$$

$$\{BAS_y \in \mathbb{N} | 0 \leq BAS_y \leq 1\} \quad (47e)$$

$$\{S_y \in \mathbb{N} | 0 \leq S_y \leq 1\} \quad (47f)$$

$$\{LH \in \mathbb{R} | 0.1 \leq LH \leq 0.3\} \quad (47g)$$

$$\{IR \in \mathbb{R} | 10 \leq IR \leq 60\} \quad (47h)$$

$$\{SN \in \mathbb{N} | 1 \leq SN \leq 3\} \quad (47i)$$

4.5.2 Optimization Results

In order to find the best solution, we implemented the problem in Python using the pymoo library [135]. In particular, we used the NSGA-II algorithm [136]. In the literature, it is possible to find some recent applications of NSGA-II on additive manufacturing optimization. E.g., in [137], the authors used the same algorithm to find a frontier of solutions that minimize the time and material consumption while keeping a sufficient level of ultimate tensile strength and surface roughness. Matos et al. studied the best manufacturing positioning while optimizing the support area, the manufacturing time, the surface roughness, and the surface quality using an NSGA-II algorithm [138].

The algorithm NSGA-II generates an initial population P_t of solutions with dimension N. Then a mutation operation is performed to create an offspring O_t of size N. The two populations, P_t and O_t, are combined to form Z_t. Then the solutions are sorted according to non-domination criteria; each solution front is ranked according to this criterion. The following population P_{t+1} is generated, taking the first-ranked front. If the first front is less than N, other solutions are taken from the least crowded region of the second front, and this procedure continues by the lower ranked fronts until a P_{t+1} population of size N is obtained [136].

The new offspring O_t, depends on two operators: the crossover probability X and the mutation probability M. Finally, to find the best solutions, four different factors have to be set: the population (N), the crossover (X) and the mutation (M)

and the number of generations to be tested (G). In the literature, it is possible to find different suggestions and methods for choosing these parameters. According to Schaffer et Al., a mutation probability higher than 0.05 never drives good results, and M of 0.005 and a X between 0.95 and 0.65, even with a small population, is suggested [139]. For these reasons, we decided to set a M = 0.005 and a X equal to 0.95. Finally in order to increase the probability to reach te convergence we set a number of generation G equal to 1000.

According to the literature, the larger the initial population, the more efficiently the algorithm finds the optimal front [140]. For this reason, we tested the difference between the optimal frontier obtained with a N equal to 1000, 35, 30 and 20. The difference between the first (N =1000) and the second (N = 35) is meagre: looking for the best solution in each performance, these were practical all the same, and only one deviated by less than 2%. While testing the first with the third, all values were identical except for one value that differed by about 10%. Finally, as expected, we got the worst results with a population of only 20 solutions. The average deviation from the first run was 20%, with peaks at 117%. For this reason, we can assume that the best value for N would be between 30 and 35. So, for this reason, we fixed N equal to 35, testing 35000 solutions. The obtained solutions are represented in **Error! Reference source not found.**.

Table 23 - Parameters of the 35 solutions

Solution ID	BAS	RE	S	SN	WT (°C)	PT (°C)	WS (mm/s)	LH (mm)	IR
1	1	0	1	1	212.95	50	40	0.1	60%
2	0	1	1	3	210.07	49.98	80	0.3	59%
3	0	0	0	1	214.72	49.67	80	0.1	52%
4	0	1	1	3	215	28.66	40	0.1	60%
5	1	1	0	1	200	25.63	80	0.3	22%
6	0	1	0	1	203.6	28.29	41.49	0.1	10%
7	1	0	1	3	200.43	25	80	0.1	10%
8	1	1	0	3	214.18	50	40.01	0.3	60%
9	0	0	0	3	210.31	49.3	80	0.3	10%
10	1	1	1	1	215	27.26	80	0.3	56%
11	1	0	1	3	213.16	26.92	40	0.3	60%
12	0	1	1	1	214.97	25.4	40	0.1	60%
13	1	0	1	3	200	49.99	40.01	0.3	55%
14	0	1	1	1	215	28.5	78.98	0.1	60%
15	0	0	0	1	215	25.03	80	0.1	10%
16	1	0	0	1	200.76	25.11	80	0.3	18%

17	0	1	1	3	215	28.5	40	0.1	60%
18	0	0	1	1	215	28.45	79.99	0.1	10%
19	0	0	0	1	201.36	25.04	40.24	0.3	15%
20	0	1	1	3	200	49.9	40	0.1	12%
21	1	0	1	1	214.05	48.36	40	0.3	60%
22	0	0	1	3	200.02	49.97	40.96	0.1	16%
23	1	1	1	3	214.94	26.89	40	0.3	60%
24	1	0	0	3	200.43	25	80	0.1	10%
25	0	1	0	3	214.25	49.97	77.76	0.3	18%
26	1	0	1	1	200.93	25	79.98	0.12	13%
27	0	1	0	1	214.73	25	80	0.3	10%
28	1	0	1	3	200	25	40	0.1	59%
29	0	1	1	3	215	50	80	0.3	57%
30	1	1	1	3	201.08	26.35	40	0.1	60%
31	1	1	1	1	213.98	48.14	40	0.3	60%
32	0	0	0	1	210.86	25.68	80	0.3	10%
33	1	0	0	1	214.72	49.67	80	0.1	58%
34	0	0	1	3	200.21	50	40	0.3	60%
35	1	1	0	3	212.7	49.29	40.01	0.29	60%

The space of solutions seems well varied and well explored. There are no similar solutions. However, it looks interesting to see that the optimal solution is often at the extremes of the parameter. This phenomenon is particularly true since the models tend to be linear.

4.5.3 Multi-Criteria Decision Method

Once the result is obtained, the second problem is determining the best solution. For this reason, we proposed a methodology to use this solution and help the designer decide. We proposed a visual method in order to facilitate decision-making.

The heatmap presented in Figure 29 represents the 35 different solutions obtained through the optimization algorithm. On the x-axis are present the 22 performances, while the y-axis shows the solution ID between 1 to 35. In each square, the value of the performance is represented using a colour scale from red to green. The best performance is represented with the green colour, while the worst one is in red. This chart can be used as a map for the designer to choose the best parameters and can be made available near the workstation or machine.

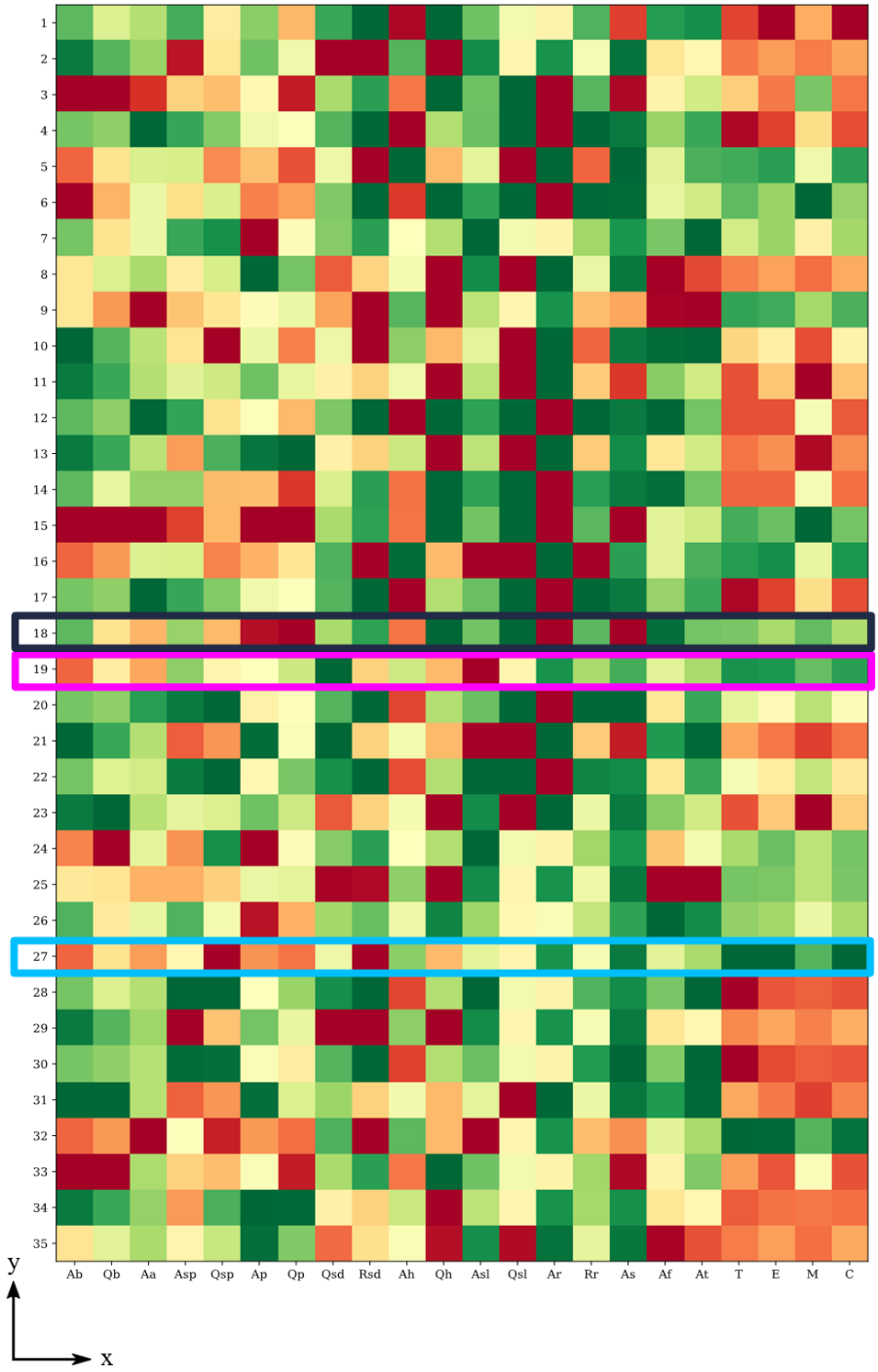

Figure 29 - Solution Heatmap with solutions 18, 19, and 27 highlighted (the last three variables, T, E, M, and C, stand for process time, energy consumption, material consumption, and CO_2eq)

For instance, if the designer has to produce a part with a bridge in the lesser time possible. A possible approach could be to see the dark green square

corresponding to the non-dominated solutions in the T column. Solution 27 (light blue) seems to be the faster one. Nevertheless, analyzing the Ab and Qb columns, we immediately see that the corresponding quality of the bridge is low. Solution 18 (navy blue) is sufficiently fast and has a satisfactory accuracy index. Finally, after thoroughly analyzing the results, it is possible to find solution 19 (magenta), which seems to be an average process time and a good bridge quality as a whole. The three proposed solutions are graphically depicted in Figure 30 and Figure 31. The former represents the status of the nine parameters in each solution, and the latter shows the value of the 22 performances. The three solutions are presented as a single-colored line (navy blue for solution 18, magenta for 19, and light blue for 27, they are also highlighted in Figure 29 with the same colors). The y-axis of the two images is normalized to represent the top and bottom levels efficiently. While in Figure 31, the y-axis is also inverted since the objective is to minimize the 22 performances, this representation can be straightforwardly understood, and the better value is on top of the graph.

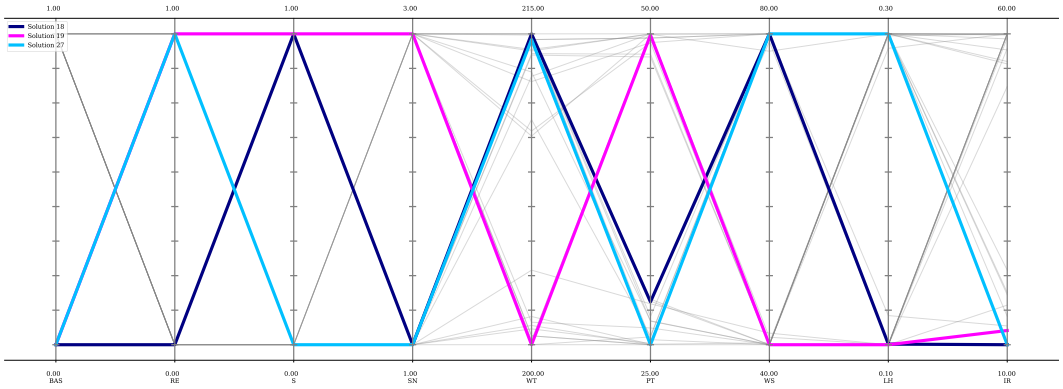

Figure 30 - Parameter selection of solutions 18, 19 and 27

As can be seen from Figure 30, the three solutions differ significantly from each other. None of the three needs a base, those with better arcs require support and have a lower layer height. In comparison, the fastest one has all the parameters set to finish as fast as possible: no base or support, only one shell number, high working speed, high layer height, and an infill rate of 10%.

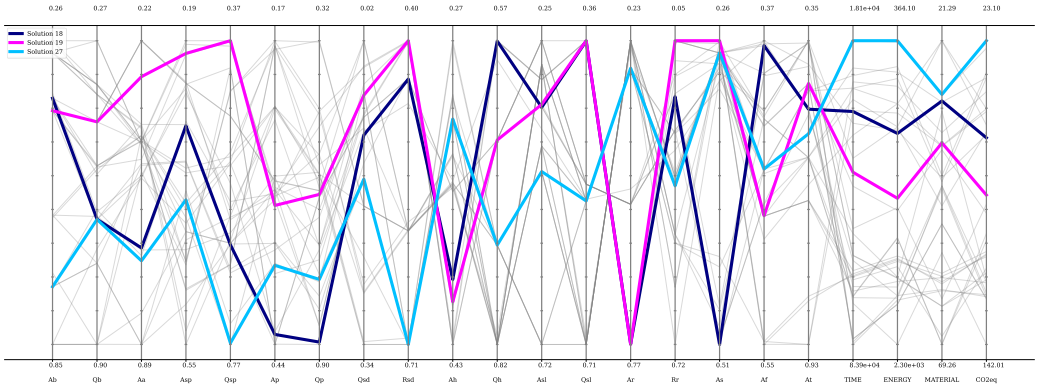

Figure 31 - Performance Representation of solutions 18, 19, and 27.

The designer should be able to decide which solution is most suitable for him, looking at Figure 31. The fastest one (27) should be enough if it is just a tester or a prototype. If he is not interested in the externally perceived quality, solution 18 can guarantee good accuracy in a short time. While if a good arc is needed, the best solution is the 19.

4.6 Conclusions and Future Developments

The paper proposes a methodology for generating knowledge in OKP additive manufacturing contexts. In such a context, testing and manufacturing various parts to evaluate the best set of production parameters is not allowed. Therefore, the designer needs decision support tools. The method presented aims to study the product both in terms of production cost (seen as consumption of energy, time, and matter) and environmental impact (evaluated by a semi-quantitative method that can estimate the CO2eq emitted) and quality, assessed through three metrics representing accuracy, resolution, and subjective perceived quality.

The methodology aims to model the impacts of parameters on the described performance through a statistical-empirical analysis. The regression models are finally used to find a set of Pareto non-dominated solutions. Ultimately, these solutions are implemented in a visualization-based decision-making support procedure.

The main limitation of the present work is the lack of validation of the method through the design of a real part. This validation can undoubtedly be a future work assuming that the heatmap presented can be used to support the design work of a

new product. A second limitation of the work is the developed benchmark. It has no joints, threaded parts, etc., and is limited to analyzing some basic geometric shapes. In addition, no analysis of the mechanical properties of the part was conducted. Mechanical performance obviously generates additional variability and complexity in the study. However, having information on this is of critical importance to the designer. Finally, we did not manage to find a satisfactory model for some performances, and some quality models can explain just a low amount of variability. According to [44], a simple regression model combined with physic/equation-based modeling can outperform machine learning approaches in small dataset applications. Generating large datasets to test manufacturing could often prove inconvenient, particularly in OKP productions. Combining the proposed experimental approach with physic-based models can be interesting as a future improvement.

In the next chapter, we present the final case study based, whose primary purpose is to study the feasibility of an innovative warehouse picking system.

Chapter 5

Sustainable Warehouse Picking

5.1 Introduction

Warehouses allow regulating the company's flow of goods, both inbound and outbound. It consists of handling and storing equipment and products, and both human and capital resources are involved. We can identify five main processes carried out within it: (i) receiving, (ii) transfer and storing, (iii) accumulation, (iv) sortation, (v) order picking, (vi) cross-docking, and (vii) shipping. The first involves the arrival of the unit load in the warehouse. Subsequently, the items are transferred to the appropriate area, stored, accumulated, sorted, and finally picked and shipped or traversed through a cross-docking area [141].

Warehouse operations management can be very complex and plays a critical role in order to avoid inefficiencies that can be reflected throughout the production process. Sufficient space is needed to optimize stock handling, cart movement, and loading and unloading procedures. Generally, the operation that requires the most significant workforce commitment and so has the highest cost is order picking [142]. For all these reasons, warehouse management represents a fundamental part of the internal organization of a company's supply chain. In recent years, it has become necessary to find solutions that allow improvements in the performance of the entire production chain. In this regard, several works have been developed that analyze the key performance indices (KPIs) used to evaluate the operations performed and improve their performance.

Sustainable warehouses provide a storage management service that satisfies customers by trying to produce as little environmental impact as possible and operating socially responsibly. Climate change is one of the greatest threats of the 21st century and, as such, is of concern to both companies and the public. For this reason, companies are looking for solutions that limit greenhouse gas emissions into the atmosphere in any process (e.g., by promoting green logistics). This sustainability is achieved through sustainable management of resources (energy,

water, raw materials) and the use of renewable energies. In fact, in recent years, the concept of sustainability has evolved profoundly to ensure the availability and quality of natural resources (environmental sustainability), the quality of life and safety of citizens (social sustainability), and the economic efficiency of businesses (economic sustainability). For example, while energy consumption and consequent emissions have continually increased, transportation and storage are perceived as essential drivers of environmental pollution in global supply chains.

5.2 Automated Warehouse System

In this paragraph, we first introduce the essential automated warehouse systems, emphasizing the picking task. Then we focus on the studies that have shown interest in evaluating warehouse performances through discrete-event simulation.

5.2.1 AWS for storing, retrieving, and picking activities

Since their initial introduction in the 1950s, Automated Storage and Retrieval Systems (AS/RS) have been a critical factor in assuring significant improvements in material handling, enhancing businesses' flexibility and competitiveness [143]. It is crucial to emphasize the increased accuracy in material handling control, inventory space efficiency, and improved responsiveness and speed during unit loads storing and retrieval among the many benefits of AS/RS [144].

Over time, the introduction of automated solutions made it possible to simplify tasks like choosing, retrieving, and storing unit loads. The necessity to store SKUs in particular places inside a warehouse is referred to as store operations. They can adhere to various regulations, from predetermined to arbitrary position allocations [145]. The order-picking tasks include retrieving SKUs and selecting the appropriate number of items in response to consumer demand to generate a non-homogeneous UL [145]. Picking activities can be accomplished in various methods, some of which require human intervention (picker) and others totally automated. In [146], it is possible to find an extensive review of the most diffused automated picking methods, e.g., parts-to-picker, in which an AS/RS brings the items to a picking area or the robots-to-part and the parts-to-robot, the first one is an AGVcarring a robot and it is the main object of this analysis. In Figure 32, the principal order picking systems are classified. In this paragraph, we focus on semi-automated technologies, Parts-to-Pikers, and fully automated technologies, Robots-to-Parts.

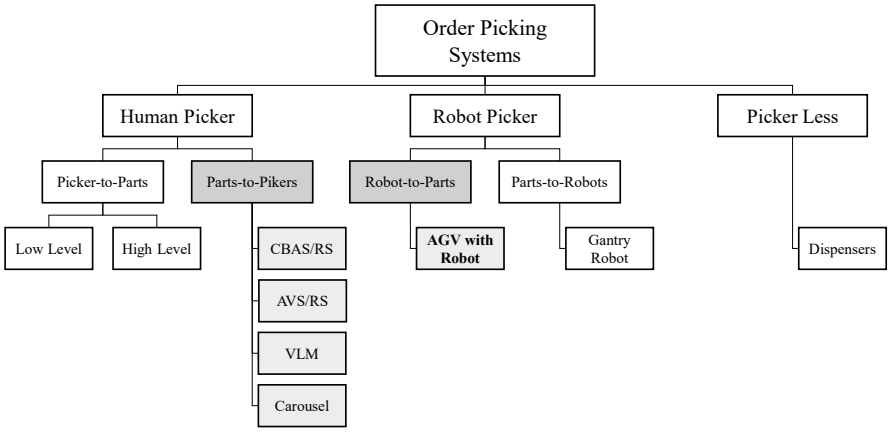

Figure 32 – Classification of the principal order picking systems, elaboration from Jaghbeer et al. [146].

CBAS/RSs (Crane-Based Automated Storage and Retrieval Systems) were the first AS/RSs to be developed. They consist in automated cranes that may move vertically and horizontally along warehouse aisles at the same time [142]. Single-deep and multi-deep storage may be utilized with crane-based systems; the cranes are fitted with double-deep telescopic prongs to make working on multi-deep storage easier [142]. The crane system is complemented for multi-deep storage by a few conveyors that make storing and retrieving pallets easier. The system is much more portable and is known as a mini-load automated storage and retrieval system if the objects being stored are totes rather than pallets [142].

Compared to the automated system based on cranes, the AVS/RS (Automated Vehicle Storage and Retrieval Systems) system offers even more versatile possibilities. Since the shuttles used to store and retrieve pallets are substantially lighter than cranes, the AVS/RS improves overall throughput while reducing energy usage [147]. The system consists of shuttles designed for horizontal movement and lifts intended for pallet or vertical shuttle movement. Both tier-captive and tier-to-tier AVS/RS systems are possible. Each tier in the first arrangement includes a dedicated shuttle responsible for storing or retrieving the pallet at that particular tier level. In the second arrangement, the lift that permits vertical movements can be used by the shuttle to go between several stages.

Vertical and horizontal carousels, often used for medium and small items, are another form of AS /RS. They consist of racks that rotate horizontally or vertically and bring the appropriate components to the picker in the retrieval sequence [142].

VLMs (Vertical Lift Modules) are similar to carousels, but they have two storage columns and a lifting crane in the middle that selects the correct goods and brings them directly to the picker [142].

As aforementioned, CBAS/RS, AVS/RS, VLM, and Carousel fall into those systems that bring parts to the picker to perform the picking activity, but picking may also be done by a robot that travels in the warehouse and chooses the suitable SKU in the correct number. The feasibility of this novel picking system is demonstrated by Kimura et al. [148], which mounts a robotic dual-arm on an AGV to provide flexible picking for a warehouse with high mixed inventory.

5.2.2 Discrete Event Simulation in the context of automated warehouses for order picking activities

Discrete event simulation and the development of analytical models, tested and validated through simulation, are the two main approaches that have been used to identify the best warehouse design configuration and evaluate its performance [149]. This second section of the literature review on AWS concentrates on the most critical studies that employ discrete event simulation (DES) and on studies that combine DES and other techniques. As expected, discrete event simulation is often used in the AV/RS literature. In particular, the articles are arranged into five clusters: (i) DES applications on CBAS/RS, (ii) DES applications on AVS/RS, (iii) DES applications on VLM, (iv) DES to compare different AS/RS typology and finally, (v) AS/RS design evaluation through other methodologies validated using DES.

5.2.2.1 DES applications on CBAS/RS

An interesting work on automated crane-based storage and retrieval systems is proposed by Colla et al. The authors used discrete-event simulation to evaluate the best storage policy, i.e., FIFO reordering, stack reordering, and space reordering. Several KPIs are monitored, like throughput, average stock, receptivity, handling potentiality, and fragmentation as a measure of space breakup [150].

[151] examines how the storage policy (random or cross-aisle full turnover) affects the performance of a crane-based automated system. Regardless of how many aisles or how many SKUs are considered, the study shows that a random storage policy improves the expected travel time per order.

In order to support the crane-based warehouse design, Lerher T et al. (2014) proposed a DES-based methodology. Travel time, throughput, and cost are thoroughly covered in the literature. For this reason, the study primarily concentrates on energy usage. The model shows that high-speed profiles led to higher CO_2 emissions [152]

5.2.2.2 DES applications on AVS/RS

An example of discrete event simulation to study AVS/RS can be found in the work of Lerher T. et al. [153]. They evaluated how the racking configuration (number of levels, number of aisles, number of columns, and therefore length and height of storage racks) and the speed of shuttles and lifts affected the performance of an AVS/RS, also known as SBS/RS, a component of AV/RS. The study concluded that the lift throughput multiplied by the aisles determines the system's throughput capacity. As a result, the system's throughput should increase if the number of floors is reduced and the number of aisles is increased. [153]. A later study by Lerher T. et al. attempted to deepen the analysis of SBS/RS performance [154]. In their work, the authors developed a discrete event simulation to evaluate the performance of an SBS/RS system, focusing on the system throughput. Nine different rack configurations were studied, and the system's throughput capacity was recorded. It was found that the whole system's performance is highly dependent on the racking configuration (number of tiers, aisles, and columns) and the shuttle/lift speed, which is, however, limited by physical constraints[154]. Since the study focuses only on throughput performance, it lacks considerations of energy consumption and recovery, which have some influence when decisions have to be made about the optimal design of the system and its environmental sustainability.

Ekren et al. propose a similar study. They use discrete event simulation to analyze the utilization of shuttles and lifts and the retrieval and storage cycle time as of an SBS/RS. The study makes some interesting contributions to warehouse design and identifies the best rack configuration for class-based storage policy through 10 different iterations of the simulation model. The authors highlighted that the study might be improved if various arrival rates and speed profiles for shuttles and lifts were included. [155].

In other studies, cycle time seems to be the main element to describe the performance of an AVS/RS System, as shown in [156]. The authors employed discrete event simulation to find the best combination of vehicles and lifts with pre-defined rack configurations. The performance measures used to evaluate each scenario are cycle time, utilization of vehicles, and utilization of lifts. It has been

concluded that the design with the more significant number of lifts performs better than the other scenarios, maintaining a fixed number of vehicles [156]. It is essential to underline that this study is not complete and exhaustive because it does not include considerations of costs.

Marchet et al. included some cost considerations in their study [157]. In their paper, discrete event simulation is used to understand the optimal racking configuration (number of aisles, tiers, and columns) for an AVS/RS autonomous warehouse. KPIs such as throughput, lead time, and cost were monitored during the simulation. The results indicate that rack configuration has an impact on throughput. Different bottlenecks can be identified depending on how many tiers or columns the storage area has. If the warehouse develops in height, the bottleneck may be the elevator so that the throughput of the aisle is equal to the throughput of the elevator. On the other hand, if the warehouse system has longer corridors and fewer floors, the bottleneck may be the vehicle. Similar to the previous case, the throughput of an aisle is then equal to the throughput of the vehicle [157]

Kriehn et al. used discrete event simulation to observe the changes in throughput in SBS/RS systems when specific memory management policies are applied instead of random memory allocation. The study's results indicate that system throughput increases significantly when class-based storage, retrieval order sequencing, and storage reorganization are introduced either individually or, in some cases, in combination. Their analysis also involves energy consumption, and they stated that the three proposed strategies could lead to lower energy consumption as a desired secondary effect [158]

In [159], it is possible to find a study with a focus on environmental sustainability. Different warehouse configurations were tested in their work to select the one that guaranteed the highest vehicle utilization and the lowest energy consumption considering an AVS/RS system. A discrete event simulation was implemented, and 81 scenarios differing in rack configuration were analyzed. It was found that energy consumption decreases when the warehouse is characterized by low floors and a high number of aisles. When the number of floors or columns increases, energy consumption also increases [159].

Lerher T. et al. performed a simulation-based Design of Experiments (DoE) applied to shuttle based AS/RS to identify the optimal parameters to maximize the throughput. The study concluded that different factors affect throughput, i.e., the number of columns and the speeds and accelerations of shuttles and lifts. The study

let these factors vary to see what the final throughput would be, and it has been observed that the best scenario is the one with the smallest number of columns and the highest number of tiers [160].

5.2.2.3. DES in the context of VLM

Rosi B. et al. explored how modifications to the lift's velocity profile and the VLM's size affect the performance of a single-tray VLM. The study compared the throughput of 4 distinct VLM configurations using discrete event simulation, and it concluded that throughput increases as VLM height decreases and lift velocity rises [161]

Battini D. et al. (2016) employ discrete event simulation to figure out how to increase throughput in a dual-tray vertical lift system. The simulation creates 10,000 random picking orders and compares different storage policies given a certain set of VLM features. It has been noted that Class-Based Storage, which keeps frequently used goods near the retrieval, has a positive impact on system throughput. The study also clarifies how the operator might improve system performance by employing batch order picking [162].

5.2.2.4 DES used to compare different AS/RS

In this section, we present studies that are broader in their analysis and involve and compare different technologies. Ekren et al. (2012), for instance, propose and discrete event simulation approach to compare the performance of an AVS/RS and CBAS/RS. In this work, the scholars focalize their analysis on tier-to-tier AVS/RS systems and aisle-to-aisle CBAS/RS. They generate 198 scenarios using considering choosing as analysis factors the number of vehicles, lifts, cranes, aisles, bays, tiers, and two demands. In contrast to the research already discussed, the range of KPIs is substantially greater in this instance. They monitored the average flow time, the system's average utilization, the average waiting time in the queue, the average number of jobs in the queue, and the system cost. The study's outcome demonstrated that AVS/RS system performs better than CBAS/RS. Furthermore, it is revealed that AVS/RS usually have fewer jobs waiting in a queue and shorter waiting times compared to CBAS/RS. Despite this, the authors point out that AVS/RS is generally much more expensive than a CBAS/RS system [163].

Bruno et al.decided to shift the focus to the concept of environmental sustainability in the evaluation of AVS/RS performance. They evaluate as KPIs the energy consumption combined with cycle time and system utilization. The study compares traditional CBAS/RS with AVS/RS. A conceptual model is first

developed, and then it is implemented through Discrete event Simulation. The results show that AVS/RS, besides giving benefits in terms of improved cycle time, also considerably reduces energy consumption [164].

Another recent analysis of energy consumption is proposed by Guerrazzi E. et al. In their article, they observed through a DES model that the utilization of AVS/RS can allow energy savings of up to 60% compared to CBAS/RS [165].

5.2.2.5 Design and performance evaluation of AS/RS with other methodologies validated through DES

Often, simulation is combined with other approaches like analytical modeling. One of the first studies linked to AVS/RS performance evaluation is given by the work of Malmborg, where an analytical model has been developed to estimate AVS/RS performance in terms of cycle time and vehicle utilization under different rack configurations. The study aims at comparing AVS/RS with AV/RS performance. The analytical model is then validated through simulation [166].

Eder M. and Kartnig G. developed an analytical model to determine the best rack configuration and geometry capable of achieving the higher throughput for an automated storage retrieval system based on shuttles. Discrete Event simulation through is used in this study to validate the analytical model. The analytical model suggests that as the height and length of the racks increase, the throughput at first improves up to a certain point, after which it worsens [167]

In [168], an analytical model is used to calculate the cycle time and throughput of a multi-tire AVS/RS, and a discrete event simulation validates the results analytically. This study could be particularly beneficial during the system design stage as it gives valuable insights into the best rack configuration and speed profile of devices [168].

5.2.3 Research Gaps and Research Aim

To the best of our knowledge, no articles use the Discrete Event Simulation to evaluate the feasibility and performance of a robot-to-parts system. Several studies use other methodologies, like mathematical models, to estimate their cost, lead time, or flexibility [146]. For this reason, we decided to focus this study on the impact different parameters can have on an AVS/RS robot-to-parts system and evaluate its performances from economic and environmental sustainability perspectives. The new automated system will consist of a shuttle with a robotic arm installed on it. It will therefore try to combine the activities already performed by

an AVS/RS with the activities of picking to create personalized pallets in the most modular and flexible way. This system enhances the AVS/RS's potential by enabling it to build mixed pallets based on the demand orders. This structure will equip the system with the skill to handle stock units of different dimensions, from pallets to small items. Moreover, implementing this system would eliminate the need for a dedicated picking area where operators manually pick the relevant units.

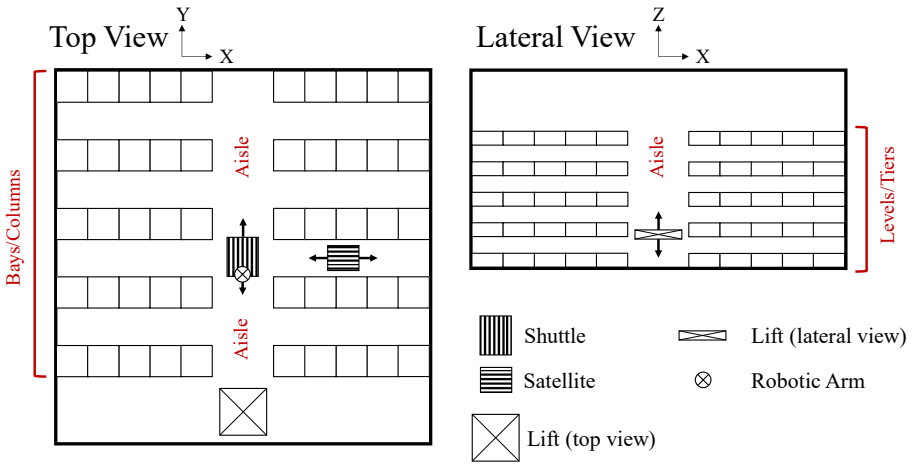

Figure 33 - Scheme of the AVS/RS object of the study.

Figure 33 shows the scheme of the studied AVS/RS. A lift moves the shuttles and the coupled satellites in each aisle on the Z-axis. The shuttles move along the aisle on Y-axis. Each shuttle is associated with a satellite moving along the X-axis bays. A robotic arm is placed on each shuttle to make the mixed pallet satisfy the order.

5.3 Methodology

The proposed methodology consists of two different parts. The first one is intended to generate new knowledge on the process, while the second one is intended to find an optimal solution for the case study.

As previously described, in order to generate new knowledge, we can use (a) computer simulation to test design aspects' impact on final product performances (hybrid approach), (b) use an analytical model based on physical law (theoretical approach), and (c) use an experimental data-driven approach (empirical approach). Since the object of this study is to evaluate the performance of a warehouse, an empirical approach would be impossible due to the high costs. Since we cannot generate a completely analytical approach to the warehouse since it would be too

complex, the most suitable solution is to use the hybrid way and develop a simulation model.

The proposed methodology is displayed in Figure 34. The first step consists in defining some performances to be analyzed and the relative parameters we want to assess. To find the most suitable performances, we performed an extensive literature review. Then, according to all these variables, we define a Design of Experiment (DoE) to investigate the impact of the selected parameters on the performances. In order to create an empirical regression model that connects the parameters mathematically with the performances, STEP 1 concludes with the statistical analysis of the dataset that was obtained. The compression of the design space is the first step in STEP 2. It is necessary to eliminate any parameters that have no effect. The same must be done with consistent performances throughout all experiments. A multi-objective optimization problem is thus developed, and the designer is then able to decide with foresight owing to the results. In order to decide the most suitable solution, we proposed a methodology called TOPIS, capable of sorting the best solution based on user preferences.

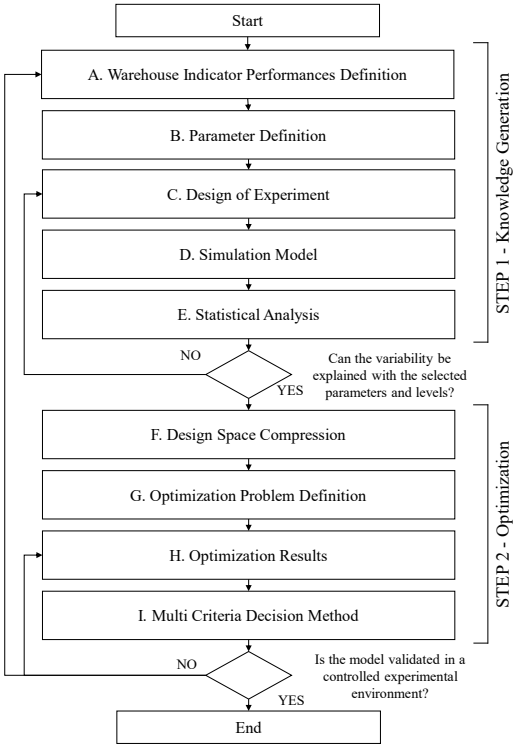

Figure 34 - Warehouse Case Study Methodology

With the proposed methodology in Figure 34 we validate the hybrid approach of the general framework. Figure 35 shows the crucial aspects validated with a dashed line with this third use case. The phases between A to C compose the design space definition. Phases D and E are the two pillars of the knowledge generation phase using a hybrid approach. Phases G and H are meant to find the optimal solutions, and finally, phase I is needed to support the designers in finding the most suited solution.

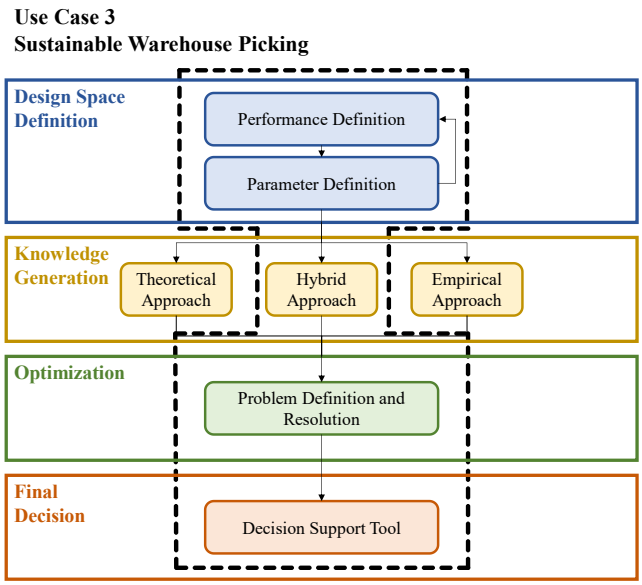

Figure 35 - General framework on the warehouse use case

5.4 Warehouse Indicator Performances Definition

The first step of this work aims to propose a set of indicators in order to evaluate the sustainability of warehouse systems from the different points of view of the Triple Bottom Line (TBL), the environmental, economic, and social sustainability [33]. In order to pursue this aim, we relied on 70 indicators found by Faveto et al. through a review of over 200 scientific articles [66]. We expanded the search to provide greater robustness to what was found. Subsequently, we introduced new indicators we felt were missing from the previous analysis through this second research. We have provided a definition, a unit of measurement, an approximate formulation, and some examples of application for each of the proposed indicators. Finally, the indicators have been ranked according to different metrics.

According to Roberts's Measurement Theory, when a phenomenon is studied, it is possible to define an empirical relational system like $U = \langle A, R, O \rangle$, in which $A = \{a_i\}$ is the set of all possible instances of the phenomenon, $R = \{r_i\}$ and $O = \{o_i\}$ are respectively the sets of possible empirical relations and operations on A. A relational system like $B = (N, S, P)$, where N is a set of numbers ($\mathbb{N}$, $\mathbb{R}$, $\mathbb{Q}$, etc.), S is a set of mathematical relation ($<$, $>$, $=$, etc.) and P is a set of mathematical operations ($+$, $\div$, $\times$, etc.), is called numerical relational system [169]. The term 'to measure' means creating an empirical relational system map in a numerical relational system, keeping all the relations and operations real. A measure is a

homomorphism of A into N and an isomorphism of R into S and O into P [169]. It also is possible to make a homomorphic map of an empirical relational system without the isomorphic map of relations and operations. This map could be called an indicator [170]. A performance indicator is a numeric value that represents a complex empirical phenomenon. For adequate support to decision-making processes, it is necessary to evaluate performances to give insights to the management office. The elementary data gathered by sensors or operators must be aggregated into valuable tools representing system performance [171]. The use of indicators is strictly linked to three different aims: (i) to assess the current status of a process in order to compare it with a benchmark, (ii) to continuously monitor the progress of a particular process in a specific time frame, and (iii) to evaluate the impact of a particular strategy or change by measuring the KPI in two different moments. A graphical representation of these three purposes is displayed in Figure 36.

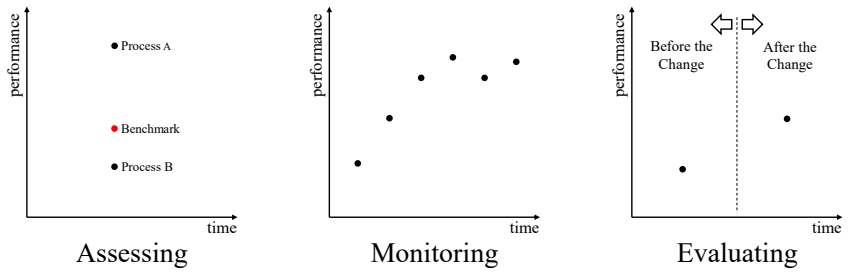

Figure 36 - The three main aims of key performance measurements

In the past few years, some scholars have focused their research on performance in order to provide an extensive set of sustainability KPIs that can be used as a valuable tool in a particular field of knowledge. One of the most used methodologies to pursue this aim is the systematic analysis of literature. For instance, [172], through literature analysis, discovered 55 sustainability indicators. It arranged them into five different clusters and ranked them based on their usefulness and practicality. At the same time, in [173], the authors proposed several indices to study the environmental, economic, and social sustainability of additive manufacturing products and process development. Another example is [174], in which the authors extracted 787 indicators to analyze ecodesign processes from the scientific literature. It is possible to find similar works aiming to develop a framework to support the definition of a complete set of indicators applicable to warehouse performance analysis. Johnson and McGinnis proposed a data envelopment analysis (DEA) approach to assess the warehouses compared to an

efficient frontier. In their work, a warehouse is represented as a system that transforms inputs like labor, space, equipment, and inventory into outputs, like the piece lines, the pallet lines, the case lines, revenue, value-added services, etc.[175] Staudt et Al. performed a literature review for the purpose of finding the most used performance indices. They defined four categories of direct, measurable KPIs: time, cost, quality, and productivity, and a general indirect measurable KPI cluster. The indirect group contains indicators like flexibility, customer perception, value-added, etc. [176]. A recent scientific trend is to study warehouses with a sustainable outlook. Torabizadeh et Al. proposed 33 different sustainability indicators and clusterized them into six distinct groups: (i) warehouse operation performance, (ii) economic performance measurement, (iii) resources, (iv) emission waste & environmental commitment, (v) labor practice & decent work, and (vi) product responsibility and society [69]. In contrast, Faveto et al., in their article, focus on the triple bottom line and the three aspects of sustainability: social, environmental, and economic [66]. It is also possible to find indicator definitions in articles that study particular warehouse logic or strategies. Gu et Al., in their work, proposed a wide selection of scientific papers that calculate the travel time and other indicators analytically according to different warehouse technology [177].

Despite the number of cited studies, a significant scientific gap is still evident. In different geographical or sectoral contexts, the indicators are not homogeneous, although they are intended to represent the same phenomena. Sometimes an indicator with the same name is calculated and used for entirely different purposes. Other times the same indicator is named differently according to the context. For instance, in [178], storage costs and holding costs are used as synonyms. In contrast, in [179], the storage costs are incurred in introducing the load unit inside the warehouse, and in [180], the holding costs are sustained in maintaining the load unit stored in the warehouse. The standard ISO 22400 [181] has the scope to create a conventional set of KPIs in the manufacturing field. However, such a norm does not present a section related to the logistic management of the warehouses. The primary purpose of the present work is to start a scientific debate on the realization of a broadly accepted performance measurement system in warehouses using the sustainability triple bottom line as a general reference.

5.4.1 Key Performance Indicators Discovery

As previously mentioned, in this analysis, we use as a general reference the 70 KPIs identified in a previous scientific work conducted by Faveto et al. [66]. The authors examined 237 articles and clusterized the indicators based on two different

perspectives: the Triple Bottom Line (TBL) accounting framework and Anthony's Pyramid structure [182]. We start from this set of indices and search them on a broader sample in order to validate and integrate them with other missing indicators.

To extract a comprehensive sample of articles focused on warehouse systems, we define the following query: TITLE (warehouse) AND NOT TITLE-ABS-KEY("data warehouse") on Scopus (https://www.scopus.com/). This query allowed us to find papers with a focus on warehouses. Searching the same keyword (warehouse) inside the whole abstract would extract too many documents without a clear direction. Therefore we limited the query to the title. We also decided to avoid all these articles containing the keyword "data warehouse" in their title since it was evident from different analyses we conducted that the central part of the out of our scope articles was in the computer science domain. In November 2020, the previous query retrieved 4402 different articles. We performed a sampling method based on quality criteria. An article in order to pass the quality filter must satisfy at least one of the following three conditions: (i) the paper is published in a journal classified as Q1, (ii) the article is published in a journal with a Scimago Journal Ranking (SJR) greater than 0.5 or (iii) the article has at least 50 citations. The filter extracted 890 articles, 20 % of the total sample. These articles were scanned and analyzed in order to pursue two different purposes: (a) to calculate the frequency of the 70 primary indicators already collected previously on a more significant sample and (b) to find new indicators to be included in this analysis.

The 890 articles were assigned to two parallel groups of engineering students to be analyzed manually (each student was in charge of 35-50 documents). After carefully reading the paper, each student identified and highlighted the presence or absence of the 70 given indicators within the article to simplify the review process, and the obtained result was recorded in a shared excel document. A second aim of the student analysis was to find and report new KPIs not included in the base set. Finally, another student's task was to identify any off-topic research (e.g., articles about warehouse insects) and report them. Of the 890, 232 documents were classified as duplicates or not found. Usually, duplicates were old versions of papers already analyzed, like errata, or editorial and notes, while the ones not found were articles whose full text was not available. Another 73 were identified as off-topic or out of scope, i.e., unrelated to the topics studied. Finally, the analyzed articles were 585, about 13 % of the total extraction. Once all articles were analyzed, we moved on to a review process. In the first phase, we merge the two results obtained. The papers were examined in parallel by the two groups. Therefore, it has been fundamental to compare the results of the two analyses to gather them in one. In 17

instances, KPIs identified by one student did not match those found in the analysis of the duplicate copy of the same paper. In these cases, we reexamined the articles. Next, a sample review of the 585 papers was conducted. A total of 363 articles and their indicators were reviewed, randomly selected from all the papers present, and if some errors were found, they would be corrected.

5.4.2 Metrics Definition

This section aims to introduce and propose some metrics for evaluating the indices. The goal of these metrics is to assess the usefulness of the indicators from different points of view to try to extract a set that can be considered complete. We have proposed two sets of metrics: (i) objective and (ii) subjective. The objective metrics are based on the literature frequency. In contrast, the subjective set is based on a qualitative assessment of the ease of use and a survey conducted in different Italian companies.

The first metric is the relative frequency f_{ϑ}^{r}, calculated by dividing the absolute frequency f_{ϑ}^{a} of a generic indicator ϑ by the total number of the analyzed papers K (585).

$$f_{\vartheta}^{r} = \frac{f_{\vartheta}^{a}}{K}, \tag{48}$$

The second metric is a citation-weighted frequency based on the number of citations of the article in which the indicator is contained. B_k^{ϑ} is a Boolean value equal to one if the i-th indicator is present in paper k and zero otherwise, while C_k is the number of citations of the k-th article.

$$f_{\vartheta}^{wc} = \frac{\sum_{k=1}^{K} C_k B_k^{\vartheta}}{\sum_{k=1}^{K} C_k}, \tag{49}$$

The third metric considers the singularity of indicators used in a research article, where M_k represents the number of different indices present in the k-th paper. The logic behind this index is that if a KPI is always used alone, it has a precise purpose and can provide knowledge without other indicators. When the frequency f_{ϑ}^{wm} is equal to 1 means that it is always used singularly in every article.

$$f_{\vartheta}^{wm} = \frac{\sum_{k=1}^{K} B_k^{\vartheta}}{\sum_{k=1}^{K} M_k B_k^{\vartheta}}, \tag{50}$$

The last metric is based on the year of publication of the paper. Each article is identified by a decimal number between 0 and 1, denoted by A_k that represents the age of the k-th article. A_k is calculated as:

$$A_k = \frac{y_k - y_{max}}{y_{min} - y_{max}}, \tag{51}$$

Where, y_{max} is the year of the most recent publication, 2021 in our case, and y_{min} is the year of the older publication decreased by a unit, in our case, 1946. A_k is then used as a discount factor in order to calculate a new frequency that assigns a larger value to a more recent occurrence than an older one.

$$f_{\vartheta}^{wa} = \frac{\sum_{k=1}^{K} A_k B_k^{\vartheta}}{K}, \tag{52}$$

In this way, we provide a discount rate to the occurrences. In particular, if an indicator is present in an article published in 2021, the presence would be worth 1. This value will decrease linearly to a minimum value of 0.0134 given to the occurrences in the articles published in 1947.

All the metrics that have been presented so far have an objective value. However, they lack contact with the industrial world; for this reason, we have created a survey to be submitted to experts working in the logistics sector. In about six months, we collected the answers from 15 people representing SMEs and big corporate firms, whose warehouses vary from a minimum of 48 m^2 to a maximum of 36000 m^2. Each respondent compiled a first section in which the company is described, mainly information about the company size, warehouse size, number of SKUs managed, the primary function of the warehouse, etc. In the second phase, they assigned a value of importance from 0 to 5 to the 70 indicators constituting the basic set. The perceived importance metric (s_{ϑ}^{q}) of the indicator ϑ is calculated through a simple arithmetic average of the answer Q_n^{ϑ} obtained by the N respondents.

$$s_{\vartheta}^{q} = \frac{\sum_{n=1}^{N} Q_{n}^{\vartheta}}{N}, \qquad (53)$$

5.4.3 Indicator List and Selected Set

The 70 selected indicators are categorized into three clusters following the Triple Triple Bottom Line (TBL) structure. The TBL is a framework that evaluates a process from three distinct points of view of sustainability: social aspects, environmental aspects, and economic aspects. According to this theory, an organization should be able to perpetuate its activities over time concerning the environment and society by generating profit [69]. Inside the three clusters, other subcategorization was made depending on the nature of KPIs. The economic cluster, as we expected, is the biggest one, with 52 different indicators (almost 80% of the total). Environmental and Social Cluster have similar dimensions, 10 hands are clustered as environment-related, and 8 indicators are clustered as Social related.

The following paragraphs describe each KPIs cluster. For each KPI, the unit measure, the questionnaire-based perceived importance (Q), the relative frequency (R), the citation-weighted frequency (C), the singularity indicator (S), and finally, the yearly weighted frequency (Y) are reported.

5.4.4.1 Economic KPIs

The indicators of this cluster refer to the economic value created by the organization. In particular, they indicate the warehouse's performances that directly influence the company's costs and profit. Inside this group, we subcategorized the indicators into four separated subclusters: (i) Generic Performances (Table 24), (ii) Time Related Performances (Table 25), (iii) Cost Related Performances (), (iv) and ICT Performances (Table 27).

Table 24 - Generic Performances

KPI	Definition	Unit	Q	R	C	S	Y
Bottleneck Rate	*Bottleneck Rate is the maximum reachable system Throughput*	[1/h]	2.60	0.04	0.04	0.14	0.03
Capacity Flexibility	*Capacity flexibility is a qualitative index that refers to the ability to adjust the total production capacity in any period with the option of utilizing contingent resources in addition to permanent resources*	[-]	3.73	0.14	0.13	0.14	0.12

Critical WIP	*Critical WIP measures the maximum number of ULs handled when the warehouse Throughput reaches the Bottleneck Rate*	[-]	2.60	0.01	0.02	0.07	0.01
Inventory Turnover	*The Inventory Turnover is calculated by dividing the cost of goods by the average inventory in the same period, and it measures the rate at which inventory is sold or consumed and replaced*	[-]	4.07	0.11	0.08	0.12	0.09
Machine Collision	*Machine Collision indicates the number of collisions between automated guided vehicles in a certain period*	[-]	2.07	0.03	0.02	0.12	0.03
Number of Failures	*The Number of Failures is the absolute number of system failure that needs extraordinary maintenance*	[-]	2.67	0.03	0.04	0.12	0.02
Object Misplacement	*Object Misplacement is the percentage of tasks performed in wrong positions: load unit stock in the wrong location or items retrieved from the bad warehouse cell*	[%]	3.27	0.01	0.00	0.11	0.00
Peak Utilization	*Peak Utilization is the system utilization when the number of items managed by the system is more than the critical value, i.e., they are enough to make the system work at its bottleneck rate.*	[%]	2.60	0.02	0.01	0.11	0.02
Picking Accuracy	*Picking Accuracy measures the percentage of items picked correctly during a time shift*	[%]	3.47	0.06	0.12	0.12	0.05
Positioning Accuracy	*Positioning Accuracy measures the number of items correctly placed in the warehouse during a storage activity during a time shift*	[%]	3.40	0.05	0.05	0.09	0.05
Receptivity	*The Receptivity index consists of the total number of load units that can be stored in the warehouse, i.e., its storage capacity*	[-]	3.60	0.09	0.18	0.12	0.08
Resource Utilization	*Resource Utilization measures the % of the time in which resources (humans, vehicles, etc.) perform operations*	[%]	3.53	0.11	0.12	0.10	0.10
Selectivity	*The Selectivity is measured as the number of directly reachable ULs divided by the receptivity, and it measures how it would be easy to perform a retrieval task in the warehouse*	[%]	3.33	0.01	0.01	0.11	0.01
Shelf Occupation	*The shelf occupation measures the space occupied only on the shelves and not in all the storage areas*	[%]	3.40	0.03	0.03	0.08	0.03
Stock Balance	*The Stock Balance Index represents the overall balance of stock volume inside the warehouse. It is calculated as a weighted sum of the difference. The index grows with an increase in system ill balance.*	[-]	2.80	0.05	0.04	0.11	0.04
Throughput	*The Throughput represents the number of ULs/orders processed in the unit of time*	[UL/h]	3.20	0.23	0.34	0.12	0.20
Travel Distance	*Travel Distance is the total distance traveled by the piker or the vehicle to move between the input/output point of the warehouse to the storage/retrieval point located in the warehouse*	[m]	3.00	0.27	0.36	0.14	0.24
Unoccupied Space	*The Unoccupied Space index is the ratio between the total volume of the warehouse and the space occupied by the items.*	[%]	3.07	0.05	0.08	0.09	0.05
Unprocessed Order	*Unprocessed Order indicates the percentage of lost orders by mistakes in each time span*	[%]	3.33	0.03	0.03	0.11	0.03

Vehicle Capacity	*Vehicle Capacity measures the carrying capacity of vehicles (can be measured in kg or in standard unit load)*	[kg]	3.20	0.07	0.09	0.14	0.06
Warehouse Exposition Ratio	*Warehouse Exposition measures the percentage of the warehouse dedicated to exposition (i.e., walkable by customers). It is based on the principle that space allocated for exposition can generate revenue, while space given for storage is a cost*	[%]	2.47	0.02	0.02	0.10	0.02

Table 25 - Time Related Performances

KPI	Definition	Unit	Q	R	C	S	Y
Charging Platform Av.	*If there are electric vehicles in the warehouse, the Charging Platform Av. measures the % of the time the charging platforms are not in use*	[%]	2.13	0.01	0.01	0.08	0.01
Charging Time	*Charging Time is the average time a vehicle must spend in the charging platform*	[s]	2.07	0.02	0.01	0.08	0.01
Cycle Time	*Cycle time is the total time required to complete a loading/unloading operation*	[s]	3.00	0.16	0.22	0.12	0.14
Inventory Time	*Inventory Time is the time required for the detection, enumeration, and description of individual objects present at a given time in the warehouse*	[days]	3.07	0.03	0.03	0.09	0.03
Lead Time	*Lead Time is the time the intercurrent between the order received by the supplier and to order arrival at the retail location*	[days]	3.67	0.19	0.19	0.15	0.17
Order Elabor. Time	*Order Elaboration Time is the time needed to elaborate the order and start to perform all the subsequent activities*	[-]	3.33	0.05	0.08	0.10	0.04
Packing Time	*Packing Time is the time it takes to perform the packaging activity before shipping the order*	[s]	2.53	0.02	0.01	0.10	0.02
Picking Time	*Picking Time is the time it takes to pick up a single item in the warehouse*	[s]	3.20	0.18	0.27	0.13	0.16
Planning Time	*Planning Time is the time to schedule the storage/retrieval activities after the system elaborates the order*	[s]	2.67	0.05	0.05	0.10	0.05
Queue Waiting Time	*The Queue Waiting Time indicates the average time a UL must wait before being in a standing-by position*	[s]	2.53	0.07	0.07	0.10	0.06
Retrieval Time	*Storage Time is the time needed to retrieve the UL from the location where it is stored*	[s]	3.00	0.08	0.12	0.09	0.07
Storage Time	*Storage Time is the time needed to allocate the UL in the location where it has to be stored*	[s]	2.87	0.07	0.05	0.10	0.06
Task Time	*Task Time is the time required to complete a grasping operation on a given shelf*	[s]	2.13	0.05	0.05	0.10	0.04
Travel Time	*Travel Time is the total time needed by the piker or the vehicle to move between the warehouse's input/output point to the storage/retrieval point located in the warehouse*	[s]	2.93	0.29	0.40	0.13	0.25
Warehouse Av.	*Warehouse Availability indicates the percentage of time during the 24-hour day that the warehouse is active for storage/retrieval or picking activities*	[-]	3.60	0.08	0.07	0.13	0.07

Table 26 - Cost Related Performances

KPI	Definition	Unit	Q	R	C	S	Y
Direct Labour Cost	*Direct labor cost is the cost of activities directly involved in the production of the finished products*	[€]	3.20	0.11	0.08	0.13	0.09
Holding Cost	*Holding Cost is the daily cost to maintain units stocked (i.g., energy consumptions, refrigeration, depreciation, insurance, etc.).*	[€/day]	2.60	0.27	0.30	0.18	0.23
Indirect Labour Cost	*Indirect labor cost is not direct labor cost but is the cost of ancillary operations that makes the business possible*	[€]	2.60	0.05	0.07	0.14	0.04
Inventory Cost	*Inventory cost is an aggregate cost generally composed of ordering cost, holding cost, shortage cost, and replenishment cost.*	[€]	3.20	0.19	0.19	0.15	0.16
Maintenance Cost	*Maintenance Cost indicates all the costs due to warehouse maintenance*	[€]	3.67	0.05	0.05	0.14	0.05
Management Cost	*Management Cost indicates all the costs due to general warehouse management*	[€]	3.47	0.10	0.06	0.12	0.08
Retrieval Cost	*Retrieval Cost is the cost needed to retrieve the UL from the location where it is stored*	[€]	2.67	0.04	0.06	0.09	0.03
Space Cost	*Space Cost includes all the costs sustained for maintaining the area in which the warehouse system's infrastructure is built*	[€]	2.93	0.10	0.09	0.13	0.09
Storage Cost	*Storage Cost is the cost needed to allocate the UL in the location where it has to be stored*	[€]	3.07	0.14	0.12	0.12	0.12

Table 27 - ICT Performances

KPI	Definition	Unit	Q	R	C	S	Y
Algorithm Reliability	*Algorithm Reliability measures the reliability of the information system, which can be calculated as the absolute number of errors generated by the system in a given time frame*	[-]	0.00	0.13	0.12	0.15	0.11
Bar/QR Code Reliability	*Bar/QR Code Reliability indicates the reliability of the object identification system by barcode or QR code. Errors can be measured in terms of incorrect erased codes or misidentifications*	[-]	3.33	0.01	0.00	0.12	0.01
Image Rec. Speed	*Image Rec. Speed measures the speed of the automated system to find by image recognition the items in the warehouse*	[ms]	2.13	0.00	0.00	0.06	0.00
Response Latency	*Response Latency is a measure of information system latency. It measures how long it takes, from when the request is entered into the system to when the command is sent to the automated system or worker.*	[ms]	2.73	0.07	0.06	0.15	0.06

Solver Iterations	*Solver Iteration is a measure of the information system indicating how often the algorithm must iterate to arrive at the optimum (e.g., minimum path, nearest object, etc.)*	[ms]	0.00	0.15	0.14	0.14	0.13

5.4.4.2 Environmental KPIs

The Environmental Performances are clustered into two different groups. The first set describes the warehouse system as an environment per se, i.e., the atmosphere in which the human resources operate and the items are stored. The first cluster is called Warehouse Environmental Measures, and it is displayed in Table 28. At the same time, the second group contains measures of the direct impact that the system has on the environment: like energy consumption and pollutant emissions (Table 29).

Table 28 – Warehouse Environmental Measures

KPI	Definition	Unit	S	R	C	U	Y
Barometric Pressure	*Energy Recovery is the amount of energy regenerated in a defined time thanks to systems like kinetic breaks*	[kWh/day]	2.20	0.03	0.01	0.13	0.02
Humidity	*Passive Consumption is the average power consumption when the system is on but inactive*	[kWh/day]	2.80	0.05	0.03	0.17	0.04
Pollutant/Dirty Conc.	*Area Occupation represents the proportion of the area used to store items, with the space for the passage of operators and vehicles to pick and handle items*	[%]	3.20	0.02	0.01	0.21	0.02
Roof Temperature	*Pollutant Emission calculates the environmental footprint of the warehouse. It can be computed in CO2eq emitted.*	[CO2eq /day]	2.80	0.01	0.01	0.16	0.01
Temperature	*Energy Consumed by the warehouse*	[kWh/day]	3.20	0.12	0.11	0.18	0.10

Table 29 – Emission, Waste, and Environmental Commitment Indicators

KPI	Definition	Unit	S	R	C	U	Y
Energy Consumption	*Energy Consumed by the warehouse*	[kWh/day]	3.67	0.09	0.07	0.15	0.09
Energy Recovery	*Energy Recovery is the amount of energy regenerated in a defined time thanks to systems like kinetic breaks*	[kWh/day]	2.73	0.02	0.01	0.15	0.02
Passive Consumption	*Passive Consumption is the average power consumption when the system is on but inactive*	[kWh/day]	2.67	0.01	0.00	0.18	0.01
Pollutant Emission	*Pollutant Emission calculates the environmental footprint of the warehouse. It can be computed in CO2eq emitted.*	[CO2eq /day]	2.67	0.04	0.02	0.16	0.03
Space occupation	*Area Occupation represents the proportion of the area used to store items, with the space for the passage of operators and vehicles to pick and handle items*	[%]	3.47	0.16	0.19	0.12	0.14

Vehicle Autonomy	*Vehicle Autonomy measures the percentage of time that vehicles operate tasks without operator supervision.*	[%]	2.40	0.03	0.02	0.11	0.03

5.4.4.3 Social KPIs

Based on activities concerning social sustainability and ISO 26000 [183], companies are responsible for considering their impact on their human resources and the human society in which they are immersed. Not many indices have been found in the literature for this category. The ones we found mainly measure the operator's safety and how much the warehouse system is based on human work or automation Labour Practice. Decent Work and Social Responsibility Indicators are reported in Table 30.

Table 30 - Labour Practice. Decent Work and Social Responsibility Indicators

KPI	Definition	Unit	S	R	C	U	Y
Activity Automation	*Activity Automation is a qualitative indicator representing the degree of automation of a warehouse*	[-]	3.27	0.07	0.11	0.12	0.06
Human Activity Time	*Human Activity Time is a measure of the automatization of the warehouse. It is calculated as the % time of tasks performed manually*	[%]	3.87	0.04	0.03	0.12	0.03
Human Error	*Human Error is a qualitative index measuring the number of errors committed by human resources during tasks. It can be determined as the number of errors in a specific period*	[-]	3.73	0.05	0.06	0.11	0.04
Human Utilization	*Human Utilization measure the utilization of human resources*	[%]	3.93	0.05	0.05	0.11	0.05
Machine Safety	*Machine Safety is a qualitative indicator measuring safety in automated machines. It can be quantified as the number of accidents reported in a given time period caused by machine failures*	[-]	3.87	0.02	0.01	0.11	0.02
Noise	*Noise is a measure of the quality of work*	[dB]	2.67	0.02	0.00	0.14	0.02
Operators per Area	*Operators per Area measures the number of operators per m2, it indicates eventual overcrowding of specific areas, and it is a measure of the quality of work*	[1/m2]	3.53	0.04	0.03	0.11	0.03
Work Safety	*Work Safety is a qualitative indicator measuring safety in the work environment. It can be calculated as the number of accidents reported in a given period*	[-]	3.67	0.08	0.08	0.14	0.07

5.4.4.4 Indicators Ranking

This section presents the indicators ranked for the five analyzed metrics: Q, R, C, U, and Y. Table 31 displays the nine top-ranked warehouse indicators according to the five metrics.

Table 31 - Top 9 Indicators ranking

Questionnaire (Q)	Rel Freq (R)	Cit Freq (C)	Unicity (U)	Yearly Freq (Y)
Inventory Turnover	Travel Time	Travel Time	Pollutant/Dirty Conc.	Travel Time
Human Utilization	Travel Distance	Travel Distance	Passive Consumption	Travel Distance
Human Activity Time	Holding Cost	Throughput	Holding Cost	Holding Cost
Machine Safety	Throughput	Holding Cost	Temperature	Throughput
Capacity Flexibility	Lead Time	Picking Time	Humidity	Lead Time
Human Error	Inventory Cost	Cycle Time	Roof Temperature	Picking Time
Work Safety	Picking Time	Lead Time	Pollutant Emission	Inventory Cost
Lead Time	Area Occupation	Inventory Cost	Inventory Cost	Area Occupation
Energy Consumption	Cycle Time	Space Occupation	Response Latency	Cycle Time

It is interesting to note that the experts interviewed found indicators analyzing human resources such as Human Utilization, Human Activity Time, and Human Error crucial. The most important indicator, according to the experts, is Inventory Turnover. This indicator is more financial than operational, and it is able to quickly provide insight into the rotation of goods and possible inventories. Data from the questionnaires also revealed the importance of safety in the workplace (machine and work safety). Finally, we mention energy consumption as the only indicator related to environmental sustainability. The three frequencies, R, C, and Y, do not exhibit excessively different results. These three classifications are able to depict the focus that research has in the area of warehouse analysis. The most studied indicators are those related to Travel Time and Travel Distance. This fact is not surprising as research often concentrates on algorithms to find the best route to reach the unit load in the warehouse. Along with these, Picking, Cycle, and Lead Time are also important. A second particularly prolific area of research is devoted to warehouse cost minimization, especially Holding and Inventory Costs through stock management. Throughput is a well-known KPI and is often used to compare different warehouses' performances. Finally, we cite Space Occupation as an essential indicator of environmental sustainability. More efficient and compact warehouses should be preferred over wider ones requiring more space. Lastly, particularly interesting is the result obtained from the uniqueness metric. In this group, we have very particular indicators linked to environmental sustainability. This may show that studies that aim to analyze warehouse environmental performance rarely combine environmental KPI with economic performance and vice versa. In addition, articles specializing in environmental sustainability performance seem to focus on a small set of indicators compared to other analyses.

5.4.4.5 New KPI

In this section, we cover some other indicators considered fundamental for an analysis of a warehouse. These indicators were not presented in the previous work.

The first indicator is the Shortage Costs (sometimes it can be found as Penalty Costs [184]). This performance aims to evaluate the effect of stock out. It represents costs incurred due to backlogging or delivery penalties for incorrect timing. Only in the case of contractual penalties does this mean an actual expense for the company, but more often, it is an opportunity cost whose estimation is particularly complex. According to [185], most researchers assume that during the stock-out phase, the shortages were either. However, in practice, some devoted potential consumers are ready to wait for these shortages, while others can be more impatient and search for the goods elsewhere.

Replenishment Costs are the costs incurred for the procurement of new items. Replenishment costs, holding costs, and shortage costs constitute inventory costs (presented in Table 26). These three costs include various sides of the same coin. It is necessary to demand large orders to lower the replenishment cost. However, implementing this strategy impacts holding costs (especially in the case of perishable products). A proper balance between order size and frequency decreases the chances of stockout and, thus, shortage costs. A heuristic application of an efficient replenishment strategy can be found in [186].

Another interesting KPI is ergonomics. Warehouses, particularly picking activities, require a significant human workload, so keeping track of workers' good physical condition is critical. In [187], an optimization model for picking is proposed to find the best solution for a storage location problem that minimizes the cycle time and the work discomfort. They estimate a measure of the work discomfort based on location factors (e.g., picking level, section number, and type of bin) and product factors (e.g., quantity, mass, and volume of the product to pick). While in [188], the authors evaluate the physical fatigue of workers through an analysis of spinal load performed in a lab environment.

5.4.4.6 Selected Performances

We decided to focus the analysis on nine performances to perform the feasibility study. Six indicators can be considered economically related, and three are environmentally related. The first indicator we chose to analyze is Throughput, undoubtedly one of the most used indicators. Then we focused on Resource Utilization. According to our analysis, it is crucial to keep track of the time needed

to perform different tasks. In particular, we decided to measure the Lead Time as the time between the order entering the warehouse and when the order is completed. While the Picking Time is defined as the time needed by the AGV to perform the complete mixed order. Finally, we chose to measure the total Travel Distance and the Average Meter per Order. The other three indices are related to environmental sustainability: Space Occupation, total Energy Consumption, and the average Energy per Order. A summary of the nine performances is reported in Table 32.

Table 32 - Nine performance measures

Class	Performance	Unit
Economic Related Performance	Throughput (TH)	order/h
	Resource Utilization (RU)	%
	Lead Time (LT)	s
	Picking Time (TT)	s
	Travel Distance (TD)	m
	Meter per Order (MpO)	m
Environmental Related Performance	Space Occupation (SO)	m^2
	Energy Consumption (EC)	kWh
	Energy per Order (EpO)	kWh

The calculation of average energy consumption was made following some studies on the subject. In [159],.the authors studied AVS/RS consumption, and they considered the energy required to move a vehicle at a constant speed equal to $EC = pc \times t$. Where pc is the power required to overcome the traction force while traveling at constant speed, and t is equal to the time the vehicle traveled at constant speed [159]. On the other hand, the work of Bruno et al. indicates the power required by the AVS/RS shuttle when it is empty (1 kW) and loaded (2kW) [164]. These elements were useful for calculating the energy consumption in the simulation model. Assuming that the maximum load that a pallet can support is 1500kg, and the power required to move 1500kg would be equal to $pe - pf$, where pe is the power when the shuttle is empty, and pf is the power required when the shuttle is fully loaded. This means that each kg needs a power of $\frac{pe - pf}{1500}$ ($1/1500$ W per kg) to be transported, assuming a linear relation between weight and power. With this information and the knowledge of the vehicles' travel times in the model, it is possible to calculate the energy consumption of the vehicles during the simulation, taking into account the different weights that the vehicles carry during the picking process. The average energy consumption index also includes an indication of the passive energy of the vehicles, i.e., the energy consumed when the vehicles are on but not performing any activity.

5.5 Parameter Definition

5.5.1 Experiment Factors and Levels

In this paragraph, we define the design space we want to analyze. In particular, we decided to study the impact of the geometrical structure of the warehouse by varying the tier number and the number of bays. We decided not to study the impact of aisles since each aisle or couple of aisles can be considered as a reference structure, and usually, in AVS/RS, the vehicles are in charge of operations aisles in close proximity. Moreover, we decided to study the impact of the vehicle number and the interarrival frequency of order as a control variable. Finally, we choose to assess the effect of four different storage logics, in particular: the class-based rule (CB), the dedicated slot rule (DS), a policy based on the association rules (AR), and finally, an approach based on SKU weights (BW). This last rule was decided to test the possible beneficial impact on energy consumption due to placing heavier items near the loading/unloading area. The warehouse object of the study should be able to manage 9 different SKUs with varying frequencies of order and correlation. As the first analysis, we opted to use the order list of an Italian company selling controllers and hardware components as an order reference. The list is modified ad hoc to generate interaction between SKUs. The orders would arrive at the warehouse following an exponential distribution with varying $1/\lambda$. Each simulation run would last for 24 consecutive hours.

Since the proposed analysis is a feasibility study, exploring the most significant space of solutions is necessary. For this reason, we decided on wide parameter intervals. For the tier number, we opted for the two levels, 3 and 9. For the bay number, we opted for the two levels, 12 and 24. The tiniest warehouse can store enough objects to satisfy the 24 hours demand. At the same time, the vehicle number varies from 1 to 6, and the $1/\lambda$ value of the exponential distribution interarrival time varies from 250s to 100s. Finally, we analyze the four previously described storage policies. A summary of the factors and their levels is reported in Table 33.

Table 33 - Factors and level of the analysis

Factors	Level (-)	Level (+)
Tier Number (TN)	3	9
Bay Number (BN)	12	24
Vehicle Number (VN)	1	6
Order Interarrival ($1/\lambda$) (OIN)	250 s	100 s
Storage Logic (SL)	CB DS	AS W

5.5.2 Storage Logic Definition

Before explaining in more detail, the design of the experiment and the discrete event simulation model developed, it is essential to explain how the storage policies are implemented in this study.

5.5.2.1 Class-Based Storage

Class-based storage policies categorize the SKUs into three classes, A, B, and C, and stored in specific areas within the warehouse. Area A usually closer to the loading/unloading area, Area B is in the middle of the warehouse, and Area C is the furthest from the loading/unloading area. Class-based storage can differentiate SKUs using various product characteristics, such as picking frequency, product volume, and product sales value [189]. In general, high-rotational products(class A) impact 80% of the total orders, medium-involvement products (class B) impact 15% of the orders, and the remaining low-involvement products (class C) impact 5% [189]. We can find percentages slightly different than the above in the literature, depending on the particular study.

Following the classification, it's crucial to define the three different classes inside the warehouse. The products in Class A will be kept closer to the depot point to ensure simple and quick access, while those in Classes B and C will be kept farther away from the depot point due to their lower demand and less frequent access.

Figure 37 shows the shape of the different areas and how they change depending on warehouse organization and where the loading/unloading area is located. These three different configurations of the areas can be defined as diagonal, within aisles, and across floors. In [190], it is possible to find other logic for the Class-Based policy

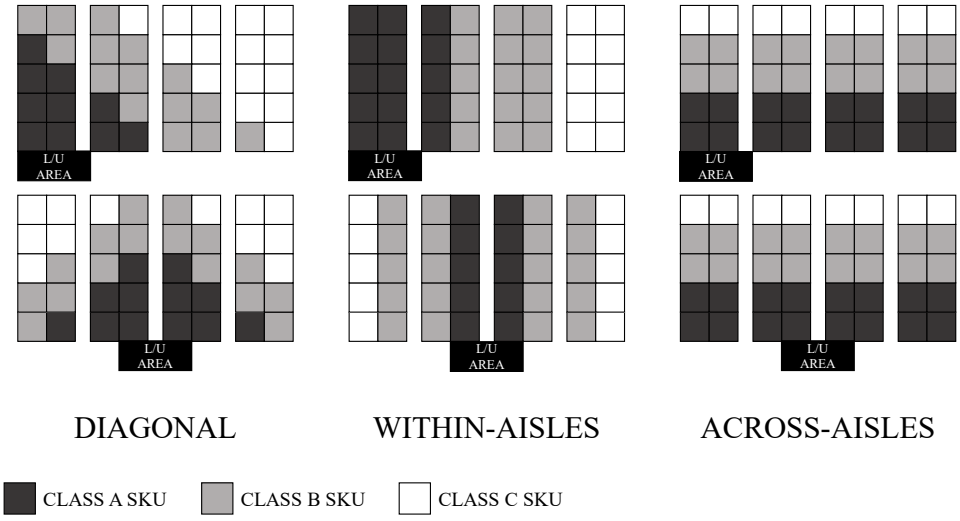

Figure 37 - Three Different Class-Based Policy [190]

In this work, the Class-Based storage is established on product order frequency, and we decided the percentages equal to 60% for Class A, 30% for Class B, and 10% for Class C.

5.5.2.2 Dedicated Slots storage

In a dedicated Slots Storage, the slots are assigned to specific products. Even if the product is out of stock, that place is only meant to be filled with that type of item [190]. In this work, the simulator randomly chooses the dedicated slots at the beginning of the run.

5.5.2.1 Storage by Association Rules

Some studies have highlighted the importance of implementing data mining techniques (e.g., the Apriori algorithm) in the context of automated warehouses to improve slot allocation so that travel distance during picking is minimized [191].

In this study, we use the Apriori algorithm to find hidden patterns in a list of several picking orders is possible. In particular, the algorithm can identify what combination of items is requested with the highest frequency through an iterative process. The definition and the procedure of the algorithm can be found in [192]. The policy used in this work is a combination of the previously described Class-Based storage. Still, with a modification, if an SKU is associated with another one, the two SKUs would be placed close to each other, even if they are not in the same

class. If a class A object and a class C object are associated, both are considered class A objects

5.5.2.1 Storage by Weight

The object weight is the product feature that influences where SKUs should be stored. This storage policy can be viewed as a Class-Based Storage variation where weight is the crucial attribute [189]. The heaviest units are stored close to the pallet retrieval point, and the lightest products are placed far from this point to assess whether such storage logic could provide any additional energy-saving benefits.

5.6 Design of Experiment

we opted to develop a full factorial experimental plan. Since we are analyzing four factors with two levels and one factor with four levels, a full factorial experimental plan requires 64 experiments ($2^4 \cdot 4$). It is possible to perform a complete factorial plan since we are in a simulation environment. Therefore, the experiment costs are low. Figure 38 represents the graphical representation of the 64 explored scenarios. Each black dot corresponds to a configuration considered during the experiment, and the cubes embody the five dimensions object of the study.

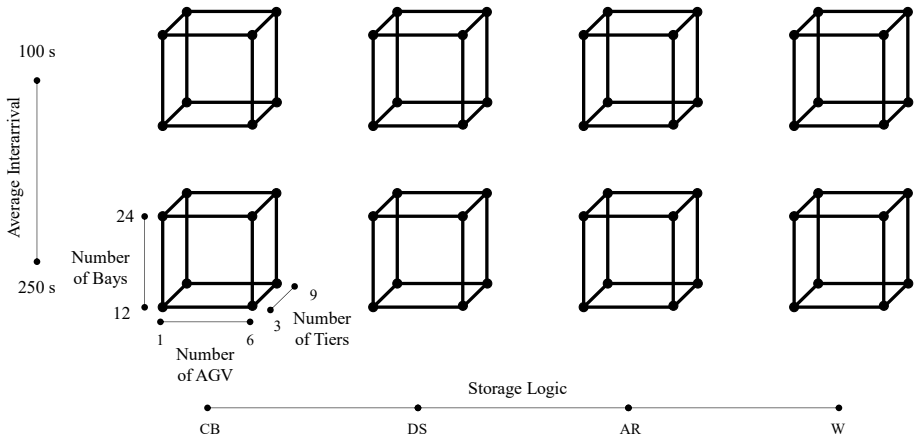

Figure 38 - Graphical Representation of the 64 scenarios

5.7 Simulation Model

In this section, we present the developed simulation model. The simulation model of the warehouse was developed using FlexSim software (www.flexsim.com). The purpose of the simulation model is to evaluate the feasibility of a robot-to-part order-picking system. The present work references the AVS/RS systems and the data provided by Eurofork S.p.A. (http://www.eurofork.com/), an Italian company leader in automated material handling. However, the system tested in this study does not currently exist, as this study seeks to evaluate its feasibility. Therefore, it is necessary to add some logic to the current system. The most significant modification is to include a robotic arm capable of performing the picking operations directly on the shuttle. The robotic arm is intended to reach the items on the homogeneous stored pallet brought to the front of the warehouse by the satellite, and the robotic arm takes the items and generates the mixed pallet over the shuttle. After the mixed pallet is complete, the shuttle exits the warehouse and deposes the order in an unloading area. Figure 39 displays the simulated vehicle. As stated before, the developed system is an AVS/RS with a shuttle and a satellite. The shuttle can enter each aisle and moves along Y-axis. Each shuttle is paired with a satellite. The satellite can only move on X-axis, entering inside the bays. A standard procedure consists of five steps: (i) the shuttle arrives in position near the correct bay, (ii) the satellite enters the bay and gets a homogeneous pallet, then (iii) the robotics arm takes the correct number of items and place them on a pallet stored on the shuttle, (iv) the satellite relocate the homogeneous pallet in its original position and finally (v) the satellite re-join the shuttle which is ready for the next task. In the case the robotic arm takes the last item on the homogeneous pallet, the shuttle is provided with a slot intended to store the empty pallet, and the shuttle will place it in the unloading area at the end of the order.

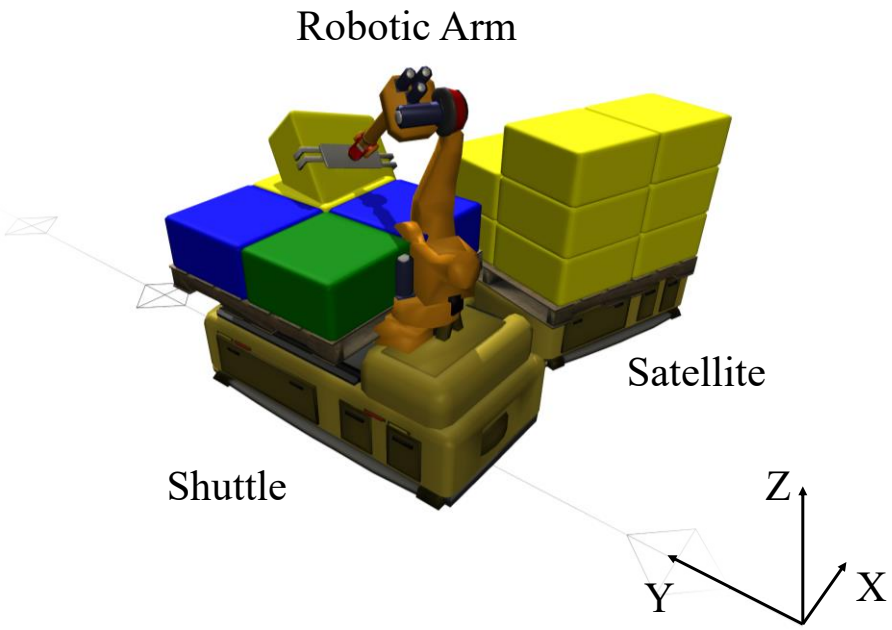

Figure 39 - Shuttle with a robotic arm mounted on top during a picking task.

The simulated system allows the handling of pallets up to a maximum size of 1000x1200mm with a weight of up to 1500kg. The shuttle, the satellite, and the lift can move autonomously at speeds up to 2 m/sec in the three directions. Figure 40 displays four simulations with different storage policies.

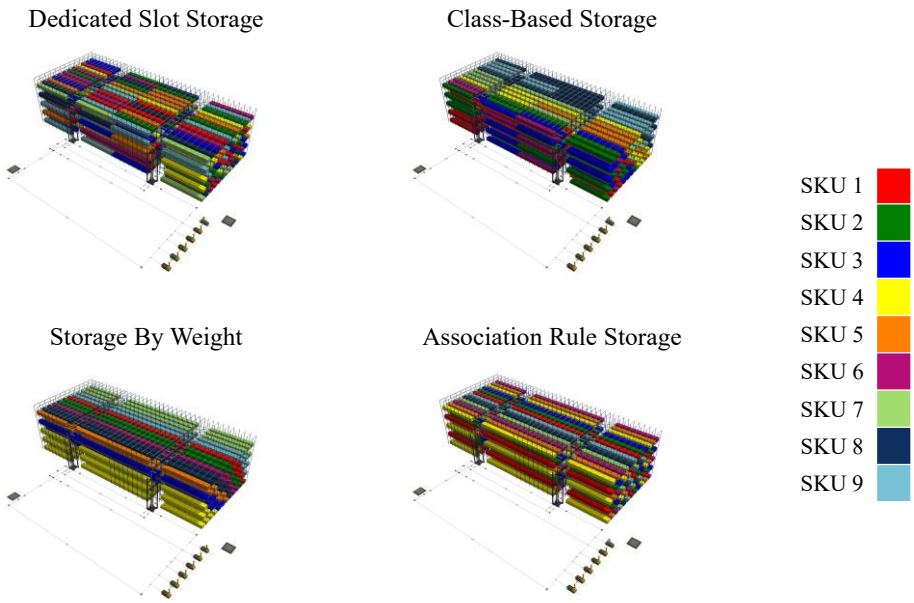

Figure 40 - Complete warehouse simulation model with the four storage logics highlighted

The studied warehouse has two parallel aisles. On the left side of the warehouse is present the loading area, where the shuttle can take empty pallets, while on the right side, there is the unloading area, where the shuttle can deposit fulfilled orders. The vehicle parking is in the bottom right corner of the facility. As aforementioned, the warehouse can manage nine SKUs, enumerated between 1 and 9, and they have the properties represented in Table 34. Moreover, the following association rules have been found: 1-2-3, 1-2-6, 1-2-7, 1-3-6, 1-6-7, 2-3-6, 2-6-7.

Table 34 - SKU proprieties

SKU ID	Weight	Class
SKU 1	10 kg	A
SKU 2	17 kg	A
SKU 3	32 kg	A
SKU 4	35 kg	B
SKU 5	25 kg	B
SKU 6	20 kg	A
SKU 7	2 kg	B
SKU 8	22 kg	C
SKU 9	6 kg	C

5.8 Statistical Analysis

The statistical analysis is divided into two parts: a qualitative analysis in which we described the obtained box plot to graphically assess some impacts between performances by changing the parameters. Then we compute regression models to explicit the relation between parameters and performances.

5.8.1 Qualitative Analysis

5.8.1.1 Number of Tiers

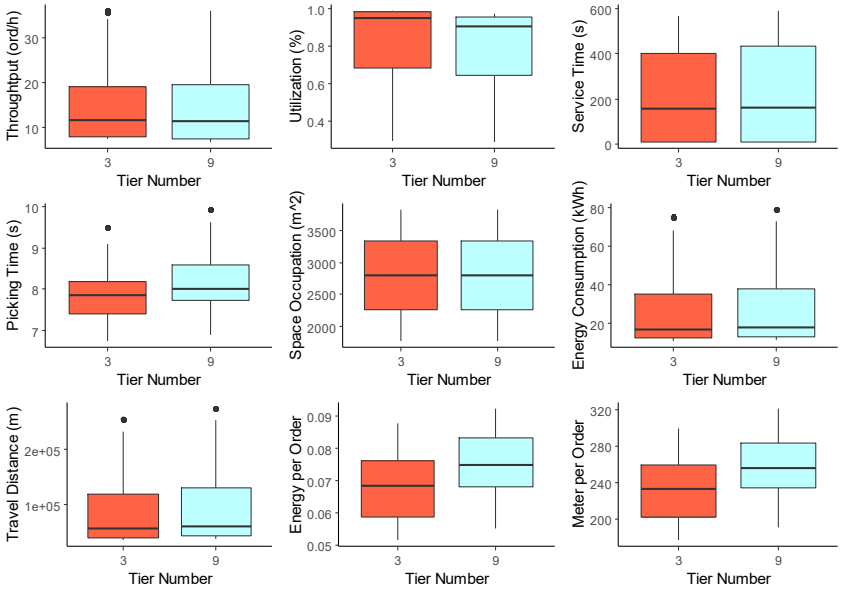

Figure 41 - Tier Number Box Plots

Figure 41 displays the box plots of the nine performances compared to the change of the tier number from 3 to 9. As it is possible to see from the graph, the variables most impacted are picking time and energy e meter per order. As the number of levels increases, the time to retrieve the goods increases. This behavior is easily understandable. Changing levels several times is necessary; therefore, a single operation takes longer and impacts the meters traveled per order and the energy consumed. Nevertheless, this improvement in picking time does not seem to improve the TH which remains relatively stable overly, because the total service time is strongly impacted by the time that orders wait in the queue.

5.8.1.2 Number of Bays

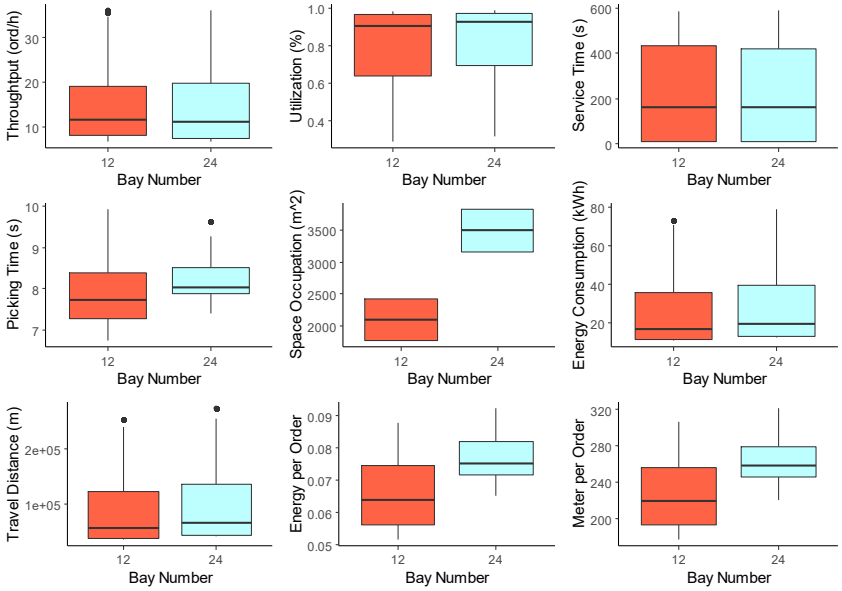

Figure 42 - Bay Number Box Plot

Precisely what was seen with the number of levels, a more significant number of bays seems to worsen the picking performance slightly. Again for the same reasons, we explained in the previous paragraph. A more extended warehouse means more meters to be traveled and thus more energy consumption per order and a longer picking time. On the other side, a more significant number of bays also results in a more extensive warehouse and so more space occupation, as it is possible to see in Figure 42.

5.8.1.3Number of AGVs

Figure 43 displays the impact of AGV number on the nine performances. The number of AGVs is probably a key element to manage since it dramatically impacts all nine performances. as expected, more AGVs cause an improvement in throughput and service time. The more vehicles are present, the more orders it is possible to fill in the same time slot. Regarding utilization, scenarios with only one AGV almost always have this parameter close to 100%, while with 6 vehicles, we measured a variable value depending on the other parameters. What is very interesting, however, is to see that the picking time with more AGVs increases. So orders would attend less time in the queue, but more time will be needed to finalize them, probably due to a gridlock inside the warehouse: vehicles have to wait until there is space to occupy a corridor, and they have to wait more time before to

ultimate the task. Obviously, in absolute terms, 6 AGVs consume more energy and travel more meters than 1 AGV alone. However, this parameter does not give us much information. More interesting is the energy and meters per order. Probably due to the same gridlock effect, we see that having more AGVs also results in the least environmentally friendly choice. Finally, the increase in AGVs also increases the Space Occupation. This phenomenon is principally due to the space needed for parking lots.

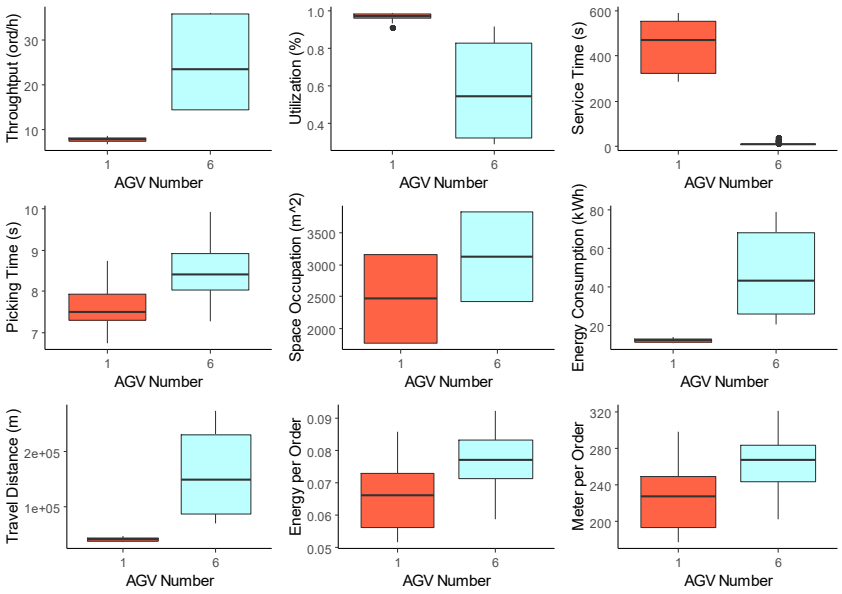

Figure 43 - AVG Number Boxplots

5.8.1.4 Order Frequency

The frequency of order interarrival is a control variable rather than a proper parameter, as seen in Figure 44. Lower interarrival always results in more significant stress on the warehouse and thus superior throughput, longer service time, higher utilization, elevated energy consumption, and greater travelled distances.

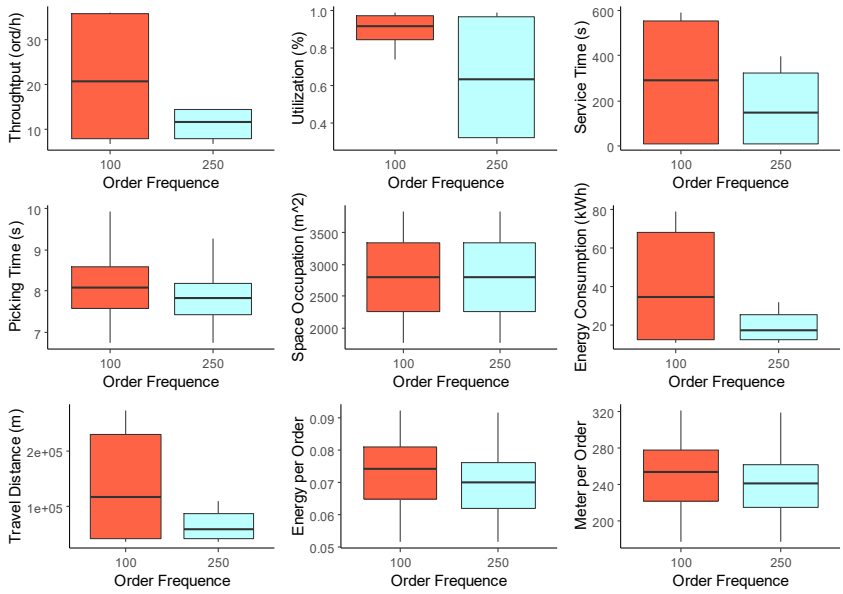

Figure 44 - Order Frequency Box Plots

5.8.1.5 Storage Logic

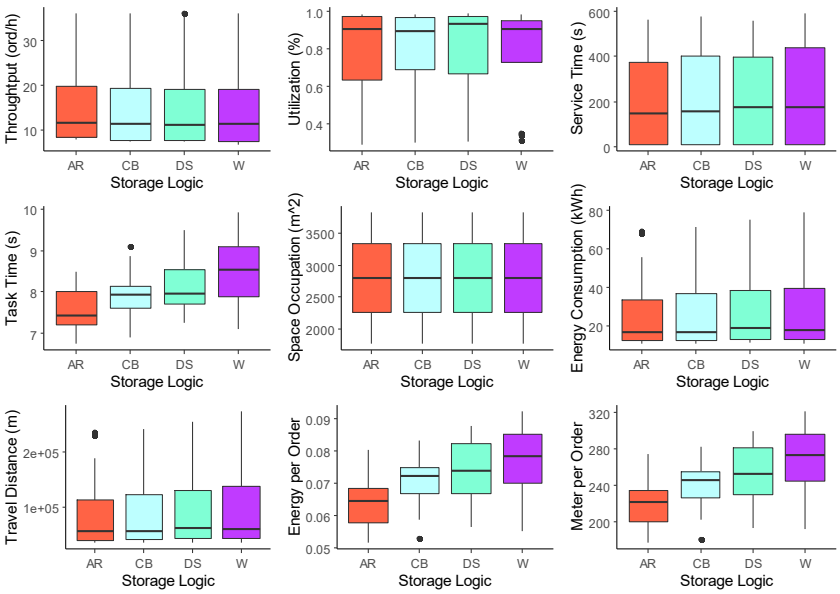

Figure 45 - Storage Logic Box Plots

Finally, Figure 45 shows the box plot for the four storage logics. As expected, the more complex and consistent the logic, the better the performance. The best logic is the association rule. The class-based ranks second, and the dedicated slot, which is nothing more than random placement, ranks third. The worst logic, on the

other hand, is weight-based logic. This was partly unexpected. It would have expected an improvement in energy compared to the other three logics. However, the objects the system carries are not excessively heavy; therefore, the impact of weight on consumption is negligible. Further analysis of this logic should be done.

5.8.2 Quantitative Analysis

We used a methodology made up of two steps to find the best model to predict the effect of parameters on performances: (i) stepwise bidirectional regression fitting minimizing the model AIC [132], (ii) and backward elimination of the less significant predictors to prevent overfitting. The three categorical variable storage logic has been replaced by four binary variables (DS, CB, W, AR). AR is never present stand-alone in order to eliminate multicollinearity, and its effect can be assessed by analyzing the models' intercepts.

All the proposed models reach an adjusted R^2 greater than 89%, meaning they can explain a considerable part of the variance. Table 35 shows the model of the TH, the parameter that most impacts performance is the number of vehicles. There is an increase of 8 orders per hour for each vehicle added. There is a visible negative effect on the throughput of all storage logic. As seen in the qualitative analysis, the AR logic is the best (parameter embedded in the intercept), then the CB, then the DS, and finally the W.

Table 35 - Throughput Model

Dep. Variable		Predictors	β	Sig
TH		(Intercept)	-0.0435	
		VN	8.2468	***
R	0.9973	OIN	0.0276	***
R-adj	0.997	CB	-0.3673	†
		DS	-0.5026	*
		W	-0.7284	**
		VN×OIN	-0.0277	***

Table 36 displays the model on resource utilization. The greater the number of vehicles, the lower the utilization. This effect is not directly seen by the single parameter VN but from its interaction with order interarrival. In particular, when the vehicle number is equal to 1 there is no interaction, while increasing the number of vehicles would result in a decrease in utilization, and this effect would increase if the order interarrival increased.

Table 36 - Utilization Model

Dep. Variable	Predictors	β	Sig

UTI		(Intercept)	0.9642	***
		VN	0.0366	***
R	0.9934	OIN	0.0007	***
R-adj	0.9921	TN	-0.0041	***
		CB	-0.0130	
		DS	-0.0090	
		W	-0.0344	*
		VN×OIN	-0.0007	***
		VN×CB	0.0050	
		VN×DS	0.0081	*
		VN×W	0.0146	***

Table 37 displays the service time model. Again, as for the throughput, we have a huge impact due to the vehicle number. Each vehicle reduces the service time by 140 seconds. We can also notice the same effect seen before with the logic. The best result is achieved with the association rule logic. Using another logic results in an increase in service time.

Table 37 - Service Time Model

Dep. Variable		Predictors	β	Sig
ST		(Intercept)	844.12	***
		VN	-139.70	***
R	0.9962	OIN	-1.85	***
R-adj	0.9958	CB	10.55	†
		DS	10.19	†
		W	25.27	***
		VN×OIN	0.30	***

The picking time model is represented in Table 38, and we can conclude the same considerations as seen so far regarding storage logic. In this case, however, we have a pejorative effect from the vehicle increase, as predicted in the qualitative analysis. The increase in the number of levels and bay interacts with the number of vehicles and partially damps the adverse effect due to the gridlock effect.

Table 38 - Picking Time Model

Dep. Variable		Predictors	β	Sig
TT		(Intercept)	5.615	***
		VN	0.448	***
R	0.9192	CB	0.625	†
R-adj	0.8918	DS	1.076	**
		W	0.597	†

	BN	0.054	***
	AR×TN	0.021	
	CB×TN	0.113	***
	DS×TN	-0.014	
	W×TN	0.200	***
	VN×OIN	-0.001	***
	CB×BN	-0.044	**
	DS×BN	-0.015	
	W×BN	-0.038	**
	VN×BN	-0.005	*
	BN×OIN	0.000	*
	VN×TN	-0.007	†

Table 39 represents the Occupied Space model. This model is deterministic, and the total warehouse area only depends on bay and vehicle numbers.

Table 39 - Occupied Space Model

Dep. Variable		Predictors	β	Sig
OS		(Intercept)	248	***
R	1	BN	116	***
R-adj	1	VN	132	***

Table 40 shows the energy consumption model, energy consumption is heavily impacted by vehicle number, and a pejorative effect can be calculated from the interaction between the vehicle number and the storage logic. A weak increase in energy may also be due to an increase in the number of bays and tiers.

Table 40 - Energy Consumption Model

Dep. Variable		Predictors	β	Sig
E		(Intercept)	-5.6834	**
		VN	14.1319	***
R	0.994	OI	0.0553	***
R-adj	0.9919	BN	0.1825	*
		VN×OIN	-0.0554	***
		TN×AR	-0.2551	
		TN×CB	0.4127	*
		TN×DS	-0.3116	
		TN×W	0.4794	*
		VN×BN	0.066	***
		VN×CB	0.5779	*
		VN×DS	1.0299	***

	VN×W	1.0202	***
	VN×TN	0.0856	*
	BN×CB	-0.2450	**
	BN×DS	-0.0254	
	BN×W	-0.2471	**

Table 41 displays the model of traveled meters. It is very similar to that of energy consumed. The two variables are closely related.

Table 41 - Travelled Meters Model

Dep. Variable		Predictors	β	Sig
M		(Intercept)	-19484.7	**
		VN	48546.1	***
R	0.9941	OI	189.5	***
R-adj	0.992	BN	606.4	†
		VN×OIN	-190.0	***
		VN×BN	220.1	***
		VN×CB	1892.3	*
		VN×DS	3452.1	***
		VN×W	3927.0	***
		AR×TN	-817.5	
		CB×TN	1328.7	†
		DS×TN	-1005.0	
		W×TN	1657.6	*
		VN×TN	297.2	*
		BN×CB	-811.6	**
		BN×DS	-80.2	
		BN×W	-809.6	**

Table 42 displays the energy per order model.

Table 42 - Energy per Order Model

Dep. Variable		Predictors	β	Sig
ExO		(Intercept)	3.92E-02	***
		VN	3.86E-03	***
R	0.9109	BN	9.08E-04	***
R-adj	0.8921	VN×OIN	-6.28E-06	***
		AR×TN	3.83E-04	
		CB×TN	2.36E-03	***
		DS×TN	6.40E-04	†
		W×TN	3.16E-03	***
		VN×TN	-1.12E-04	†

		BN×CB	-3.70E-04	**
		BN×DS	3.45E-04	**
		BN×W	-2.76E-04	*

Table 43 shows the meter-per-order model. Again the most impactful variable is the number of vehicles. This phenomenon is due to the gridlock effect presented precedently. This time the number of bays and the number of tiers also significantly impact by significantly increasing the number of meters traveled per order. The gridlock effect is evidenced by the fact that increasing the number of floors improves the situation both in this example and in the case of energy per order.

Table 43 - Meter per Order Model

Dep. Variable		Predictors	**β**	Sig
MxO		(Intercept)	114.9	***
		VN	13.2	***
R	0.9265	BN	3.7	***
R-adj	0.9055	CB	23.7	
		DS	40.1	*
		W	16.6	
		TN	2.5	*
		CB×TN	5.3	***
		DS×TN	-1.1	
		W×TN	8.7	***
		VN×OIN	-0.02	***
		BN×CB	-2.1	**
		BN×DS	-0.3	
		BN×W	-1.3	†
		VN×TN	-0.4	*

5.9 Optimization

The optimization method we used in this case study is identical to the approach in chapter 5 on additive manufacturing. We used a multi-objective genetic algorithm to find a set of non-dominated solutions. What we propose to be different from the last chapter is the multicriteria choice methodology. We proposed a graphical method based on a colored heatmap in the previous chapter. In this analysis, we suggest a quantitative approach. In order to find the best solution. Paragraph 6.9.1 contains the definition of the optimization problem, while paragraph 6.9.2 describes the optimization results.

5.9.1 Optimization Problem Definition

The optimization problem is described in this paragraph. The 9 objectives to minimize are represented by equation 54. In order to have a single minimization problem, the performance TH is transformed TH^{-1}, while the resource utilization is transformed in the resource underutilization equal to $RUN = 1 - RU$.

Equations 55a–i are exact representations of the empirical regression models for each of the nine performances from the previous chapter that were statistically analyzed. Equation 56a forces a single storage logic. Only one logic can be utilized. Finally, equations 56b-h stand for the minimum and maximum bound of the decisional variables. We can only infer inside this domain because it is all that we have researched.

$$\min_{NV,BN,TN,DS,CB,AR,W} TH^{-1}, RUN, LT, TT, OS, CE, TD, EpO, MpO \tag{54}$$

$$TH^{-1} = 1/(k_{TH} + \hat{\beta}_{1TH} \cdot NV + \hat{\beta}_{2TH} \cdot OIN + \hat{\beta}_{3TH} \cdot CB + \hat{\beta}_{4TH} \cdot DS + \hat{\beta}_{5TH} \cdot W + \hat{\beta}_{6TH}\, NV \cdot OIN); \tag{55a}$$

$$RUN = 1 - (k_{RU} + \hat{\beta}_{1RU} \cdot NV + \hat{\beta}_{2RU} \cdot OIN + \hat{\beta}_{3RU} \cdot TN + \hat{\beta}_{4RU} \cdot CB + \hat{\beta}_{5RU} \cdot DS + \hat{\beta}_{6RU} \cdot W + \hat{\beta}_{7RU} \cdot NV \cdot OIN + \hat{\beta}_{8RU} \cdot NV \cdot CB + \hat{\beta}_{9RU} \cdot NV \cdot DS + \hat{\beta}_{10RU} \cdot NV \cdot W); \tag{55b}$$

$$LT = k_{LT} - \hat{\beta}_{1LT} \cdot NV + \hat{\beta}_{2LT} \cdot NB + \hat{\beta}_{3LT} \cdot CB + \hat{\beta}_{4LT} \cdot DS + \hat{\beta}_{5LT} \cdot W + \hat{\beta}_{6LT} \cdot NV \cdot OIN; \tag{55c}$$

$$TT = k_{TT} + \hat{\beta}_{1TT} \cdot NV + \hat{\beta}_{2TT} \cdot CB + \hat{\beta}_{3TT} \cdot DS + \hat{\beta}_{4TT} \cdot W + \hat{\beta}_{5TT} \cdot NB + \hat{\beta}_{6TT} \cdot AR \cdot NT + \hat{\beta}_{7TT} \cdot CB \cdot NT + \hat{\beta}_{8TT} \cdot DS \cdot NT + \hat{\beta}_{9TT} \cdot W \cdot NT + \hat{\beta}_{10TT} \cdot NV \cdot OIN + \hat{\beta}_{11TT} \cdot CB \cdot NB + \hat{\beta}_{12TT} \cdot DS \cdot NB + \hat{\beta}_{13TT} \cdot W \cdot NB + \hat{\beta}_{14TT} \cdot NV \cdot NB + \hat{\beta}_{15TT} \cdot NB \cdot OIN + \hat{\beta}_{16TT} \cdot NV \cdot NT; \tag{55d}$$

$$OS = k_{OS} + \hat{\beta}_{1OS} \cdot NB \cdot + \hat{\beta}_{2OS} \cdot NV; \tag{55e}$$

$$CE = k_{CE} + \hat{\beta}_{1CE} \cdot NV + \hat{\beta}_{2CE} \cdot OIN + \hat{\beta}_{3CE} \cdot NB - \hat{\beta}_{4CE} \cdot NV \cdot OIN + \hat{\beta}_{5CE} \cdot NT \cdot AR + \hat{\beta}_{6CE} \cdot NT \cdot CB + \hat{\beta}_{7CE} \cdot NT \cdot DS + \hat{\beta}_{8CE} \cdot NT \cdot W + \hat{\beta}_{9CE} \cdot NV \cdot NB + \hat{\beta}_{10CE} \cdot NV \cdot CB + \hat{\beta}_{11CE} \cdot A \cdot DS + \hat{\beta}_{12CE} \cdot NV \cdot W + \hat{\beta}_{13CE} \cdot NV \cdot R + \hat{\beta}_{14CE} \cdot NB \cdot CB + \hat{\beta}_{15CE} \cdot NB \cdot DS + \hat{\beta}_{16CE} \cdot NB \cdot W; \tag{55f}$$

$$TD = k_{TD} + \hat{\beta}_{1TD} \cdot NV + \hat{\beta}_{2TD} \cdot OIN + \hat{\beta}_{3TD} \cdot NB + \hat{\beta}_{4TD} \cdot NV \cdot OIN + \hat{\beta}_{5TD} \cdot NV \cdot NB + \hat{\beta}_{6TD} \cdot NV \cdot CB + \hat{\beta}_{7TD} \cdot NV \cdot DS + \hat{\beta}_{8TD} \cdot NV \cdot W + \hat{\beta}_{9TD} \cdot AR \cdot TN + \hat{\beta}_{10TD} \cdot CB \cdot TN + \hat{\beta}_{11TD} \cdot DS \cdot TN + \hat{\beta}_{12TD} \cdot W \cdot TN + \hat{\beta}_{13TD} \cdot NV \cdot TN + \hat{\beta}_{14TD} \cdot NB \cdot CB + \hat{\beta}_{15TD} \cdot NB \cdot DS + \hat{\beta}_{16TD} \cdot NB \cdot W; \quad (55g)$$

$$EpO = k_{EpO} + \hat{\beta}_{1EpO} \cdot NV + \hat{\beta}_{2EpO} \cdot NB + \hat{\beta}_{3EpO} \cdot NV \cdot OIN + \hat{\beta}_{4EpO} \cdot AR \cdot NT + \hat{\beta}_{5EpO} \cdot CB \cdot NT + \hat{\beta}_{6EpO} \cdot DS \cdot NT + \hat{\beta}_{7EpO} \cdot W \cdot NT + \hat{\beta}_{8EpO} \cdot NV \cdot R + \hat{\beta}_{9EpO} \cdot NB \cdot CB + \hat{\beta}_{10EpO} \cdot NB \cdot DS + \hat{\beta}_{11EpO} \cdot NB \cdot W \quad (55h)$$

$$MpO = k_{MpO} + \hat{\beta}_{1MpO} \cdot NV + \hat{\beta}_{2MpO} \cdot NB + \hat{\beta}_{3MpO} \cdot CB + \hat{\beta}_{4MpO} \cdot DS + \hat{\beta}_{5MpO} \cdot W + \hat{\beta}_{6MpO} \cdot NT + \hat{\beta}_{7MpO} \cdot CB \cdot NT + \hat{\beta}_{8MpO} \cdot DS \cdot NT + \hat{\beta}_{9MpO} \cdot W \cdot NT + \hat{\beta}_{10MpO} \cdot NV \cdot OIN + \hat{\beta}_{11MpO} \cdot NB \cdot CB + \hat{\beta}_{12MpO} \cdot NB \cdot DS + \hat{\beta}_{13MpO} \cdot NB \cdot W + \hat{\beta}_{14MpO} \cdot NV \cdot NT \quad (55i)$$

$s.t.$

$$CB + DS + AR + W = 1 \quad (56a)$$

$$\{NV \in \mathbb{N} | 1 \leq NV \leq 6\} \quad (56b)$$

$$\{BN \in \mathbb{N} | 12 \leq BN \leq 24\} \quad (56c)$$

$$\{TN \in \mathbb{N} | 3 \leq TN \leq 9\} \quad (56d)$$

$$\{DS \in \mathbb{N} | 0 \leq DS \leq 1\} \quad (56e)$$

$$\{CB\mathbb{N} | 0 \leq CB \leq 1\} \quad (56f)$$

$$\{AN \in \mathbb{N} | 0 \leq AN \leq 1\} \quad (56g)$$

$$\{W \in \mathbb{R} | 0.1 \leq W \leq 0.3\} \quad (56h)$$

5.9.2 Optimization Results

As previously stated, we implemented the problem previously described in Python using the pymoo library [135] using the NSGA-II algorithm [136].

As mentioned in paragraph 5.5.2, in order to implement the NSGA-II algorithm, four different factors have to be defined: the population (N), the crossover (X), and the mutation (M) and the number of generations to be tested (G We chose to set an M = 0.005 and an X equal to 0.95 for the same reasons described in paragraph 5.5.2, and we set a G equal to 10000.

The scientific literature claims that the NSGA-II algorithm discovers the ideal front more efficiently the greater the original population N [140]. We tested the difference between the optimal frontier obtained with an N equal to 15, 30, and 100. The difference between the first (N =15) and the second (N = 30) is slight: Looking for the best solution in each performance, these were very similar, and an average difference of 4% is computed. Testing the first ($N = 30$) with the third ($N = 100$), again, a slight difference between performances is recorded. Again an average improvement of 4% for the solutions obtained with $N = 100$. We, therefore, fixed N equal to 30, testing 350000 solutions. The obtained solutions parameter are represented in Table 44.

Table 44 - Parameters of the 30 solutions

ID	NB	NT	NV	CB	AR	DS	W
1	24	3	6	0	0	0	1
2	24	3	6	0	0	0	1
3	12	3	1	1	0	0	0
4	12	3	1	1	0	0	0
5	12	3	1	1	0	0	0
6	12	3	1	0	0	0	1
7	20	3	6	1	0	0	0
8	24	3	6	1	0	0	0
9	24	3	6	1	0	0	0
10	12	3	1	1	0	0	0
11	12	3	1	0	0	0	1
12	24	3	5	1	0	0	0
13	12	3	2	0	0	0	1

14	24	3	3	1	0	0	0
15	24	3	1	1	0	0	0
16	16	3	6	0	0	0	1
17	12	3	3	0	0	0	1
18	24	3	2	0	0	0	1
19	12	3	6	0	0	0	1
20	12	3	2	1	0	0	0
21	12	3	2	1	0	0	0
22	24	3	4	0	0	0	1
23	12	3	5	0	0	0	1
24	20	3	4	1	0	0	0
25	19	3	4	1	0	0	0
26	12	3	4	0	0	0	1
27	12	3	6	1	0	0	0
28	12	3	3	0	0	0	1
29	24	3	4	1	0	0	0
30	16	3	4	0	0	0	1

5.10 Multi-Criteria Decision Method

A Multiple-Criteria Decision Analysis (MCDA) approach is used to evaluate which of all the possible alternatives is the best solution. These methods are able to compare a set of options according to their suitability. The "Technique for Order Preference by Similarity to Ideal Solution" (TOPSIS) has been applied since it is more suitable for this study case with many criteria and alternatives, as explained by Ching-Lai Hwang and Yoon Yoon [193]. The methodology is based on choosing the best option through the similarity with the ideal solution. Starting from a matrix $a \times c$ with a alternatives to be evaluated on c criterias, it consists of five distinct steps. (i) the normalization of the matrix, (ii) the generation of the normalized weighted matrix based on the weights assigned to each criterion a priori. (iii) the definition of the two ideal best V^+ and ideal worst V^- solutions. (iv) the distances of each alternative from the ideal best d_{ab} and from the ideal worst d_{aw}, and finally, (v) the similarity of each solution with the worst solution $p_{aw} = \frac{d_{aw}}{d_{aw}+d_{ab}}$. The similarity value would be equal to 1 if the solution is farest as possible from the worst one and equal to 0 if it is precisely the same as the worst solution. After that, to find the best solution, it is easy to rank the alternatives and search for the highest p_{aw} In Figure 46, different weights assigned to performance indicators are

represented, and an arrow is shown to clarify which functions must be maximized (↑) and which are minimized (↓).

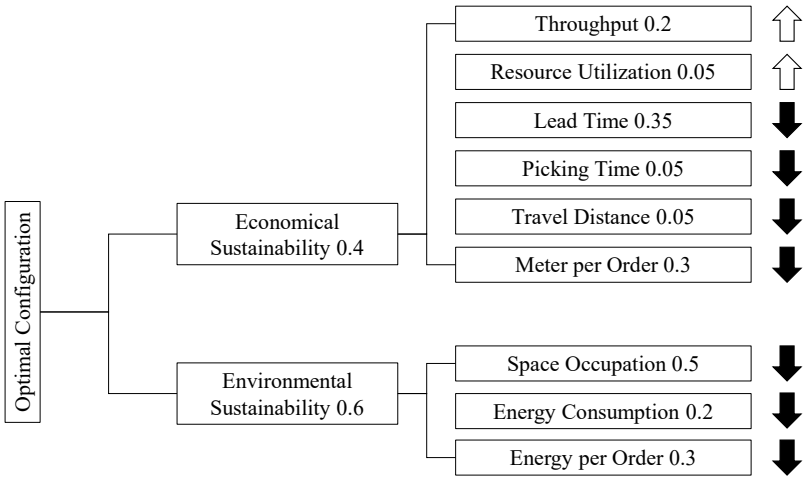

Figure 46 - Topsis Weight Tree Distribution

In this analysis, we propose a methodology to support warehouse designers in finding their best alternative in terms of economic and environmental aspects. This part of the study is highly dependent form the chosen weight. According to Franco and Montibeller, multi-criteria decision methods consist of two different phases, high-level problem structuring, in which the main goal is to define the main goal and purpose of the analysis, and a profound definition of the multi-criteria evaluation model. This second phase aims to find the criteria, evaluate the alternatives, and define a value tree in which the criteria are decomposed and hierarchized[194]. The value tree decomposes the overall objective operational objectives, which allows an efficient assessment of alternatives' performances [194]. Since this part is particularly critical, the end of the analysis must follow sensitivity analysis, robustness analysis, and solution legitimation [195].

In order to give an example of the proposed methodology, we supposed the weights sown in Figure 46. In particular, we give a weight of 0.4 out of 1 to the economic sustainability perspective and importance of 0.6 to the environmental sustainability perspective. Then going to the third level of the value tree, from the economic point of view, we give the maximum importance to the lead time, meters per order, and throughput, and then we give 0.05 to the other remaining criteria. From the

environmental perspective, we split the in 0.5 to space occupation and 0.5 to energy-related performance (0.2 for energy consumption and 0.3 for energy per order). Both meter and energy per order are considered more important than the absolute value criteria since the absolute value is dependent on the order satisfied. The higher the number of orders, the more meters traveled; thus, the energy consumption while dividing the absolute value by the number of orders is an improved efficiency measure.

Proceeding with the application of the TOPSIS algorithm, we obtain the solution ranking. Table 45 shows the three best and worst solutions. As required, the algorithm prefers more environmentally sustainable solutions at the expense of throughput and lead time. Less-performing and small warehouses are favored.

Table 45 - Ranking of the three best and worst solutions

		0.08	**0.02**	**0.14**	**0.02**	**0.2**	**0.12**	**0.03**	**0.18**	**0.12**
Rank	**ID**	**TH**	**RU**	**LT**	**TT**	**SO**	**MpO**	**TD**	**EpO**	**EC**
1	**21**	9.1	0.848	704.0	7.2	1904	12.5	42374	0.063	195.0
2	**20**	9.1	0.848	704.0	7.2	1904	12.5	42374	0.063	195.0
3	**3**	7.8	0.980	768.2	7.1	1772	10.5	35899	0.058	188.2
…	[…]	[…]	[…]	[…]	[…]	[…]	[…]	[…]	[…]	[…]
28	**16**	14.1	0.426	454.2	8.1	2896	24.2	85965	0.089	244.7
29	**1**	14.1	0.426	439.4	8.2	3824	26.9	94903	0.094	263.9
30	**2**	14.1	0.426	439.4	8.2	3824	26.9	94903	0.094	263.9

Figure 47 and Figure 48 depict the feasible best and the feasible worst solutions with a dark blue line and a red line, respectively. Figure 47 shows the parameters, while Figure 48 the performances

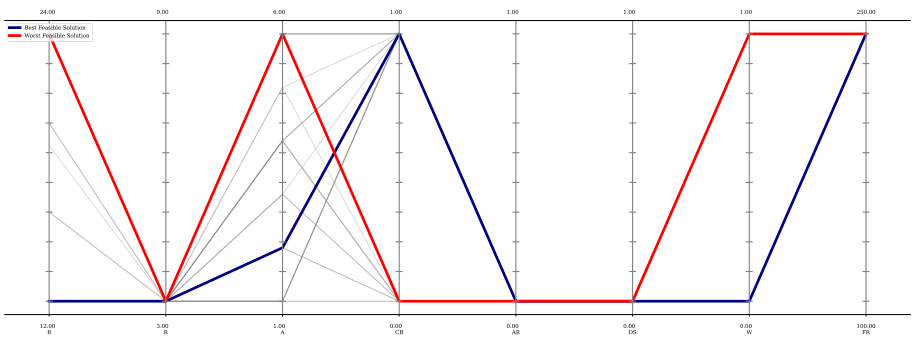

Figure 47 - Graphical representation of the parameters of the best and worst feasible solutions

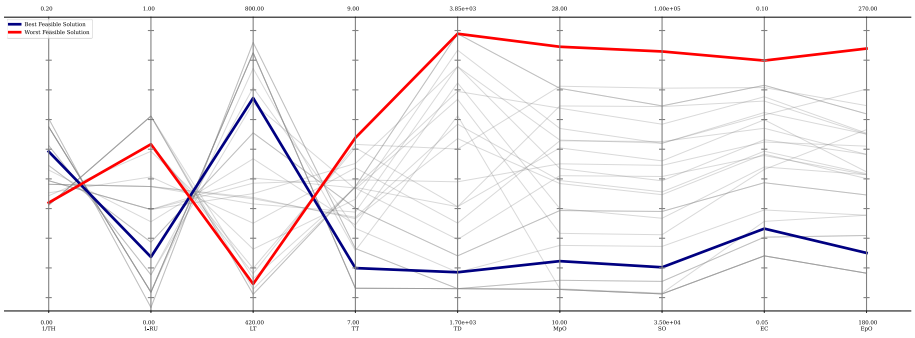

Figure 48 – Graphical representation of the performances of the best and worst feasible solutions

In the next chapter, we draw the conclusion of this thesis.

Chapter 6

Conclusions and Future Work

6.1 Summary of the work

The primary motivation for this research was to investigate decision-support approaches in the design stages for one-of-a-kind products. We directed the analysis through the study of three case studies of very different products. The study of these applications allowed us to find standard guidelines that could give rise to a generic framework. In particular, we presented an initial project in which the general purpose was to create a tool for decision support in the disposal of an industrial forklift charging system. This first problem falls into the category of the knowledge generation theoretical approach. Of the three case studies, it is the only one having a single optimization variable (cost minimization) and provides a fairly certain answer as to the amount of charging systems to insert to meet a given demand.

The second case study aimed to create a tool for decision support in additive manufacturing or prototyping small objects. In this case, several indicators of sustainability (environmental and economic) and indicators representing product quality were studied. The multiobjective problem was solved through a generic algorithm that allowed for different non-dominated solutions. These solutions were finally used to generate a colored heatmap representing the different solutions and usable as a map to move through parameter decisions. Such a graphical solution to multiobjective decision-making is an option mainly used in design or management support.

Finally, the third case study aimed to identify a tool to study the feasibility of an innovative warehouse picking system. Specifically, different economically related and environmentally related KPIs were analyzed, and the optimal warehouse layout and storage logic under varying order frequency was studied. A classical multi-criteria decision analysis (MCDA) method called TOPSIS was chosen to support multiobjective decision-making. This approach can allow the designer to decide the

importance of his or her objectives by describing a value tree without generating bias.

Figure 49 displays what critical elements of the general framework are validated with the three different use cases. In particular, as previously described, the first use case proposed an entirely theoretical approach, the second use case proposed a wholly empirical approach, and the third use case applied a hybrid approach.

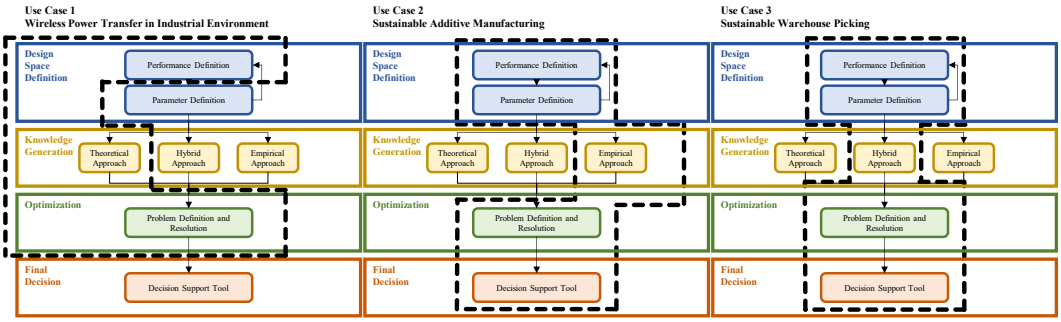

Figure 49 - General framework applied to the three use cases

6.2 Conclusive Remarks

The research methodology applied in this thesis is a use-case-based approach. We could call define it as a bottom-up approach. Specifically, to investigate the research question, we started with three very different case studies, all of which had a one-of-a-kind product element in common. By laying the foundation for these case studies, we could outline key steps or elements that then composed and validated the final proposed framework. This approach thus allowed us to base our assumptions on something practical and tangible rather than something overly theoretical and cast from above. Although this approach has degrees of advantages, it also has some limitations: its abstraction is particularly complicated. This generic framework worked within the three circumscribed case studies; however, applying it in other contexts may raise further doubts, and new critical issues may open up. Despite this limitation, we believe that using this framework as a map for defining a decision-aid tool in one-of-a-kind products may prove particularly useful. As stated earlier, one-of-a-kind product contentions generate great difficulties in dealing with decisions without adequate precognition in the designer. The proposed framework would undoubtedly help the designer understand where to look for that knowledge and, in its absence, how to generate it through experimentation.

6.3 Discussion on the Research Question

The research question we tried to address was to define a generic framework capable of supporting designers in generating a knowledge-based decision tool. In particular, to find a way to overcome the limitations of lack of knowledge by adding an intermediate step of knowledge generation. We have succeeded through the proposed framework to provide the crucial foundations and steps to accomplish this task. We believe that it is fascinating the knowledge generation step through three possible approaches, one fully data-driven, one entirely theoretical, and finally a hybrid one, makes it particularly effective for the designer to understand which direction to move towards depending on his problem and then develop a methodology that best suits his purpose. The bottom-up approach described above has limitations. However, we believe that the general framework proposed in this thesis (Figure 6) may be sufficiently generic to apply to a wide variety of case studies; conversely, it nonetheless succeeds in providing essential help through scanning key milestones. This work is only the beginning of a definition of a complete methodology, which is why we have always spoken of a generic framework. In the following paragraph, we will discuss in more detail what we believe may be the future developments of this work in the short, medium, and long term.

6.4 Limitations and Future Work

As stated before, the proposed framework has certain limitations. The main limitation described in the previous paragraphs is its use-case-based origin. It only lies on three case studies, and its abstraction could be problematic. In particular, if this method is applied to another problem, we do not have the certainty that all the issues have been thoroughly analyzed. Therefore, new case studies could generate the updating of the framework and, thus, its evolution to a more complete and articulated phase composed of more phases and sub-phases. A first future work that could be developed in the short to medium term would be to try to apply the methodology to other case studies to validate each of its parts more and thus improve it. A second exciting work that could be developed in the short term is to provide more comprehensive guidance on what kind of knowledge generation approach is most appropriate. In this work, we have exclusively defined that a theoretical approach is recommended when one has complete knowledge of the laws governing the system studied, and the product has a large size and cost. An empirical approach is recommended when the scale of the product is small and it is

possible to test various parameters without raising development costs too high. Finally, a hybrid approach is recommended when we straddle the two described above: some basic rules are known, and the cost of experimentation is high. However, these evaluations should be studied more in the future.

Finally, this framework only outlines the steps the designer must follow to make conscious decisions. In this thesis, we have never investigated all the opportunities of existing methods to define the design space, generate knowledge, optimize the problem, and decide on the most appropriate solution. The object of future long-term work that would undoubtedly make the proposed framework extremely interesting will be to propose all possible alternatives to achieve the four identified goals and then guide the designer to those most suitable in his or her specific case study. Specifically, explore all possible techniques and approaches that can be used in each element of the framework.

References

[1] L. Panza, A. Faveto, G. Bruno, F. Lombardi, Open product development to support circular economy through a material lifecycle management framework, (2022) 27. https://doi.org/10.1504/IJPLM.2022.125826.

[2] K.T. Ulrich, S.D. Eppinger, Product design and development, Sixth edition, McGraw-Hill Education, New York, NY, 2016.

[3] M. Hertwig, A. Barwasser, J. Lentes, F. Adam, J. Kalkuhl, M. Siee, Crowd Engineering – Produktentwicklung in der Community: Innovation in der Produktentwicklung durch die Einbindung einer Community, ZWF. 115 (2020) 36–39. https://doi.org/10.3139/104.112226.

[4] Y. Koren, X. Gu, W. Guo, Reconfigurable manufacturing systems: Principles, design, and future trends, Front. Mech. Eng. 13 (2018) 121–136. https://doi.org/10.1007/s11465-018-0483-0.

[5] X. Gong, R. Jiao, A. Jariwala, B. Morkos, Crowdsourced manufacturing cyber platform and intelligent cognitive assistants for delivery of manufacturing as a service: fundamental issues and outlook, Int J Adv Manuf Technol. 117 (2021) 1997–2007. https://doi.org/10.1007/s00170-021-07789-7.

[6] O. Fisher, N. Watson, L. Porcu, D. Bacon, M. Rigley, R.L. Gomes, Cloud manufacturing as a sustainable process manufacturing route, Journal of Manufacturing Systems. 47 (2018) 53–68. https://doi.org/10.1016/j.jmsy.2018.03.005.

[7] A. Barni, E. Carpanzano, G. Landolfi, P. Pedrazzoli, Urban Manufacturing of Sustainable Customer-Oriented Products, in: L. Monostori, V.D. Majstorovic, S.J. Hu, D. Djurdjanovic (Eds.), Proceedings of the 4th International Conference on the Industry 4.0 Model for Advanced Manufacturing, Springer International Publishing, Cham, 2019: pp. 128–141. https://doi.org/10.1007/978-3-030-18180-2_10.

[8] M. Lanz, E. Järvenpää, Social manufacturing and open design, Responsible Consumption and Production. (2020) 668–678.

[9] T. Pereira, J.V. Kennedy, J. Potgieter, A comparison of traditional manufacturing vs additive manufacturing, the best method for the job, Procedia Manufacturing. 30 (2019) 11–18. https://doi.org/10.1016/j.promfg.2019.02.003.

[10] J.S. Srai, M. Kumar, G. Graham, W. Phillips, J. Tooze, S. Ford, P. Beecher, B. Raj, M. Gregory, M.K. Tiwari, B. Ravi, A. Neely, R. Shankar, F. Charnley, A. Tiwari, Distributed manufacturing: scope, challenges and opportunities, International Journal of Production Research. 54 (2016) 6917–6935. https://doi.org/10.1080/00207543.2016.1192302.

[11] G. Bruno, A. Faveto, E. Traini, An open source framework for the storage and reuse of industrial knowledge through the integration of PLM and MES, Management and Production Engineering Review. (2020).

[12] G. d'Antonio, F. Segonds, F. Laverne, J. Sauza-Bedolla, P. Chiabert, A framework for manufacturing execution system deployment in an advanced additive manufacturing process, International Journal of Product Lifecycle Management. 10 (2017) 1–19. https://doi.org/10.1504/IJPLM.2017.082996.

[13] E.G. Carayannis, D.F.J. Campbell, "Mode 3" and "Quadruple Helix": toward a 21st century fractal innovation ecosystem, IJTM. 46 (2009) 201. https://doi.org/10.1504/IJTM.2009.023374.

[14] M. Rosienkiewicz, J. Helman, M. Cholewa, M. Molasy, G. Krause-Juettler, Analysis and Assessment of Bottom-Up Models Developed in Central Europe for Enhancing Open Innovation and Technology Transfer in Advanced Manufacturing, in: S.G. Scholz, R.J. Howlett, R. Setchi (Eds.), Sustainable Design and Manufacturing 2020, Springer, Singapore, 2021: pp. 119–128. https://doi.org/10.1007/978-981-15-8131-1_11.

[15] P. Jiang, J. Leng, K. Ding, P. Gu, Y. Koren, Social manufacturing as a sustainable paradigm for mass individualization, Proceedings of the Institution of Mechanical Engineers, Part B: Journal of Engineering Manufacture. 230 (2016) 1961–1968. https://doi.org/10.1177/0954405416666903.

[16] S. Wilkinson, N. Cope, Chapter 10 - 3D Printing and Sustainable Product Development, in: M. Dastbaz, C. Pattinson, B. Akhgar (Eds.), Green Information Technology, Morgan Kaufmann, Boston, 2015: pp. 161–183. https://doi.org/10.1016/B978-0-12-801379-3.00010-3.

[17] H.K. Kwon, K.K. Seo, Development of a Hybrid Life Cycle Cost Model for Estimating Product Design Alternatives in Cloud Computing Based Collaborative Design Environment, Advanced Materials Research. 658 (2013) 614–619. https://doi.org/10.4028/www.scientific.net/AMR.658.614.

[18] L. Rocha, A. Gomez, N. Araújo, C. Otero, D. Rodrigues, Cloud Management Tools for Sustainable SMEs, Procedia CIRP. 40 (2016) 220–224. https://doi.org/10.1016/j.procir.2016.01.106.

[19] P. Smith, J. Baille, L.-S. McHattie, Sustainable Design Futures: An open design vision for the circular economy in fashion and textiles, The Design

Journal. 20 (2017) S1938–S1947. https://doi.org/10.1080/14606925.2017.1352712.

[20] S. Bracke, J. Michalski, M. Inoue, T. Yamada, CDMF-RELSUS concept: reliable products are sustainable products – influences on product design, manufacturing and use phase, International Journal of Sustainable Manufacturing. 3 (2013) 57–73. https://doi.org/10.1504/IJSM.2013.058634.

[21] S. Bracke, M. Inoue, B. Ulutas, T. Yamada, CDMF-RELSUS Concept: Reliable and Sustainable Products–influences on Design, Manufacturing, Layout Integration and Use Phase, Procedia CIRP. 15 (2014) 8–13. https://doi.org/10.1016/j.procir.2014.06.083.

[22] J. Bonvoisin, Implications of Open Source Design for Sustainability, in: R. Setchi, R.J. Howlett, Y. Liu, P. Theobald (Eds.), Sustainable Design and Manufacturing 2016, Springer International Publishing, Cham, 2016: pp. 49–59. https://doi.org/10.1007/978-3-319-32098-4_5.

[23] J. Bonvoisin, Limits of ecodesign: the case for open source product development, International Journal of Sustainable Engineering. 10 (2017) 198–206. https://doi.org/10.1080/19397038.2017.1317875.

[24] A. Rebensdorf, A. Gergert, G.A. Oosthuizen, S. Böhm, Open Community Manufacturing – Development Challenge as a Concept for Value Creation for Sustainable Manufacturing in South Africa, Procedia CIRP. 26 (2015) 167–172. https://doi.org/10.1016/j.procir.2015.01.012.

[25] R.K. Yin, Case study research: Design and methods (applied social research methods), Sage publications Thousand Oaks, CA, 2014.

[26] B. Flyvbjerg, Five misunderstandings about case-study research, Qualitative Inquiry. 12 (2006) 219–245.

[27] K.M. Eisenhardt, M.E. Graebner, Theory building from cases: Opportunities and challenges, Academy of Management Journal. 50 (2007) 25–32.

[28] S. Keivanpour, D. Ait Kadi, Strategic eco-design map of the complex products: toward visualisation of the design for environment, International Journal of Production Research. 56 (2018) 7296–7312. https://doi.org/10.1080/00207543.2017.1388931.

[29] A. Kengpol, C. O'Brien, The development of a decision support tool for the selection of advanced technology to achieve rapid product development, International Journal of Production Economics. 69 (2001) 177–191. https://doi.org/10.1016/S0925-5273(00)00016-5.

[30] A.T. Olewnik, K. Lewis, On Validating Engineering Design Decision Support Tools, Concurrent Engineering. 13 (2005) 111–122. https://doi.org/10.1177/1063293X05053796.

[31] S. Stewart, J. Giambalvo, J. Vance, J. Faludi, C. a un sito esterno I. contenuti a cui indirizza il collegamento verranno aperti in una nuova finestra, S. Hoffenson, C. a un sito esterno I. contenuti a cui indirizza il collegamento verranno aperti in una nuova finestra, A Product Development Approach Advisor for Navigating Common Design Methods, Processes, and Environments, Designs. 4 (2020). https://doi.org/10.3390/designs4010004.

[32] G.A. Hazelrigg, A Framework for Decision-Based Engineering Design, Journal of Mechanical Design. 120 (1998) 653–658. https://doi.org/10.1115/1.2829328.

[33] J. Elkington, The Triple Bottom Line, Environmental Management: Readings and Cases. 2 (1997) 49–66.

[34] United Nations, Transforming our world: the 2030 Agenda for Sustainable Development, (2015). https://www.un.org/ga/search/view_doc.asp?symbol=A/RES/70/1&Lang=E.

[35] D. Hunkeler, E. Vanakari, G. Biswas, K. Kawamura, R. Dhingra, L. Caffey, E. Huang, A decision support system for life cycle management, in: Proceedings First International Symposium on Environmentally Conscious Design and Inverse Manufacturing, 1999: pp. 728–732. https://doi.org/10.1109/ECODIM.1999.747706.

[36] S.W. Lye, S.G. Lee, M.K. Khoo, ECoDE – An Environmental Component Design Evaluation Tool, (2002) 10.

[37] M. Cristofari, A. Deshmukh, B. Wang, Green quality function deployment, in: Proceedings of the 4th International Conference on Environmentally Conscious Design and Manufacturing, 1996: pp. 297–304.

[38] Y. Zhang, Green QFD-II: A life cycle approach for environmentally conscious manufacturing by integrating LCA and LCC into QFD matrices, International Journal of Production Research. 37 (1999) 1075–1091. https://doi.org/10.1080/002075499191418.

[39] C. Mehta, B. Wang, Green Quality Function Deployment III: A Methodology for Developing Environmentally Conscious Products, Journal of Design and Manufacturing Automation. 1 (2001) 1–16. https://doi.org/10.1080/15320370108500198.

[40] A. Romli, P. Prickett, R. Setchi, S. Soe, Integrated eco-design decision-making for sustainable product development, International Journal of Production Research. 53 (2015) 549–571. https://doi.org/10.1080/00207543.2014.958593.

[41] A. Olewnik, V.G. Hariharan, Conjoint-HoQ: evolving a methodology to map market needs to product profiles, IJPD. 10 (2010) 338. https://doi.org/10.1504/IJPD.2010.031978.

[42] A. Romli, R. Setchi, P. Prickett, M.P. de la Pisa, Eco-design case-based reasoning tool: The integration of ecological quality function deployment and case-based reasoning methods for supporting sustainable product design, Proceedings of the Institution of Mechanical Engineers, Part B: Journal of Engineering Manufacture. 232 (2018) 1778–1797. https://doi.org/10.1177/0954405416668928.

[43] F. Dell'Anna, M. Bottero, C. Becchio, S.P. Corgnati, G. Mondini, Designing a decision support system to evaluate the environmental and extra-economic performances of a nearly zero-energy building, SASBE. 9 (2020) 413–442. https://doi.org/10.1108/SASBE-09-2019-0121.

[44] R. Rai, C.K. Sahu, Driven by Data or Derived Through Physics? A Review of Hybrid Physics Guided Machine Learning Techniques With Cyber-Physical System (CPS) Focus, IEEE Access. 8 (2020) 71050–71073. https://doi.org/10.1109/ACCESS.2020.2987324.

[45] A. Faveto, F. Serio, V. Lunetto, P. Chiabert, Methodology for Commodity Cost Estimation Through Production Line Analysis and Simulation, in: Product Lifecycle Management. Green and Blue Technologies to Support Smart and Sustainable Organizations, Springer, Cham, 2022: pp. 28–43. https://doi.org/10.1007/978-3-030-94335-6_3.

[46] European Commission, A Roadmap for moving to a competitive low carbon economy in 2050, (2011). https://eur-lex.europa.eu/LexUriServ/LexUriServ.do?uri=COM:2011:0112:FIN:EN:PDF.

[47] E. Ferrero, S. Alessandrini, A. Balanzino, Impact of the electric vehicles on the air pollution from a highway, Applied Energy. 169 (2016) 450–459. https://doi.org/10.1016/j.apenergy.2016.01.098.

[48] J. Gould, T.F. Golob, Clean air forever? A longitudinal analysis of opinions about air pollution and electric vehicles, Transportation Research Part D: Transport and Environment. 3 (1998) 157–169. https://doi.org/10.1016/S1361-9209(97)00018-7.

[49] S. Sagaria, R.C. Neto, P. Baptista, Modelling approach for assessing influential factors for EV energy performance, Sustainable Energy Technologies and Assessments. 44 (2021) 100984. https://doi.org/10.1016/j.seta.2020.100984.

[50] J.V. Renquist, B. Dickman, T.H. Bradley, Economic comparison of fuel cell powered forklifts to battery powered forklifts, International Journal of

Hydrogen Energy. 37 (2012) 12054–12059. https://doi.org/10.1016/j.ijhydene.2012.06.070.

[51] R.S. Widrick, S.G. Nurre, M.J. Robbins, Optimal Policies for the Management of an Electric Vehicle Battery Swap Station, Transportation Science. 52 (2018) 59–79. https://doi.org/10.1287/trsc.2016.0676.

[52] L. Unterreiner, V. Jülch, S. Reith, Recycling of Battery Technologies – Ecological Impact Analysis Using Life Cycle Assessment (LCA), Energy Procedia. 99 (2016) 229–234. https://doi.org/10.1016/j.egypro.2016.10.113.

[53] V. Cirimele, M. Diana, F. Freschi, M. Mitolo, Inductive Power Transfer for Automotive Applications: State-of-the-Art and Future Trends, IEEE Trans. on Ind. Applicat. 54 (2018) 4069–4079. https://doi.org/10.1109/TIA.2018.2836098.

[54] R. Ruffo, V. Cirimele, M. Diana, M. Khalilian, A.L. Ganga, P. Guglielmi, Sensorless Control of the Charging Process of a Dynamic Inductive Power Transfer System With an Interleaved Nine-Phase Boost Converter, IEEE Transactions on Industrial Electronics. 65 (2018) 7630–7639. https://doi.org/10.1109/TIE.2018.2803719.

[55] W. Shi, J. Dong, T.B. Soeiro, P. Bauer, Integrated Solution for Electric Vehicle and Foreign Object Detection in the Application of Dynamic Inductive Power Transfer, IEEE Transactions on Vehicular Technology. 70 (2021) 11365–11377. https://doi.org/10.1109/TVT.2021.3112278.

[56] M. Xia, S. Aissa, On the Efficiency of Far-Field Wireless Power Transfer, IEEE Transactions on Signal Processing. 63 (2015) 2835–2847. https://doi.org/10.1109/TSP.2015.2417497.

[57] Z. Zhang, H. Pang, A. Georgiadis, C. Cecati, Wireless Power Transfer—An Overview, IEEE Trans. Ind. Electron. 66 (2019) 1044–1058. https://doi.org/10.1109/TIE.2018.2835378.

[58] G.A. Covic, J.T. Boys, Modern Trends in Inductive Power Transfer for Transportation Applications, IEEE Journal of Emerging and Selected Topics in Power Electronics. 1 (2013) 28–41. https://doi.org/10.1109/JESTPE.2013.2264473.

[59] C.C. Mi, G. Buja, S.Y. Choi, C.T. Rim, Modern Advances in Wireless Power Transfer Systems for Roadway Powered Electric Vehicles, IEEE Transactions on Industrial Electronics. 63 (2016) 6533–6545. https://doi.org/10.1109/TIE.2016.2574993.

[60] V. Cirimele, F. Freschi, L. Giaccone, L. Pichon, M. Repetto, Human Exposure Assessment in Dynamic Inductive Power Transfer for Automotive Applications, IEEE Transactions on Magnetics. 53 (2017) 1–4. https://doi.org/10.1109/TMAG.2017.2658955.

[61] V. Cirimele, M. Diana, F. Bellotti, R. Berta, N.E. Sayed, A. Kobeissi, P. Guglielmi, R. Ruffo, M. Khalilian, A. La Ganga, J. Colussi, A.D. Gloria, The Fabric ICT Platform for Managing Wireless Dynamic Charging Road Lanes, IEEE Transactions on Vehicular Technology. 69 (2020) 2501–2512. https://doi.org/10.1109/TVT.2020.2968211.

[62] S. Laporte, G. Coquery, V. Deniau, A. De Bernardinis, N. Hautière, Dynamic Wireless Power Transfer Charging Infrastructure for Future EVs: From Experimental Track to Real Circulated Roads Demonstrations, WEVJ. 10 (2019) 84. https://doi.org/10.3390/wevj10040084.

[63] R. Tavakoli, Z. Pantic, Analysis, Design, and Demonstration of a 25-kW Dynamic Wireless Charging System for Roadway Electric Vehicles, IEEE Journal of Emerging and Selected Topics in Power Electronics. 6 (2018) 1378–1393. https://doi.org/10.1109/JESTPE.2017.2761763.

[64] S.-J. Huang, T.-S. Lee, W.-H. Li, R.-Y. Chen, Modular On-Road AGV Wireless Charging Systems Via Interoperable Power Adjustment, IEEE Transactions on Industrial Electronics. 66 (2019) 5918–5928. https://doi.org/10.1109/TIE.2018.2873165.

[65] A. Zaheer, G.A. Covic, D. Kacprzak, A Bipolar Pad in a 10-kHz 300-W Distributed IPT System for AGV Applications, IEEE Transactions on Industrial Electronics. 61 (2014) 3288–3301. https://doi.org/10.1109/TIE.2013.2281167.

[66] A. Faveto, E. Traini, G. Bruno, F. Lombardi, Development of a key performance indicator framework for automated warehouse systems, IFAC-PapersOnLine. 54 (2021) 116–121. https://doi.org/10.1016/j.ifacol.2021.08.013.

[67] M. Bartolini, E. Bottani, E.H. Grosse, Green warehousing: Systematic literature review and bibliometric analysis, Journal of Cleaner Production. 226 (2019) 242–258. https://doi.org/10.1016/j.jclepro.2019.04.055.

[68] M. Dotoli, N. Epicoco, M. Falagario, N. Costantino, B. Turchiano, An integrated approach for warehouse analysis and optimization: A case study, Computers in Industry. 70 (2015) 56–69. https://doi.org/10.1016/j.compind.2014.12.004.

[69] M. Torabizadeh, N.M. Yusof, A. Ma'aram, A.M. Shaharoun, Identifying sustainable warehouse management system indicators and proposing new weighting method, Journal of Cleaner Production. 248 (2020) 119190. https://doi.org/10.1016/j.jclepro.2019.119190.

[70] Z. Liu, Z. Song, Robust planning of dynamic wireless charging infrastructure for battery electric buses, Transportation Research Part C: Emerging Technologies. 83 (2017) 77–103. https://doi.org/10.1016/j.trc.2017.07.013.

[71] S. Helber, J. Broihan, Y. Jang, P. Hecker, T. Feuerle, Location Planning for Dynamic Wireless Charging Systems for Electric Airport Passenger Buses, Energies. 11 (2018) 258. https://doi.org/10.3390/en11020258.

[72] Z. Khan, S.M. Khan, M. Chowdhury, I. Safro, H. Ushijima-Mwesigwa, Wireless charging utility maximization and intersection control delay minimization framework for electric vehicles, Computer-Aided Civil and Infrastructure Engineering. 34 (2019) 547–568. https://doi.org/10.1111/mice.12439.

[73] X. Sun, Z. Chen, Y. Yin, Integrated planning of static and dynamic charging infrastructure for electric vehicles, Transportation Research Part D: Transport and Environment. 83 (2020) 102331. https://doi.org/10.1016/j.trd.2020.102331.

[74] T. Kawakami, S. Takata, Battery Life Cycle Management for Automatic Guided Vehicle Systems, in: M. Matsumoto, Y. Umeda, K. Masui, S. Fukushige (Eds.), Design for Innovative Value Towards a Sustainable Society, Springer Netherlands, Dordrecht, 2012: pp. 403–408. https://doi.org/10.1007/978-94-007-3010-6_77.

[75] J. Matheys, J.M. Timmermans, J.V. Mierlo, S. Meyer, P.V. den Bossche, Comparison of the environmental impact of five electric vehicle battery technologies using LCA, IJSM. 1 (2009) 318. https://doi.org/10.1504/IJSM.2009.023977.

[76] J.L. Sullivan, L. Gaines, Status of life cycle inventories for batteries, Energy Conversion and Management. 58 (2012) 134–148. https://doi.org/10.1016/j.enconman.2012.01.001.

[77] C.A. Janicak, T.L. Cekada, Regulating forklift safety: Strategies to prevent injury and improve compliance, Professional Safety. 61 (2016) 38–44.

[78] C.H. Dharmakeerthi, N. Mithulananthan, T.K. Saha, Impact of electric vehicle fast charging on power system voltage stability, International Journal of Electrical Power & Energy Systems. 57 (2014) 241–249. https://doi.org/10.1016/j.ijepes.2013.12.005.

[79] TMHE-Toyota Material Handling Europe, Technical specifications - Toyota Traigo 48, (2020). https://media.toyota-forklifts.eu/published/21449_Original%20document_toyota%20mh.pdf.

[80] VDI-Fachbereich Technische Logistik, VDI 2198 - Type sheets for industrial trucks, (2019). https://www.vdi.de/richtlinien/details/vdi-2198-typenblaetter-fuer-flurfoerderzeuge.

[81] P.E. Hart, N.J. Nilsson, B. Raphael, A Formal Basis for the Heuristic Determination of Minimum Cost Paths, IEEE Transactions on Systems

Science and Cybernetics. 4 (1968) 100–107. https://doi.org/10.1109/TSSC.1968.300136.

[82] L.M. Pohl, R.D. Meller, K.R. Gue, An analysis of dual-command operations in common warehouse designs, Transportation Research Part E: Logistics and Transportation Review. 45 (2009) 367–379. https://doi.org/10.1016/j.tre.2008.09.010.

[83] H. Bikas, A.K. Lianos, P. Stavropoulos, A design framework for additive manufacturing, Int J Adv Manuf Technol. 103 (2019) 3769–3783. https://doi.org/10.1007/s00170-019-03627-z.

[84] F. Sini, G. Bruno, P. Chiabert, F. Segonds, A Lean Quality Control Approach for Additive Manufacturing, in: F. Nyffenegger, J. Ríos, L. Rivest, A. Bouras (Eds.), Product Lifecycle Management Enabling Smart X, Springer International Publishing, Cham, 2020: pp. 59–69. https://doi.org/10.1007/978-3-030-62807-9_6.

[85] S. Singh, G. Singh, C. Prakash, S. Ramakrishna, Current status and future directions of fused filament fabrication, Journal of Manufacturing Processes. 55 (2020) 288–306. https://doi.org/10.1016/j.jmapro.2020.04.049.

[86] T.D. Ngo, A. Kashani, G. Imbalzano, K.T.Q. Nguyen, D. Hui, Additive manufacturing (3D printing): A review of materials, methods, applications and challenges, Composites Part B: Engineering. 143 (2018) 172–196. https://doi.org/10.1016/j.compositesb.2018.02.012.

[87] M.-A. de Pastre, S.-C. Toguem Tagne, N. Anwer, Test artefacts for additive manufacturing: A design methodology review, CIRP Journal of Manufacturing Science and Technology. 31 (2020) 14–24. https://doi.org/10.1016/j.cirpj.2020.09.008.

[88] G. Moroni, S. Petrò, W. Polini, Geometrical product specification and verification in additive manufacturing, CIRP Annals. 66 (2017) 157–160. https://doi.org/10.1016/j.cirp.2017.04.043.

[89] G. Ameta, R. Lipman, S. Moylan, P. Witherell, Investigating the Role of Geometric Dimensioning and Tolerancing in Additive Manufacturing, Journal of Mechanical Design. 137 (2015) 111401. https://doi.org/10.1115/1.4031296.

[90] F. Segonds, Design By Additive Manufacturing: an application in aeronautics and defence, Virtual and Physical Prototyping. 13 (2018) 237–245. https://doi.org/10.1080/17452759.2018.1498660.

[91] H.D. Budinoff, S. McMains, Will it print: a manufacturability toolbox for 3D printing, Int J Interact Des Manuf. 15 (2021) 613–630. https://doi.org/10.1007/s12008-021-00786-w.

[92] O.A. Mohamed, S.H. Masood, J.L. Bhowmik, Optimization of fused deposition modeling process parameters: a review of current research and future prospects, Adv. Manuf. 3 (2015) 42–53. https://doi.org/10.1007/s40436-014-0097-7.

[93] V. Cojocaru, D. Frunzaverde, C.-O. Miclosina, G. Marginean, The Influence of the Process Parameters on the Mechanical Properties of PLA Specimens Produced by Fused Filament Fabrication—A Review, Polymers. 14 (2022) 886. https://doi.org/10.3390/polym14050886.

[94] S. Vyavahare, S. Teraiya, D. Panghal, S. Kumar, Fused deposition modelling: a review, RPJ. 26 (2020) 176–201. https://doi.org/10.1108/RPJ-04-2019-0106.

[95] M.U. Obi, P. Pradel, M. Sinclair, R. Bibb, A bibliometric analysis of research in design for additive manufacturing, RPJ. ahead-of-print (2022). https://doi.org/10.1108/RPJ-11-2020-0291.

[96] N. Bocken, P. Ritala, Six ways to build circular business models, Journal of Business Strategy. ahead-of-print (2021). https://doi.org/10.1108/JBS-11-2020-0258.

[97] F.L. Garcia, V.A. da S. Moris, A.O. Nunes, D.A.L. Silva, Environmental performance of additive manufacturing process – an overview, Rapid Prototyping Journal. 24 (2018) 1166–1177. https://doi.org/10.1108/RPJ-05-2017-0108.

[98] C.A. Griffiths, J. Howarth, G. De Almeida-Rowbotham, A. Rees, R. Kerton, A design of experiments approach for the optimisation of energy and waste during the production of parts manufactured by 3D printing, Journal of Cleaner Production. 139 (2016) 74–85. https://doi.org/10.1016/j.jclepro.2016.07.182.

[99] V. Lunetto, P.C. Priarone, M. Galati, P. Minetola, On the correlation between process parameters and specific energy consumption in fused deposition modelling, Journal of Manufacturing Processes. 56 (2020) 1039–1049. https://doi.org/10.1016/j.jmapro.2020.06.002.

[100] P. Mognol, D. Lepicart, N. Perry, Rapid prototyping: energy and environment in the spotlight, Rapid Prototyping Journal. 12 (2006) 26–34. https://doi.org/10.1108/13552540610637246.

[101] A. Drizo, J. Pegna, Environmental impacts of rapid prototyping: an overview of research to date, Rapid Prototyping Journal. 12 (2006) 64–71. https://doi.org/10.1108/13552540610652393.

[102] S. Chong, G.-T. Pan, M. Khalid, T.C.-K. Yang, S.-T. Hung, C.-M. Huang, Physical Characterization and Pre-assessment of Recycled High-Density

Polyethylene as 3D Printing Material, J Polym Environ. 25 (2017) 136–145. https://doi.org/10.1007/s10924-016-0793-4.

[103] N. Vidakis, M. Petousis, A. Maniadi, E. Koudoumas, A. Vairis, J. Kechagias, Sustainable Additive Manufacturing: Mechanical Response of Acrylonitrile-Butadiene-Styrene over Multiple Recycling Processes, Sustainability. 12 (2020) 3568. https://doi.org/10.3390/su12093568.

[104] C.G. Schirmeister, T. Hees, E.H. Licht, R. Mülhaupt, 3D printing of high density polyethylene by fused filament fabrication, Additive Manufacturing. 28 (2019) 152–159. https://doi.org/10.1016/j.addma.2019.05.003.

[105] C. Liu, A.C.C. Law, D. Roberson, Z. (James) Kong, Image analysis-based closed loop quality control for additive manufacturing with fused filament fabrication, Journal of Manufacturing Systems. 51 (2019) 75–86. https://doi.org/10.1016/j.jmsy.2019.04.002.

[106] A.M.M.S. Ullah, H. Hashimoto, A. Kubo, N.A. Jun', ichi Tamaki, Sustainability analysis of rapid prototyping: material/resource and process perspectives, IJSM. 3 (2013) 20. https://doi.org/10.1504/IJSM.2013.058640.

[107] V. KEK, V. S., B. P., M. R., Rapid prototyping process selection using multi criteria decision making considering environmental criteria and its decision support system, Rapid Prototyping Journal. 22 (2016) 225–250. https://doi.org/10.1108/RPJ-03-2014-0040.

[108] F. Laverne, E. Bottacini, F. Segonds, N. Perry, G. D'Antonio, P. Chiabert, TEAM: A Tool for Eco Additive Manufacturing to Optimize Environmental Impact in Early Design Stages, in: P. Chiabert, A. Bouras, F. Noël, J. Ríos (Eds.), Product Lifecycle Management to Support Industry 4.0, Springer International Publishing, Cham, 2018: pp. 736–746. https://doi.org/10.1007/978-3-030-01614-2_67.

[109] L. Yi, M. Glatt, P. Sridhar, K. de Payrebrune, B.S. Linke, B. Ravani, J.C. Aurich, An eco-design for additive manufacturing framework based on energy performance assessment, Additive Manufacturing. 33 (2020) 101120. https://doi.org/10.1016/j.addma.2020.101120.

[110] N.M. Khorram, F. Nonino, G. Palombi, S.A. Torabi, Economic sustainability of additive manufacturing: Contextual factors driving its performance in rapid prototyping, Journal of Manufacturing Technology Management. 30 (2018) 353–365. https://doi.org/10.1108/JMTM-05-2018-0131.

[111] M. Baldinger, G. Levy, P. Schönsleben, M. Wandfluh, Additive manufacturing cost estimation for buy scenarios, Rapid Prototyping Journal. 22 (2016) 871–877. https://doi.org/10.1108/RPJ-02-2015-0023.

[112] B.T. Wittbrodt, A.G. Glover, J. Laureto, G.C. Anzalone, D. Oppliger, J.L. Irwin, J.M. Pearce, Life-cycle economic analysis of distributed

manufacturing with open-source 3-D printers, Mechatronics. 23 (2013) 713–726. https://doi.org/10.1016/j.mechatronics.2013.06.002.

[113] F. Segonds, G. Cohen, P. Veron, J. Peyceré, PLM and early stages collaboration in interactive design, a case study in the glass industry, International Journal on Interactive Design and Manufacturing. (2014). https://doi.org/10.1007/s12008-014-0217-4.

[114] F. Markou, F. Segonds, M. Rio, N. Perry, A methodological proposal to link Design with Additive Manufacturing to environmental considerations in the Early Design Stages, Int J Interact Des Manuf. 11 (2017) 799–812. https://doi.org/10.1007/s12008-017-0412-1.

[115] B. Rocheton, F. Segonds, F. Laverne, N. Perry, HESAM: A Human cEntered Sustainable Additive Manufacturing Tool for Early Design Stages, CADandA. 18 (2020) 258–271. https://doi.org/10.14733/cadaps.2021.258-271.

[116] R. Agrawal, Sustainable design guidelines for additive manufacturing applications, Rapid Prototyping Journal. 28 (2022) 1221–1240. https://doi.org/10.1108/RPJ-09-2021-0251.

[117] M. Alizadeh, M.N. Esfahani, W. Tian, J. Ma, Data-Driven Energy Efficiency and Part Geometric Accuracy Modeling and Optimization of Green Fused Filament Fabrication Processes, Journal of Mechanical Design. 142 (2020) 041701. https://doi.org/10.1115/1.4044596.

[118] ISO 52902: 2019 - Additive manufacturing - Test artifacts - Geometric capability assessment of additive manufacturing systems, BSI, 2019.

[119] K. Kumar, V. Singh, P. Katyal, N. Sharma, EDM μ-drilling in Ti-6Al-7Nb: experimental investigation and optimization using NSGA-II, Int J Adv Manuf Technol. 104 (2019) 2727–2738. https://doi.org/10.1007/s00170-019-04012-6.

[120] Q. Feng, L. Liu, X. Zhou, Automated multi-objective optimization for thin-walled plastic products using Taguchi, ANOVA, and hybrid ANN-MOGA, Int J Adv Manuf Technol. 106 (2020) 559–575. https://doi.org/10.1007/s00170-019-04488-2.

[121] D. Mavris, D. DeLaurentis, O. Bandte, M. Hale, A stochastic approach to multi-disciplinary aircraft analysis and design, in: 36th AIAA Aerospace Sciences Meeting and Exhibit, American Institute of Aeronautics and Astronautics, Reno,NV,U.S.A., 1998. https://doi.org/10.2514/6.1998-912.

[122] M.F. Ashby, Chapter 6 - Eco-data: values, sources, precision, in: M.F. Ashby (Ed.), Materials and the Environment (Third Edition), Butterworth-Heinemann, 2021: pp. 107–147. https://doi.org/10.1016/B978-0-12-821521-0.00006-2.

[123] M.F. Ashby, ed., Appendix B—Eco- and supply-chain data, in: Materials and the Environment (Third Edition), Butterworth-Heinemann, 2021: pp. 403–429. https://doi.org/10.1016/B978-0-12-821521-0.15002-9.

[124] L. Yu, Y. Pan, Y. Wu, Research on Data Normalization Methods in Multi-Attribute Evaluation, in: 2009 International Conference on Computational Intelligence and Software Engineering, IEEE, Wuhan, 2009: pp. 1–5. https://doi.org/10.1109/CISE.2009.5362721.

[125] M.S. Tootooni, A. Dsouza, R. Donovan, P.K. Rao, Z. (James) Kong, P. Borgesen, Assessing the Geometric Integrity of Additive Manufactured Parts From Point Cloud Data Using Spectral Graph Theoretic Sparse Representation-Based Classification, in: American Society of Mechanical Engineers Digital Collection, 2017. https://doi.org/10.1115/MSEC2017-2794.

[126] W. Lin, Online quality monitoring in material extrusion additive manufacturing processes based on laser scanning technology, Precision Engineering. (2019) 9.

[127] S. Romano, A. Abel, J. Gumpinger, A.D. Brandão, S. Beretta, Quality control of AlSi10Mg produced by SLM: Metallography versus CT scans for critical defect size assessment, Additive Manufacturing. 28 (2019) 394–405. https://doi.org/10.1016/j.addma.2019.05.017.

[128] A. du Plessis, P. Sperling, A. Beerlink, W.B. du Preez, S.G. le Roux, Standard method for microCT-based additive manufacturing quality control 4: Metal powder analysis, MethodsX. 5 (2018) 1336–1345. https://doi.org/10.1016/j.mex.2018.10.021.

[129] B. Redwood, F. Schöffer, B. Garret, The 3D Printing Handbook: Technologies, design and applications, 3D Hubs, 2017. https://lib.hpu.edu.vn/handle/123456789/31395 (accessed September 13, 2022).

[130] R.V. Pazhamannil, J.N. V. N., G. P., A. Edacherian, Property enhancement approaches of fused filament fabrication technology: A review, Polymer Engineering & Sci. (2022) pen.25948. https://doi.org/10.1002/pen.25948.

[131] X. Liu, M. Zhang, S. Li, L. Si, J. Peng, Y. Hu, Mechanical property parametric appraisal of fused deposition modeling parts based on the gray Taguchi method, Int J Adv Manuf Technol. 89 (2017) 2387–2397. https://doi.org/10.1007/s00170-016-9263-3.

[132] P. McCullagh, J.A. Nelder, Generalized linear models, Routledge, 2019.

[133] P. Royston, Remark AS R94: A Remark on Algorithm AS 181: The W-test for Normality, Journal of the Royal Statistical Society. Series C (Applied Statistics). 44 (1995) 547–551. https://doi.org/10.2307/2986146.

[134] T.S. Breusch, A.R. Pagan, A Simple Test for Heteroscedasticity and Random Coefficient Variation, Econometrica. 47 (1979) 1287–1294. https://doi.org/10.2307/1911963.

[135] J. Blank, K. Deb, Pymoo: Multi-Objective Optimization in Python, IEEE Access. 8 (2020) 89497–89509. https://doi.org/10.1109/ACCESS.2020.2990567.

[136] K. Deb, A. Pratap, S. Agarwal, T. Meyarivan, A fast and elitist multiobjective genetic algorithm: NSGA-II, IEEE Transactions on Evolutionary Computation. 6 (2002) 182–197. https://doi.org/10.1109/4235.996017.

[137] E. Asadollahi-Yazdi, J. Gardan, P. Lafon, Multi-Objective Optimization of Additive Manufacturing Process, IFAC-PapersOnLine. 51 (2018) 152–157. https://doi.org/10.1016/j.ifacol.2018.08.250.

[138] M.A. Matos, A.M.A.C. Rocha, L.A. Costa, Many-objective optimization of build part orientation in additive manufacturing, Int J Adv Manuf Technol. 112 (2021) 747–762. https://doi.org/10.1007/s00170-020-06369-5.

[139] J.D. Schaffer, R. Caruana, L.J. Eshelman, R. Das, A Study of Control Parameters Affecting Online Performance of Genetic Algorithms for Function Optimization, in: Proceedings of the 3rd International Conference on Genetic Algorithms, Morgan Kaufmann Publishers Inc., San Francisco, CA, USA, 1989: pp. 51–60.

[140] H. Muhlenbein, D. Schlierkamp-Voosen, Optimal Interaction of Mutation and Crossover in the Breeder Genetic Algorithm, (n.d.) 10.

[141] L. Custodio, R. Machado, Flexible automated warehouse: a literature review and an innovative framework, Int J Adv Manuf Technol. 106 (2020) 533–558. https://doi.org/10.1007/s00170-019-04588-z.

[142] K. Azadeh, R. De Koster, D. Roy, Robotized and Automated Warehouse Systems: Review and Recent Developments, Transportation Science. 53 (2019) 917–945. https://doi.org/10.1287/trsc.2018.0873.

[143] F.H. Mohammad Khasasi, Z. Mohd Yusof, M. Alias, I. Adam, M. Rasin, Development of Automated Storage and Retrieval System (ASRS) for Flexible Manufacturing System (FMS), Journal of Engineering Technology 2231-8798. 4 (2016) 43–50.

[144] M.R. Vasili, S.H. Tang, M. Vasili, Automated Storage and Retrieval Systems: A Review on Travel Time Models and Control Policies, in: R. Manzini (Ed.), Warehousing in the Global Supply Chain, Springer London, London, 2012: pp. 159–209. https://doi.org/10.1007/978-1-4471-2274-6_8.

[145] J. Habazin, A. Glasnović, I. Bajor, Order Picking Process in Warehouse: Case Study of Dairy Industry in Croatia, PROMET. 29 (2017) 57–65. https://doi.org/10.7307/ptt.v29i1.2106.

[146] Y. Jaghbeer, R. Hanson, M.I. Johansson, Automated order picking systems and the links between design and performance: a systematic literature review, International Journal of Production Research. 58 (2020) 4489–4505. https://doi.org/10.1080/00207543.2020.1788734.

[147] G. Bruno, G. D'Antonio, Flexible reconfiguration of AVS/RS operations for improved integration with manufacturing processes, Procedia CIRP. 78 (2018) 196–201. https://doi.org/10.1016/j.procir.2018.09.052.

[148] N. Kimura, K. Ito, T. Fuji, K. Fujimoto, K. Esaki, F. Beniyama, T. Moriya, Mobile dual-arm robot for automated order picking system in warehouse containing various kinds of products, in: 2015 IEEE/SICE International Symposium on System Integration (SII), IEEE, Nagoya, Japan, 2015: pp. 332–338. https://doi.org/10.1109/SII.2015.7404942.

[149] M. Eder, An approach for a performance calculation of shuttle-based storage and retrieval systems with multiple-deep storage, Int J Adv Manuf Technol. 107 (2020) 859–873. https://doi.org/10.1007/s00170-019-04831-7.

[150] V. Colla, G. Nastasi, Modelling and Simulation of an Automated Warehouse for the Comparison of Storage Strategies, in: G. Romero, L. Martinez (Eds.), Modelling Simulation and Optimization, InTech, 2010. https://doi.org/10.5772/7658.

[151] V. Singbal, G.K. Adil, A simulation analysis of impact of design and storage policy on performance of single-crane multi-aisle AS/RS, IFAC-PapersOnLine. 52 (2019) 1620–1625. https://doi.org/10.1016/j.ifacol.2019.11.432.

[152] T. Lerher, M. Edl, B. Rosi, Energy efficiency model for the mini-load automated storage and retrieval systems, Int J Adv Manuf Technol. 70 (2014) 97–115. https://doi.org/10.1007/s00170-013-5253-x.

[153] T. Lerher, Y.B. Ekren, Z. Sari, Simulation Analysis of Shuttle Based Storage and Retrieval Systems, Int. j. Simul. Model. (2015) 48–59. https://doi.org/10.2507/IJSIMM14(1)5.281.

[154] T. Lerher, B.Y. Ekren, Z. Sari, B. Rosi, Method for evaluating the throughput performance of shuttle based storage and retrieval systems, Teh. Vjesn. 23 (2016). https://doi.org/10.17559/TV-20141022121007.

[155] B.Y. Ekren, Z. Sari, T. Lerher, Warehouse Design under Class-Based Storage Policy of Shuttle-Based Storage and Retrieval System, IFAC-PapersOnLine. 48 (2015) 1152–1154. https://doi.org/10.1016/j.ifacol.2015.06.239.

[156] B.Y. Ekren, S.S. Heragu, Simulation based performance analysis of an autonomous vehicle storage and retrieval system, Simulation Modelling

Practice and Theory. 19 (2011) 1640–1650. https://doi.org/10.1016/j.simpat.2011.02.008.

[157] G. Marchet, M. Melacini, S. Perotti, E. Tappia, Development of a framework for the design of autonomous vehicle storage and retrieval systems, International Journal of Production Research. 51 (2013) 4365–4387. https://doi.org/10.1080/00207543.2013.778430.

[158] T. Kriehn, F. Schloz, K.-H. Wehking, M. Fittinghoff, Impact of class-based storage, sequencing of retrieval requests and warehouse reorganisation on throughput of shuttle-based storage and retrieval systems, FME Transaction. 46 (2018) 320–329. https://doi.org/10.5937/fmet1803320K.

[159] A. Akpunar, E. Yetkin, T. Lerher, Energy efficient design of autonomous vehicle based storage and retrieval system, Istrazivanja i Projektovanja Za Privredu. 15 (2017) 25–34. https://doi.org/10.5937/jaes15-12132.

[160] T. Lerher, Design of Experiments for Identifying the Throughput Performance of Shuttle-Based Storage and Retrieval Systems, Procedia Engineering. 187 (2017) 324–334. https://doi.org/10.1016/j.proeng.2017.04.382.

[161] B. Rosi, L. Grasic, G. Dukic, Simulation-Based Performance Analysis of Automated Single-Tray Vertical Lift Module, Int. j. Simul. Model. 15 (2016) 97–108. https://doi.org/10.2507/IJSIMM15(1)8.328.

[162] D. Battini, M. Calzavara, A. Persona, F. Sgarbossa, Dual-tray Vertical Lift Modules for Fast Order Picking, (n.d.) 14.

[163] B.Y. Ekren, S.S. Heragu, Performance comparison of two material handling systems: AVS/RS and CBAS/RS, International Journal of Production Research. 50 (2012) 4061–4074. https://doi.org/10.1080/00207543.2011.588627.

[164] G. Bruno, G. D'Antonio, M.D. Maddis, Sustainability Analysis of Autonomous Vehicle Storage and Retrieval Systems, 12 (2016) 8.

[165] E. Guerrazzi, V. Mininno, D. Aloini, R. Dulmin, C. Scarpelli, M. Sabatini, Energy Evaluation of Deep-Lane Autonomous Vehicle Storage and Retrieval System, Sustainability. 11 (2019) 3817. https://doi.org/10.3390/su11143817.

[166] C.J. Malmborg, Conceptualizing tools for autonomous vehicle storage and retrieval systems, International Journal of Production Research. 40 (2002) 1807–1822. https://doi.org/10.1080/00207540110118668.

[167] M. Eder, G. Kartnig, Throughput analysis of S/R shuttle systems and ideal geometry for high performance, FME Transaction. 44 (2016) 174–179. https://doi.org/10.5937/fmet1602174E.

[168] T. Lerher, M. Ficko, I. Palčič, Throughput performance analysis of Automated Vehicle Storage and Retrieval Systems with multiple-tier shuttle

vehicles, Applied Mathematical Modelling. 91 (2021) 1004–1022. https://doi.org/10.1016/j.apm.2020.10.032.

[169] F.S. Roberts, Measurement theory: with applications to decisionmaking, utility and the social sciences, Cambridge Univ. Press, Cambridge, 1985.

[170] F. Franceschini, M. Galetto, E. Turina, Service quality monitoring by performance indicators: a proposal for a structured methodology, IJSOM. 5 (2009) 251. https://doi.org/10.1504/IJSOM.2009.023235.

[171] A. Neely, M. Gregory, K. Platts, Performance measurement system design: A literature review and research agenda, International Journal of Operations & Production Management. 25 (2005) 1228–1263. https://doi.org/10.1108/01443570510633639.

[172] K. Park, G.E.O. Kremer, Text mining-based categorization and user perspective analysis of environmental sustainability indicators for manufacturing and service systems, Ecological Indicators. 72 (2017) 803–820. https://doi.org/10.1016/j.ecolind.2016.08.027.

[173] G. Taddese, S. Durieux, E. Duc, Sustainability performance indicators for additive manufacturing: a literature review based on product life cycle studies, Int J Adv Manuf Technol. 107 (2020) 3109–3134. https://doi.org/10.1007/s00170-020-05249-2.

[174] V.P. Rodrigues, D.C.A. Pigosso, T.C. McAloone, Process-related key performance indicators for measuring sustainability performance of ecodesign implementation into product development, Journal of Cleaner Production. 139 (2016) 416–428. https://doi.org/10.1016/j.jclepro.2016.08.046.

[175] A. Johnson, L. McGinnis, Performance measurement in the warehousing industry, IIE Transactions. 43 (2010) 220–230. https://doi.org/10.1080/0740817X.2010.491497.

[176] F.H. Staudt, G. Alpan, M. Di Mascolo, C.M.T. Rodriguez, Warehouse performance measurement: a literature review, International Journal of Production Research. 53 (2015) 5524–5544. https://doi.org/10.1080/00207543.2015.1030466.

[177] J. Gu, M. Goetschalckx, L.F. McGinnis, Research on warehouse design and performance evaluation: A comprehensive review, European Journal of Operational Research. 203 (2010) 539–549. https://doi.org/10.1016/j.ejor.2009.07.031.

[178] G. Alpan, A.-L. Ladier, R. Larbi, B. Penz, Heuristic solutions for transshipment problems in a multiple door cross docking warehouse, Computers & Industrial Engineering. 61 (2011) 402–408. https://doi.org/10.1016/j.cie.2010.09.010.

[179] M. Ang, Y.F. Lim, How to optimize storage classes in a unit-load warehouse, European Journal of Operational Research. 278 (2019) 186–201. https://doi.org/10.1016/j.ejor.2019.03.046.

[180] N.H. Shah, H.N. Soni, K.A. Patel, Optimizing inventory and marketing policy for non-instantaneous deteriorating items with generalized type deterioration and holding cost rates, Omega. 41 (2013) 421–430. https://doi.org/10.1016/j.omega.2012.03.002.

[181] ISO 22400: 2014 Automation systems and integration — Key performance indicators (KPIs) for manufacturing operations management — Part 1: Overview, concepts and terminology — Part 2: Definitions and descriptions, BSI, 2014.

[182] G.A. Gorry, M.S. Scott Morton, A framework for management information systems, (1971).

[183] T. Hemphill, The ISO 26000 guidance on social responsibility international standard: what are the business governance implications?, Corporate Governance: The International Journal of Business in Society. 13 (2013) 305–317. https://doi.org/10.1108/CG-08-2011-0062.

[184] rinivas Bollapragada, R. Akella, R. Srinivasan, Centralized ordering and allocation policies in a two-echelon system with non-identical warehouses, European Journal of Operational Research. 106 (1998) 74–81. https://doi.org/10.1016/S0377-2217(97)00148-3.

[185] C. Xu, D. Zhao, J. Min, J. Hao, An inventory model for nonperishable items with warehouse mode selection and partial backlogging under trapezoidal-type demand, Journal of the Operational Research Society. 72 (2021) 744–763. https://doi.org/10.1080/01605682.2019.1708822.

[186] T. Singh, H. Pattnayak, A two-warehouse inventory model for deteriorating items with linear demand under conditionally permissible delay in payment, International Journal of Management Science and Engineering Management. 9 (2014) 104–113. https://doi.org/10.1080/17509653.2013.862931.

[187] J.A. Larco, R. de Koster, K.J. Roodbergen, J. Dul, Managing warehouse efficiency and worker discomfort through enhanced storage assignment decisions, International Journal of Production Research. 55 (2017) 6407–6422. https://doi.org/10.1080/00207543.2016.1165880.

[188] W.S. Marras, K.P. Granata, K.G. Davis, W.G. Allread, M.J. Jorgensen, Effects of box features on spine loading during warehouse order selecting, Ergonomics. 42 (1999) 980–996. https://doi.org/10.1080/001401399185252.

[189] A. Lorenc, T. Lerher, Effectiveness of product storage policy according to classification criteria and warehouse size, FME Transactions. 47 (2019) 142–150. https://doi.org/10.5937/fmet1901142L.

[190] A. Burinskiene, Order picking process at warehouses, IJLSM. 6 (2010) 162. https://doi.org/10.1504/IJLSM.2010.030958.

[191] H.L. Chan, K.W. Pang, Association Rule Based Approach for Improving Operation Efficiency in a Randomized Warehouse, (n.d.) 8.

[192] R. Agrawal, Fast Algorithms for Mining Association Rules, (n.d.) 13.

[193] Y.-J. Lai, T.-Y. Liu, C.-L. Hwang, Theory and Methodology TOPSIS for MODM, 1994.

[194] L.A. Franco, G. Montibeller, Problem Structuring for Multicriteria Decision Analysis Interventions, in: Wiley Encyclopedia of Operations Research and Management Science, John Wiley & Sons, Inc., Hoboken, NJ, USA, 2011: p. eorms0683. https://doi.org/10.1002/9780470400531.eorms0683.

[195] A. Tsoukiàs, On the concept of decision aiding process: an operational perspective, Ann Oper Res. 154 (2007) 3–27. https://doi.org/10.1007/s10479-007-0187-z.